الجمهورية الجزائرية الديمقراطية الشعبية
People's Democratic Republic of Algeria

وزارة التعليم العالي والبحث العلمي
Ministry of Higher Education and Research

جـــامعة 20 أوت 1955 سكيـــكـــدة
University of August 20th, 1955, Skikda
كلية التكنولوجيا
Faculty of Technology
قسم :الهندسة الكهربائية
Department of Electrical Engineering

Réf: D012121017D

THESIS

Presented to obtain

Doctoral Degree

Option: Electrotechnics

THEME

Contribution to the Study and Modelling of Photovoltaic System Dynamic Behaviour

By: **Mohammed Salah BOUAKKAZ**

Publicly Defended at **18/11/2021**

Discerned by committee members:

Z. AHMIDA	Professor	University of Skikda	President
A. BOUKADOUM	Professor	University of Skikda	Supervisor
O. BOUDEBBOUZ	A. Professor	University of Skikda	Co-Supervisor
H. LABAR	Professor	University of Annaba	Examiner
D. DIB	Professor	University of Tebessa	Examiner
R. LALALOU	A. Professor	Université de Skikda	Examiner

Year : 2020/2021

ACKNOWLEDGEMENTS

Thanks to Allah first and foremost.

Thanks to my parents, wife and family members for their unconditional love, support and prayers that have carried and sustained me on this journey.

I would like to thank my supervisor, Prof. Ahcene Boukadoum and my co-supervisor Dr. Omar Boudebbouz for their assistance and guidance throughout the process of this research.

My special honor is addressed to Prof. Zahir Ahmida, Prof. Hocine Labar, Prof. Djalel Dib and Dr. Rachid Lalalou for accepting to be part of the scientific examination committee.

My thanks should go to the University of Skikda, the Unit of Research in Renewable Energy in Saharan Region (URER-MS/CDER)-Adrar-Algeria and the Unit of Research in Advanced Materials (URMA/CRTI)-Annaba-Algeria managers and employees who provided me with data and information which I needed for the research, however, I would like to mention and extend my special thanks to a few of them, special thanks should go to Dr. Issam Attoui, Dr. Nadir Boutasseta, Dr. Nadir Frgani, Dr. Ahmed Bouraiou, Dr. Ammar Necaibia, Prof. Saad Motahhir, Dr. Abdallah Faleh and Dr. Rabah Khmis, for their devotion to go through my thesis draft, advising and guiding me on various issues regarding the thesis.

ملخص

تتعلق الاستطاعة التي توفرها أنظمة الطاقة الكهروضوئية (PV) بشكل أساسي على الظروف المناخية وحدوث الأعطال. إن خصائص تيار - جهد تحتوي على مناطق تشغيل يمكن أن تعبر على استجابات انتقالية متنوعة وم جهدة في غالب الأحيان. الاستجابة الناتجة عن التظليل الجزئي تمثل إحدى ه اته الحالات ذات الأهمية الخاصة في تقييم أداء الأنظمة الكهروضوئية. ضمن هذا المنظور، انحصر العمل البحثي لهذه الأطروحة والتي تم فيها تقييم الأداء الديناميكي لنظام كهروضوئي ثلاثي الألواح بحلقة مفتوحة و مغلقة.

إن النظام الكهروضوئي المدروس قد أخضع لزاما لتأثيرات ظروف بيئية مختلفة نتج على إثره ا إصدار أحكامًا مختلفة على مناطق التشغيل للتيار وللجهد و للاستطاعة.

في الواقع، لوحظ سلوك ديناميكي معقد تم تحسينه بفضل إستراتيجية تحكم مقترحة. أعتمد ضمن هذه الأخيرة على تعديل التيار الكهروضوئي باستخدام وحدة تحكم في الوضع المنزلق من جهة ، ومن جهة أخرى على تعديل جهد الخرج باستخدام منظم PID ذو رتب عشرية (FOPID) الذي تم تعديل معاملاته باستخدام استمثال عناصر السرب (PSO). هذا الأخير سمح بتحديد وحدة التحكم المثلى لمختلف مناطق التشغيل ونماذج التظليل الجزئي. لم يتطلب تعديل النظام الكهروضوئي استخدام تعديل عرض النبضة (PWM).

لقد لوحظت بعض النقائص بسبب النهج المستخدم لوضع وسائط التعديل على مستوى خوارزميات البحث عن نقطة الاستطاعة القصوى (MPPT). معالجتها تمت بتحديث تقنية MPPT بإقحام خوارزمية استمثال عثة اللهب (MFO) ودمجها مع إستراتيجية التحكم المقترحة.

إن إستراتيجية تحسين الأداء الديناميكي المقترحة تظهر نتائج فعالة للغاية لدرجة أنها أظهرت استجابات عابرة ممتازة لسيناريوهات تشغيل مختلفة.

الكلمات المفتاحية : الكهروضوئية (PV), تتبع نقطة الاستطاعة القصوى (MPPT), استمثال عناصر السرب (PSO), استمثال عثة اللهب (MFO), تعديل عرض النبضة (PWM), متحكم تناسبي تكاملي تفاضلي ذو رتب عشرية (FOPID)

ABSTRACT

The output power of Photovoltaic (PV) energy generation systems depends mainly on climatic conditions and the occurrence of faults. The current-voltage characteristics of PV systems have regions of operation with various, most often constraining, transient responses. Significantly, the presence of partial shading is a case of particular interest in performance evaluation. The research work of this thesis comes under this perspective. Thus, the dynamic evaluation of a PV system's performances composed of three panels was carried out in an open and closed loop.

The studied PV system had to undergo the effects of different environmental conditions, which gave different evaluations on the operating regions of current, voltage, and power.

Indeed, a complex dynamic behavior has been identified, the improvement of which was obtained thanks to a proposed control strategy. The latter was based on one hand on regulating the PV current using a sliding mode controller, and on the other hand on regulating the output voltage using a Fractional Order PID (FOPID) controller whose parameters have been adjusted using Particle Swarm Optimization (PSO). The last one was able to determine the optimal controller for different operating regions and partial shading patterns. The regulation of the PV system did not require the use of Pulse Width Modulation (PWM).

Certain imperfections due to the regulation parameterization approach were observed at the levels of the Maximum Power Point Tracking (MPPT) algorithms. To remedy this, the MPPT technique based on the Moth-Flame Optimization (MFO) algorithm was implemented and combined with the proposed control strategy.

The proposed dynamic performance improvement strategy is highly effective which shows excellent transient responses in various operating scenarios.

Keywords : Photovoltaic (PV), Maximum Power Point Tracking (MPPT), Particle Swarm Optimization (PSO), Moth-Flame Optimization (MFO), Pulse Width Modulation (PWM), Fractional Order Proportional-Integral-Derivative (FOPID).

RESUME

La puissance fournie par les systèmes photovoltaïques (PV) dépend, principalement, des conditions climatiques et de la survenance des défauts. Les caractéristiques courant-tension des systèmes PV ont des régions de fonctionnement susceptibles de contenir diverses réponses transitoires le plus souvent contraignantes. Notamment la présence d'ombrage partiel en est un cas qui intéresse, particulièrement, l'évaluation des performances. Le travail de recherche de la présente thèse s'inscrit dans cette optique. Ainsi, l'évaluation des performances dynamiques d'un système PV composé de trois panneaux a été effectuée en boucle ouverte et fermée.

Le système PV étudié a dû subir les effets de différentes conditions environnementales qui ont donné, à leur tour, différentes appréciations sur les régions de fonctionnement du courant, de la tension et de la puissance.

En effet, un comportement dynamique complexe a été relevé dont l'amélioration a été obtenue grâce à une stratégie de contrôle proposée. Cette dernière s'est articulée d'une part, sur la régulation du courant PV à l'aide d'un contrôleur à mode glissant et d'autre part, sur la régulation de la tension de sortie à l'aide d'un régulateur PID d'ordre fractionnaire (FOPID) dont les paramètres ont été ajustés en utilisant l'optimisation par essaim de particules (PSO). Ce dernier a pu déterminer le contrôleur optimal pour différents régions de fonctionnement et modèles d'ombrage partiel. La régulation du system PV n'a pas nécessité un usage de la modulation à largeur d'impulsion (PWM).

Certaines imperfections dues à l'approche utilisée pour le paramétrage de la régulation ont été observées aux niveaux des algorithmes de recherche de point de puissance maximale (MPPT). Pour y remédier, la technique MPPT basée sur l'algorithme d'optimisation Hétérocère - Flamme (MFO) a été implémentée et associée à la stratégie de contrôle proposée.

La stratégie d'amélioration des performances dynamiques proposée est très efficace jusqu'à même montrer d'excellentes réponses transitoires dans divers scénarios d'exploitation.

Mots Clés : Photovoltaïque (PV), Poursuit du point de puissance maximal (MPPT), Optimisation par essaims particulaires (PSO), Optimisation par Hétérocère - Flamme (MFO), modulation à largeur d'impulsion (PWM), Proportionnel-Intégral-Dérivé d'ordre fractionnaire (FOPID).

TABLE OF CONTENTS

LIST OF TABLES

LIST OF FIGURES

LIST OF ABBREVIATIONS

PV PhotoVoltaic

GHI Global Horizontal Irradiation

DNI Direct Normal Irradiation

NREL National Renewable Energy Laboratory

CIGS Copper Indium Gallium Selenide

CdTe Cadmium Telluride

PSCs Perovskite Solar Cells

OPV Organic PhotoVoltaic

DSSC Dye-Sensitized Solar Cell

QDs Quantum Dots

DC-DC Direct current-Direct current

MPPT Maximum Power Point Tracking

PI Proportional Integral

FOPID Fractional-Order Proportional Integral Derivative

MPC Model Predictive Control

SMC Sliding Mode Control

LQR Linear Quadratic Regulator

MFO Moth Flame Optimization

PSO Particle Swarm Optimization

PWM Pulse Width Modulation

HC Hill Climbing

FV Fractional Voltage

CV Constant voltage

LT	Look-up Table
LCC	Linear Current Control
LC	Load Current
CF	Curve Fitting
CS	Current Sweep
IC	Incremental Conductance
FLC	Fuzzy Logic Control
ANN	Artificial Neural Network
P&O	Perturb and Observe
AR	Array Reconfirmation
POS	PV-Output Senseless
AI	Artificiel intelligence
BI	Biological intelligence
ANFIS	Adaptive Neuro-Fuzzy Inference System
BN	Bayesian Network
WOA	Whale Optimization Algorithm
GA	Genetic Algorithm
CSAM	Current Sensor Auto Modulation
RCC	Ripple Correlation Control
GSA	Gravitational Search Algorithm
SA	Simulated Annealing
DE	Differential Evolutionary
GMPP	Global Maximum Power Point Tracking
I-V	Current-Voltage

P-V Power-Voltage

STC Standard Test Condition

PSC Partial Shading Condition

CPR Constant Power Region

VSR Voltage Source Region

CSR Current Source Region

GREEK SYMBOLS

λ fractional-order integration parameter

μ fractional-order derivation parameter

LIST OF SYMBOLS

D Duty Cycle

$\mathbf{K_v}$ Fractional voltage constant

$\mathbf{V_{oc}}$ Open-Circuit Voltage

$\mathbf{V_{mpp}}$ Voltage at maximum power point

$\mathbf{I_{mpp}}$ Current at maximum power point

$\mathbf{K_{ii}}$ Fractional current constant

$\mathbf{I_{sc}}$ Short-circuit current

$\mathbf{K_i}$ Short-circuit current/temperature coefficient

$\mathbf{P_{pv}}$ PV array output power

$\mathbf{V_{pv}}$ PV array output voltage

$\mathbf{I_{pv}}$ PV array output current

G Solar Irradiation

T Temperature

$\mathbf{I_m}$ Mutual Current

S	Power Switch
I_P	Current in the parallel branch
R_P	Parallel resistances of the PV panel
R_s	Series resistances of the PV panel
N_{ss}	Number of series panels
I_{ph}	Photocurrent
n	Nominal generated current
I_d	Current in the diode
I_o	Reverse saturation current
a	Diode ideality constant
V_t	Thermal voltage of the PV array
s	Sliding surface
u	Switching signal
k_D	Derivative gain
k_I	Integral gain
k_P	Proportional gain
V_i	Velocity of a particle (i)
X_i	Position of a particle (i)
P_i	The personal best fitness
G_b	The global best fitness
M_i	position of the searching agents
ΔV_{pv}	Steady state oscillations
Tr	Tracking time
ξ	Tracking accuracy

CHAPTER I

INTRODUCTION

CHAPTER I

I.1 PREAMBLE

The chapter presents the motivations which led to the realization of the thesis research work. Also, the background is dressed to emphasize the necessary correlation of solar energy study with all the environmental, climatic, and conceptual properties and characteristics. The main objectives, contributions, and the thesis organization are presented as well.

I.2 MOTIVATIONS AND BACKGROUND

Almost all types of human activity require electrical energy. On the other hand, demographic growth and the search for well-being which depend on the availability of energy products, in particular, that of electricity, make the consumption of electrical energy constantly evolving. As a consequence, the electrical energy produced from fossil sources will be unable to meet human needs and it will also be avoided due to its detrimental effect on ecosystems. The burning of fossil fuels raises major concerns about global warming and the risky environmental effects of greenhouse gas emissions. To that fact, the eventual rapid depletion of fossil reserves can cause an increase in their costs despite their poor environmental profile.

The aforementioned drawbacks turn out to be an ideal orientation for researchers and users of the electrical product to promote clean alternative sources.

Like the causes of influence cited above, the covid-19 pandemic also appears to have been very influential on human activities for more than a year from December 2019.

The daily country-level CO2 emissions estimated for different regions based on real-time activity data show a decline in global CO2 emissions by 8.8% (1,551 Mt CO2) in the first half of 2020, compared to the same period in 2019. Other estimations show that the scale

of this decline is greater than in the previous economic recession or World War II as shown in figure I.1 [1].

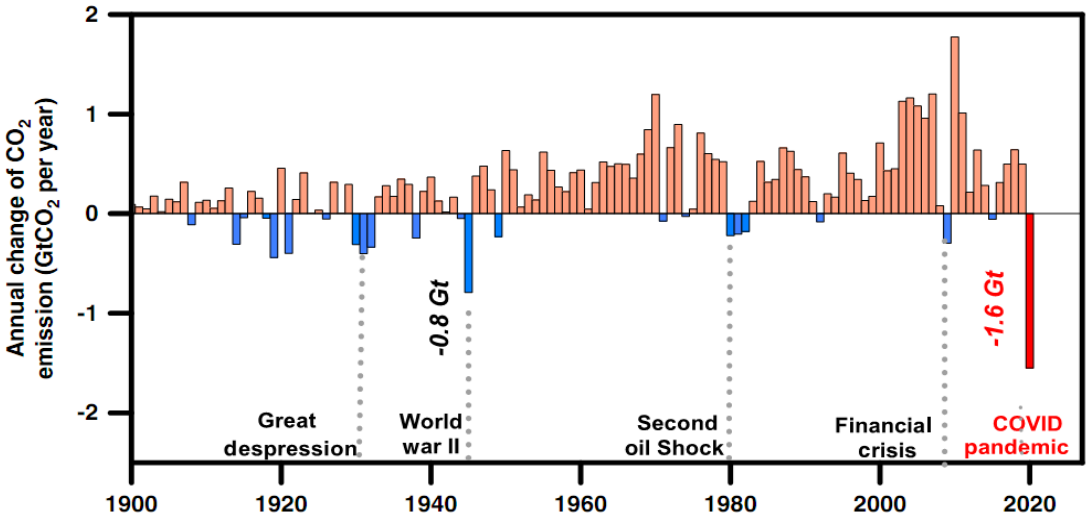

Figure I.1 Annual decrease of CO2 emission since 1900 [1].

Due to the increasing electricity demand and resulting high greenhouse emissions which is the highest among emitting sectors (figure I.2) [2] and the decreasing availability of conventional energy sources, such as coal, oil, etc. renewable energy, one of the manifestations of energy that earth receives from the sun plays an important role in the production of electrical energy.

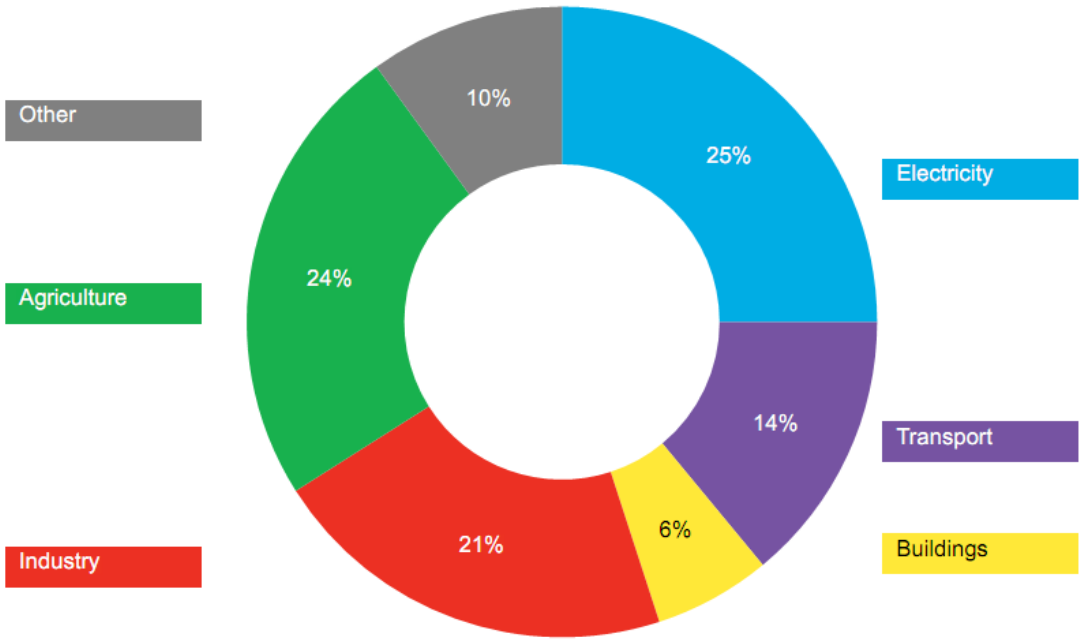

Figure I.2 Greenhouse gas emissions by sector [2].

Solar energy has a worldwide great potential and very interesting environmentally friendly properties (figure I.3) [3]. Based on photovoltaic cells, the direct conversion of solar radiation to electrical energy could be considered an outstanding energy production process. The free availability of solar energy which is clean and abundant with also almost zero noise and maintenance-free noise characteristics reinforces its profile as the energy of the future.

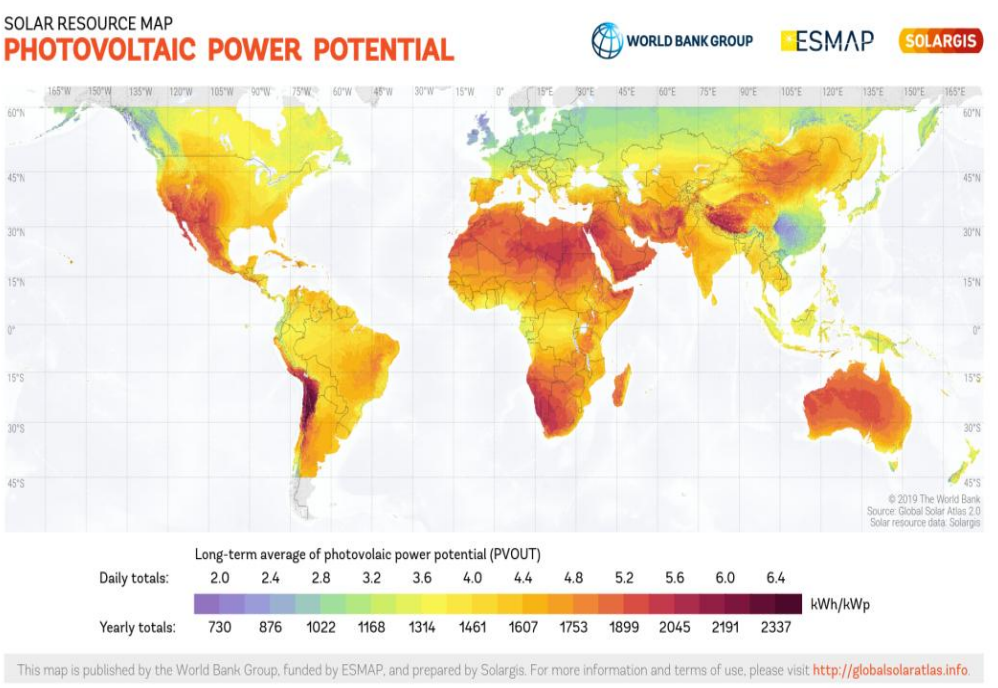

Figure I.3 PVOUT, GHI and DNI–Word [3].

In this context, Algerian relief is characterized by a large Sahara region exposed to high amounts of incoming sunlight. It could be a better choice for both testing and permanent installation of photovoltaic panels based solar energy generation systems. Algeria is the largest country in Africa with an area that reaches 2.381.741 km^2 of which 86% is the desert. It is situated in the gateway of North Africa between the 38–35 of latitude north and 8–12 longitude east, which is limited by the Mediterranean Sea to the north and by the Sahara to the south. The areas of northern Algeria are more heavily covered than those of the south. The Saharan regions receive a greater amount of energy but are characterized by a higher air temperature. Figure I.4 summarizes the estimated solar photovoltaic (PV) power generation potential, Global Horizontal Irradiation GHI, and Direct Normal Irradiation DNI– a long-term average of daily and yearly totals for Algeria [4].

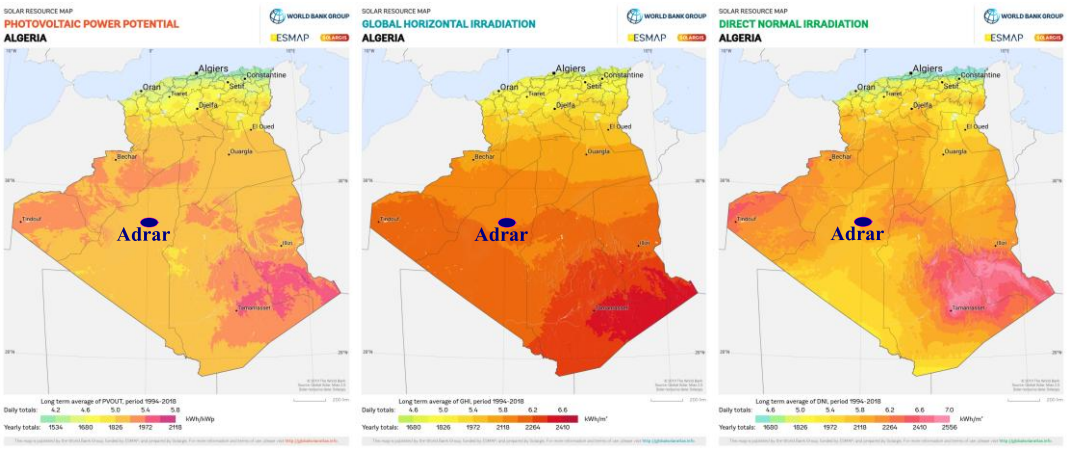

Figure I.4 PVOUT, GHI and DNI–Algeria [4].

The change in global demand for modules has always been an important factor in price adjustments. However, there are currently several mixed trends and demand forecasts. In Europe, the solar energy industry is growing rapidly, despite corona virus restrictions. Essentially strong demand is expected from China itself, and this should have gone smoothly, but has not been felt in the global market yet. (figure I.5) [5].

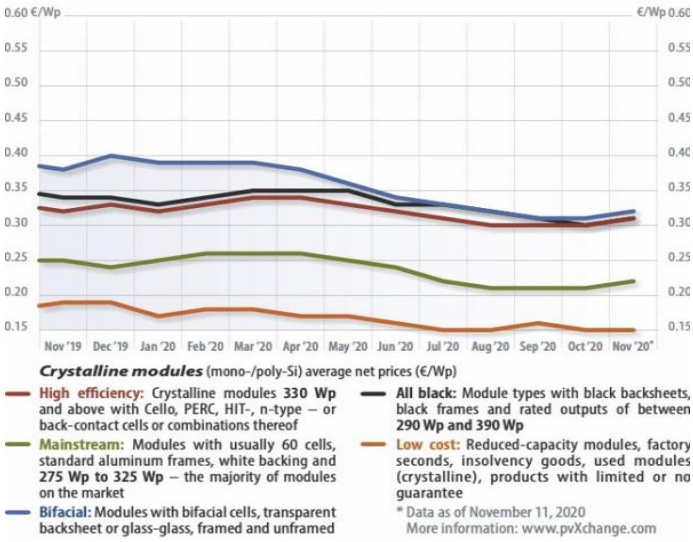

Figure I.5 Market module prices by technology [5].

In recent decades, scientists and engineers in national laboratories, universities and private companies have tried to search and develop new types of cells and expand the capabilities of existing cells because the ideal technology has yet to be developed.

The National Renewable Energy Laboratory (NREL) maintains some of the highest validated assembly conversion efficiency values for research cells since 1976 of various PV technologies

The first-generation solar cells are based on silicon chips and the energy conversion is usually around 15-20% (Table I.1). Generally, compared to non-silicon solar cells, these solar cell technologies are more efficient and durable, but at higher temperatures, they are more likely to lose some of their efficiency. Currently, four types of silicon-based photovoltaic batteries are used commercially in the production of solar panels. These types are monocrystalline, polycrystalline, amorphous and hybrid solar cells (figure I.6) [6].

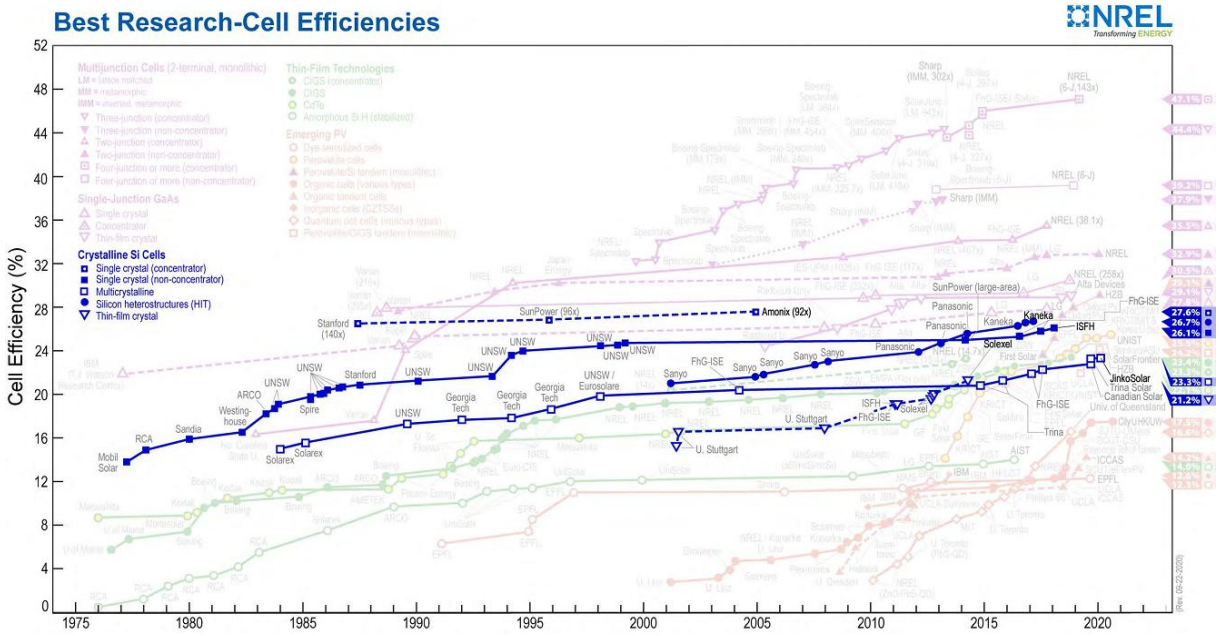

Figure I.6 1st Generations Solar Cells Efficiency Milestones [6].

Table I.1 Comparisons of 1st Generation solar cells [7].

1st Generation PV Cells: Silicon Based Solar Cells (-Si)			
Silicon is still the most common material used in PV modules, thanks to its excellent electronic, chemical and mechanical properties. Solar technologies based on this semiconductor are considered the most mature. In general, the fabrication of silicon wafers is made through Czochralski (CZ) process.			
Types	Efficiency	Advantages	Disadvantages
sc-Si	• 25–27% in laboratory • 16–22% commercial efficiency • The band gap is 1.11–1.15eV	This type of solar panel is the purest one and has a high efficiency	Manufacturing process (CZ process) is both material and energy intensive
mc-Si	• 15–18% • The band gap is 1.11 eV	A suitable alternative to reduce PV module cost	Less efficient than sc-Si cells

The second-generation solar cells are based on amorphous silicon and non-silicon materials which are Copper Indium Gallium Selenide (CIGS) and Cadmium Telluride (CdTe), where the energy conversion efficiency is usually around 10-15% (Table I.2) . This class of cell generation is also known as thin-film solar cells because it uses only a micrometer thickness for several different layers of material compared to crystalline-based silicon cells. This type of technology is used commercially due to lower manufacturing costs and fewer materials being used (figure I.7) [6].

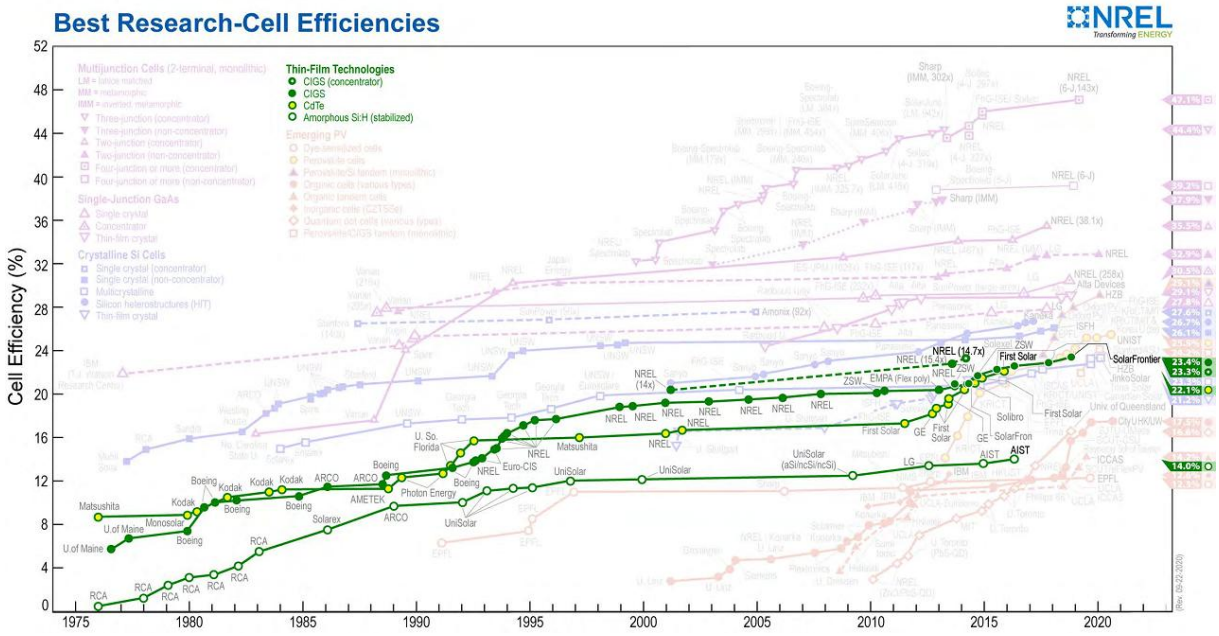

Figure I.7 2nd Generations Solar Cells Efficiency Milestones [6].

Table I.2. Comparisons of 2nd Generation solar cells [7].

2nd Generation PV Cells: Thin Film Solar Cells (TFSCs)			
Film layers thickness ranges from few nanometers (nm) to tens of micrometers (µm). The main advantage of this technology is the low cost of manufacturing and materials, due to the limited amount of semiconductor material required for each cell. Due to low thickness, TFSC are flexible, lower in weight, and have less drag compared to first generation PV. TFSCs are made by the deposition of thin layers of certain materials on glass, plastic, or stainless steel substrates using sputtering tools. Some of these technologies are not yet commercialized.			
Types	Efficiency	Advantages	Disadvantages
a-Si	• 4–8% for modules placed on the market. • Small cells in lab can reach 12%.	a-Si solar cells are the cheapest on the market	• The layers are much thinner and there is less material to absorb solar radiation • Degradation in their power output when exposed to the sun
GaAs	• 29% record efficiency in laboratory • The band gap is 1.43 eV	High efficiency and less thickness than silicon ones	High cost
CdTe	• 10–15% • (21% record efficiency) • The band gap is 1.45 eV	CdTe cells can exploit a broader wavelength spectrum than Si cells, close to the natural one. Low costs, as cadmium is abundant and generated as a by-product of important industrial materials	Cadmium by itself is one of the most toxic materials known, and cadmium telluride has some toxic properties
CIGS	• 20% (under certain conditions) • The band gap is 1.68 eV	• Process is less energy intensive than manufacturing of the Crystalline Si solar cell • Good resistance to heat	• Less efficient than Si solar cells • CIGS cells use toxic chemicals • Currently very expensive to produce
CIS	10–13%	• Processes are less energy intensive than Cry-Tech • Good resistance to heat compared to silicon based modules	Relatively expensive due to the materials used

In this new technology, solar cells are made from a variety of new materials instead of using silicon, such as ink used in printing technology, silicon wires, nanotubes, conductive plastics and organic materials. Polymeric solar cells are a subclass of organic solar cells.

The third-generation solar cells are expensive high-performance, multi-functional experimental solar cells. Most of the work is performed in the laboratory and is not commercially available. This type of device shows great potential with a standard power conversion efficiency of around 20% (Table I.3) in very small areas. Polymeric solar cells are made for roller technology and are comparable to newspaper printing (figure I.8) [6].

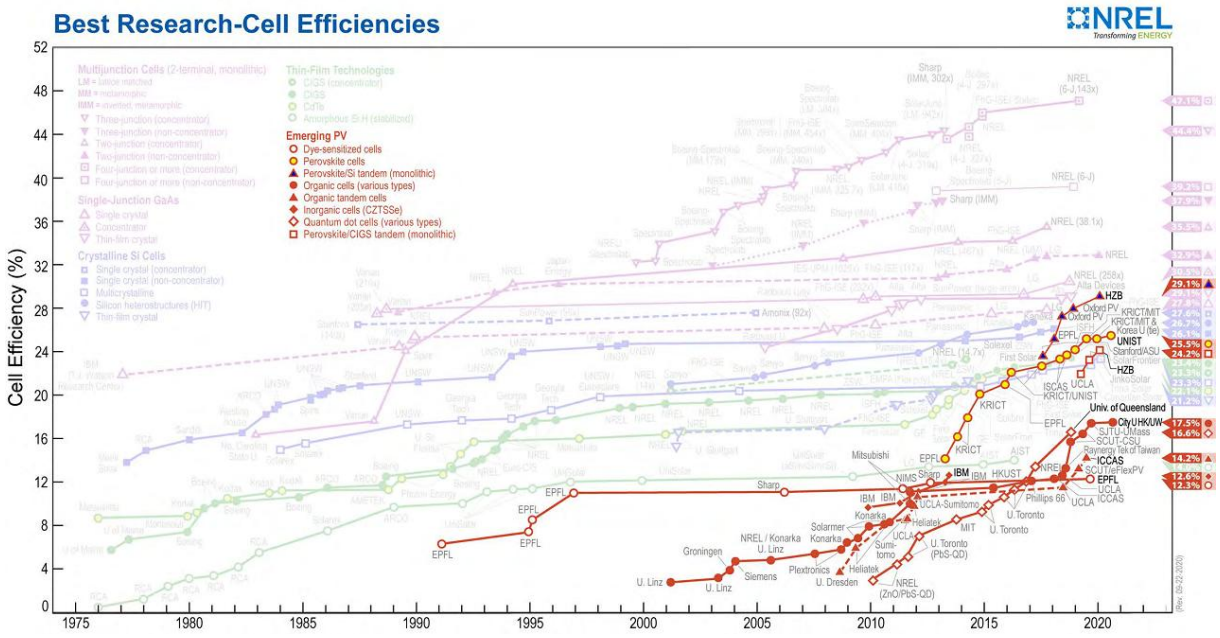

Figure I.8 3rd Generations Solar Cells Efficiency Milestones [6].

Table I.3 Comparisons of 3rdGeneration solar cells [7].

Third Generation Solar Cells			
3rd generation solar panels include several innovative technologies and most of them are still in the research or development phase. Some cells generate electricity by using organic, semi-organic or inorganic materials, hybrid systems, or new technology processes based on nanometer and molecular-scale components. These solar modules are made, in most cases, by thin film type cells.			
Types	Efficiency	Advantages	Disadvantages
PSC	19–22%	• Good efficiency and possibilities for improvement • Perovskite is cheaper to produce than silicon	• Perovskite breaks down quick when exposed to heat, snow, moisture, etc. • The presence of lead in perovskite is largely debated for toxicity concerns
OPV and polymer solar cells	4–5%, up to 9%	Lightweight, mechanical flexibility, disposability and large-scale roll-to-roll production capability	Low efficiency, low durability and low stability
DSSC	Around 10%	• Flexibility, not pollutant, easily recyclability. Low cost due to the simple manufacturing process • DSSC work even in low-light conditions • High efficiency also at high temperatures	• The electrolyte can freeze at low temperatures cutting power production and causing physical damage • Electrolyte contains volatile organic solvents and must be carefully sealed
QDs	Around 1.9%	Easy synthesis and preparation	Low efficiency

This class of solar cells combines the third-generation technology to form the fourth-generation solar cell technology. Examples include nanocrystalline solar cells and composite photovoltaic technology that combines solid-state cells with organic

photovoltaic to form hybrid nanopolymer cells. Although most of these technologies are still embryonic, it is expected that, given the low cost of materials, these types of solar cells will make the use of solar energy affordable for everyone. Another area in which solar photovoltaic technology has achieved high efficiency in centralized solar cell technology (figure I.9) [6]. An example is a multi-junction solar cell (III-V), whose efficiency exceeds 41%.

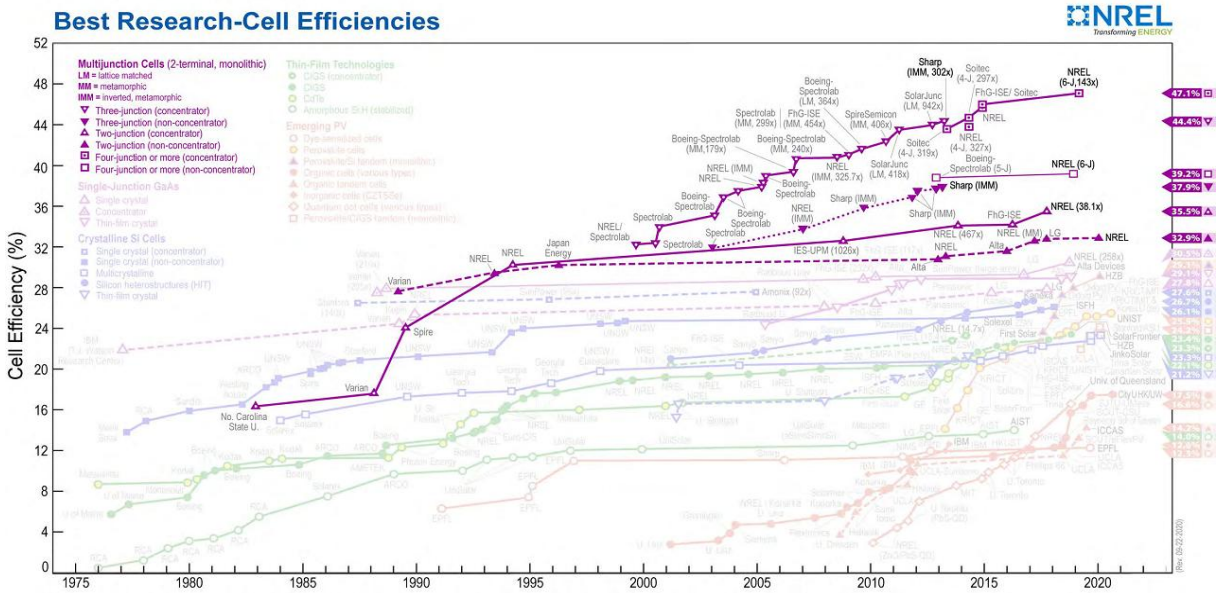

Figure I.9 4th Generations Solar Cells Efficiency Milestones [6].

PV systems are classified into three types: standalone, grid-connected, and hybrid (figure I.10) [8].

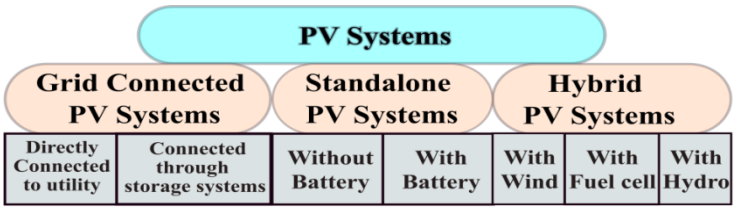

Figure I.10 PV System Classifications.

The main factor affecting PV systems performance is the solar radiation behavior. Its instantaneous unavailability can cause the most concern about panels output variables. To solve this problem and to provide a constant output voltage, various DC/DC power transducers are used. Since the 1920s, a DC-DC converter has been developed for use with photovoltaic solar panels. The main purpose of electronic transducers has been to replace the use of traditional circuits such as voltage dividers, which are often referred to as simple

voltage divider circuits. The disadvantage of this method is that the output voltage is lower compared to the input voltage, which leads to a decrease of efficiency [9].

Currently, there are several structures of DC to DC converters that are used to regulate the input voltage according to application requirements (figure I.11) .

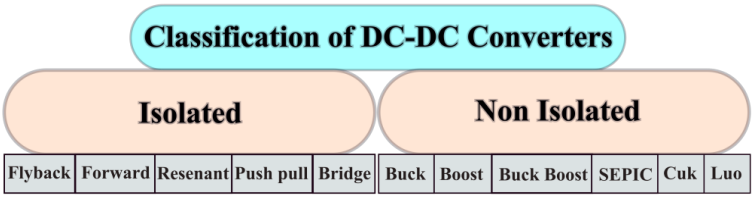

Figure I.11 Classification of the DC-DC converters.

Since the early use of the off-grid or grid-connected PV systems, many researchers have proposed and developed several methods in order to extract the maximum power for the PV panels. Accordingly, the methods have witnessed rapid improvement. Due to that, some researchers have put another classification of updated MPPT methods. As presented in figure I.12, updated MPPT methods can be classified as conventional methods, soft computing methods, or hybrid methods [10].

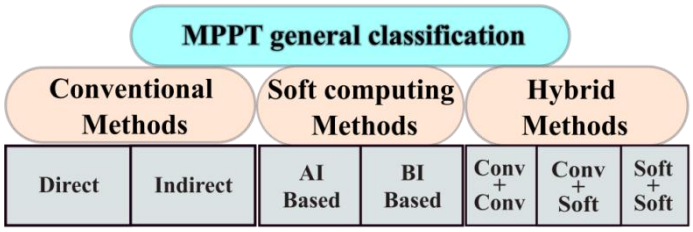

Figure I.12 MPPT Classifications.

Indeed, PV system mismatch and unpredictable internal and atmospheric variations causing the change of travel points as controllers and parameter errors are two major factors that must be carefully studied [11]. Therefore, the main purpose of PV systems is to ensure high performance at low cost by choosing an appropriate control strategy. Over the past decade, much progress has been made in optimization technologies (see figure I.13).

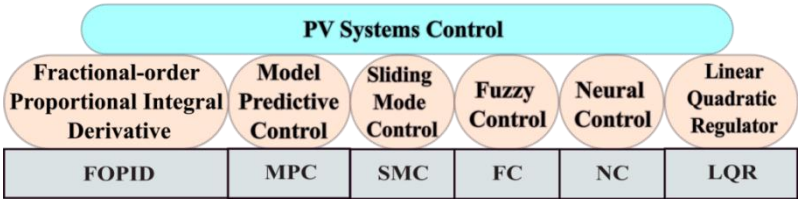

Figure I.13 PV System Classification.

I.3 PROBLEM FORMULATION

The use of renewable energy in the power generation process is among the main features of modern power systems. Distributed generators have been used in distribution electrical networks a few decades ago. The main primary sources were from sunlight and wind. The main first concern was focused on the stand-alone device for, generally, an emergency or for particular use in exceptional conditions.

Our century would, probably, be turned towards a massive use of new energy sources. This trend is strongly suited for our contemporary era where fossil sources are in the phase of extinction and the technology is in the phase of profiling.

However, research on the physical devices relating to these new energies ensuring the best compromise between costs and performance is the major challenge of any possible study. Our research is part of this perspective where the main areas of interest are more to highlight an advantageous correlation between algorithmic aspects with those of natural dynamic conditions.

In this thesis, the main research focus is on electricity production using photovoltaic panels by highlighting the beneficial attributes of the geographical situation of our country where the solar potential of the Sahara is among the sunniest areas in the world. However, the actual energy production from PV panels is considered low when compared with the incoming energy from solar sunlight.

The produced energy is also subject to multiple effects that further lower its level due to environmental conditions and the occurrence of faults that alter performance, reliability and introduce multiple maximal operating points. Current - Voltage characteristic curves exhibit various operating regions which could be characterized by different transient responses. They also vary as climatic conditions change, particularly, with the presence of the partial shading condition.

I.4 OBJECTIVES AND MAIN CONTRIBUTIONS OF THE THESIS

- The objectives of this work have been to develop appropriate methods and techniques to support strategies for getting optimal photovoltaic panels operation with the presence of dynamic conditions. Interesting results have been obtained performing important control aspects such as those relating to the fractional order regulator and those relating to Meta heuristic optimization methods applied to the MPPT.

1- In order to overcome the issues related to photovoltaic panels efficiency, a Maximum Power Point Tracking algorithm is proposed to remedy this issue.
2- Conventional MPPT algorithms have been proven to be ineffective in the presence of rapidly changing climatic conditions and also in the presence of partial shading. In such conditions, bio-inspired algorithms such as the proposed Moth Flame Optimization technique (MFO) is used to track the global MPP.
3- The Analysis of the transient response of the PV array in various operating regions and environmental conditions.
4- Design of a control strategy that takes into consideration the transient behavior for changing operating conditions.

- The main contributions of this research work are as follows:

1- The analysis shows complex dynamic behavior has been found for the first time in the current study to characterize the transient response of the PV array when operating in different regions along the characteristic curve and also in the case of changes in environmental conditions.
2- A control strategy has been proposed to take into account the complex dynamic behavior of the PV array. Fractional Order PID combined tuned in various regions and partial shading patterns using Particle Swarm Optimization (PSO) has been designed to control the PV array voltage, whereas the PV current has been regulated using a sliding mode controller that does not require Pulse Width Modulation (PWM). A dynamic performance evaluation of the PV system has been performed both in open-loop and in the presence of a feedback controller.

3- The global search problem of the maximum power point has been solved using the Moth Flame Optimization technique combined with the proposed control strategy to improve the performance PV system in different operating conditions.

I.5 LIST OF PUBLICATIONS

The obtained results in this thesis have been published in research papers. Those directly related to the objectives of the thesis have been published by the candidate (appendix A) while others have been involved in papers through collaborative efforts.

I.5.1 LIST OF PUBLICATIONS WITHIN THE THESIS FRAMEWORK

1. **M. S. Bouakkaz**, A. Boukadoum, O. Boudebbouz, A. Bouraiou, N. boutasseta and I. Attoui, "ANN based MPPT Algorithm Design using Real Operating Climatic Condition," 2020 2nd International Conference on Mathematics and Information Technology (ICMIT); IEEE; Adrar, Algeria, 2020, pp. 159-163, doi: 10.1109/ICMIT47780.2020.9046972.

2. **M. S. Bouakkaz**, A. Boukadoum, O. Boudebbouz, N. Fergani, N. Boutasseta, I. Attoui, A. Bouraiou, and A. Necaibia, "Dynamic performance evaluation and improvement of PV energy generation systems using Moth Flame Optimization with combined fractional order PID and sliding mode controller," Solar Energy, vol. 199, pp. 411- 424, 2020.

3. **M. S. Bouakkaz**, A. Boukadoum, O. Boudebbouz, I. Attoui, N. Boutasseta and A. Bouraiou, "Fuzzy Logic based Adaptive Step Hill Climbing MPPT Algorithm for PV Energy Generation Systems," 2020 International Conference on Computing and Information Technology (ICCIT-1441), Tabuk, Saudi Arabia, 2020, pp. 1-5, doi: 10.1109/ICCIT-144147971.2020.9213737.

4. **M. S. Bouakkaz,** A. Boukadoum, O. Boudebbouz, N. Boutasseta, I. Attoui, N. Fergani, A. Bouraiou, and A. Necaibia, "ANFIS-BASED MAXIMUM POWER POINT TRACKING USING GENETIC ALGORITHM TUNED FRACTIONAL-ORDER PROPORTIONAL-INTEGRAL-DERIVATIVE CONTROLLER AND ON-SITE MEASURED CLIMATIC DATA," International Journal of Energy for a Clean Environment, vol. 22, pp. 63- 82, 2021. doi: 10.1615/InterJEnerCleanEnv.2020035458

5. **M. S. Bouakkaz,** A. Boukadoum, O. Boudebbouz, I. Attoui, N. Boutasseta and A. Bouraiou,. (2021). Survey of Six Maximum Power Point Tracking Algorithms under Standard Test conditions. Algerian Journal of Renewable Energy and Sustainable Development, 3(01), 1-11.

6. **Bouakkaz M.S.** et al. (2021) Global Maximum Power Point Tracking Using Genetic Algorithm Combined with PSO Tuned PID Controller. In: Motahhir S., Bossoufi B. (eds) Digital Technologies and Applications. ICDTA 2021. Lecture Notes in Networks and Systems, vol 211. Springer, Cham. https://doi.org/10.1007/978-3-030-73882-2_107

I.5.2 LIST OF PUBLICATIONS INVOLVEMENT IN OTHER PROJECTS

1. N. Boutasseta, **M. S. Bouakkaz**, A. Bouraiou, A. Neçaibia, I. Attoui and N. Fergani, "Practical Implementation of Computational Algorithms for Efficient Power Conversion in Photovoltaic Energy Generation Systems," 2020 International Conference on Computing and Information Technology (ICCIT-1441), Tabuk, Saudi Arabia, 2020, pp. 1-5, doi: 10.1109/ICCIT-144147971.2020.9213761.

2. Attoui I., Fergani N., Boutasseta N., Oudjani B., **Bouakkaz M.S.**, Bouraiou A. (2021) Multiclass Support Vector Machine Based Bearing Fault Detection Using Vibration Signal Analysis. In: Bououden S., Chadli M., Ziani S., Zelinka I. (eds) Proceedings of the 4th International Conference on Electrical Engineering and Control Applications. ICEECA 2019. Lecture Notes in Electrical Engineering, vol 682. Springer, Singapore. https://doi.org/10.1007/978-981-15-6403-1_61.

3. Attoui, I., Oudjani, B., Boutasseta, N., Fergani, N., **Bouakkaz, M.S.,** &Bouraiou, A. (2020). Novel predictive features using a wrapper model for rolling bearing fault diagnosis based on vibration signal analysis. The International Journal of Advanced Manufacturing Technology. doi:10.1007/s00170-019-04729-4.

4. Bouraiou A. **Bouakkaz, M.S.**et al. (2021) Supervision and Monitoring of Photovoltaic Systems Using Siemens PLC and HMI. In: Motahhir S., Bossoufi B. (eds) Digital Technologies and Applications. ICDTA 2021. Lecture Notes in Networks and Systems, vol 211. Springer, Cham. https://doi.org/10.1007/978-3-030-73882-2_105

I.6 THESIS ORGANIZATION

The general classification of existing Maximum Power Techniques is presented in Chapter II. They have been categorized based on different criteria which can be classified as 1) classification based on a tracking mechanism 2) Implementation based classification 3) **c**lassification based on modernity.

Chapter III emphasizes some topics related to the output power of Photovoltaic (PV) energy generation systems. A dynamic performance evaluation of the PV system is performed in the presence of varying operating conditions and in the special case of the presence of the partial shading condition.

Chapter IV presents the global search algorithm associated with the proposed control strategy and corresponding results and discussions.

Finally, the conclusions of the thesis are pointed out in Chapter V as well as suggestions for future works are given.

CHAPTER II

CLASSIFICATION OF MPPT TECHNIQUES

CHAPTER II

II.1 INTRODUCTION

Maximum Power Point Tracking is the algorithm that facilitates the accurate tracking of the optimal operating point (MPP) that has to be applied for driving the load. The two important factors that are required to track an MPP are solar irradiation and temperature. Several MPPT techniques have been developed and implemented to reach the maximum operating power point for rapidly changing values of solar irradiation and temperature. In this work, existing MPPT classification techniques are highlighted and additional classification based on conventional (direct and indirect approaches), Soft Computing (Artificial intelligence (AI), and Bio-Inspired (BI)), and a hybrid approach are carried out.

Due to the advantages of MPPT in terms of performance and cost of energy produced by a photovoltaic system, a lot of research works have been carried out in the scientific community and have proven its importance. The recent MPPT research database for two of the most important and trusted publishers such as Elsevier and IEEE show a quick grouping of this research topic over the past 3 years which is summarized in Table II.1.

Table II.1 Number of MPPT articles publication

TYPE OF JOURNAL		Years		
		2019	2020	2021/03
IEEE	Books	0	0	0
	Articles	710	568	50
	Other	0	0	0
	Total	710	568	50
Elsevier	Books	29	8	39
	Articles	454	572	271
	Other	9	3	16
	Total	492	583	326

II.2 CLASSIFICATION OF MPPT TECHNIQUES

A large number of MPPT algorithms and designs have recently been proposed in the literature [12]–[21]. In this review, MPPT methods are categorized on the basis of different criteria such as tracking technology, sensing and existing…etc [22]. In this work, the classification proposed has been adopted. The general structure of the different approaches is shown in figure II.1.

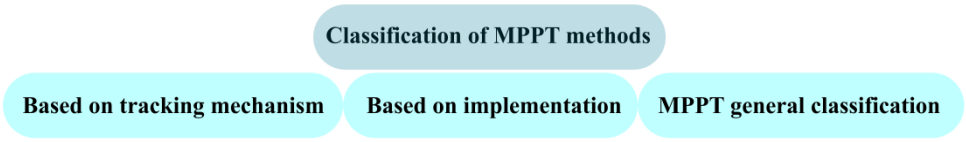

Figure II.1 Classification of MPPT methods.

II.2.1 CLASSIFICATION BASED ON TRACKING MECHANISM

An increasing number of MPPT classifications of tracking techniques have been applied to MPPT algorithms. Consequently, several research papers in the literature have categorized MPPT algorithms depending on their tracking techniques. It can be inferred that the tracking techniques are divided into five classes, as shown in figure II.2.

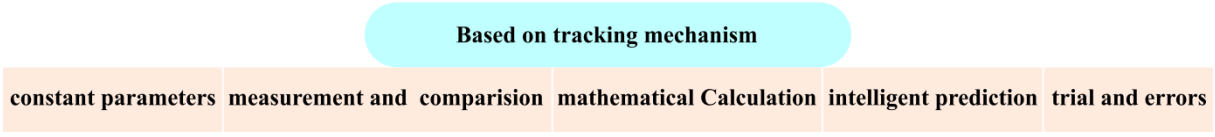

Figure II.2 Categorisation of MPPT based on tracking strategies.

A few of these approaches depend on constant parameters such as Fractional current (FC), Constant voltage (CV), and Fractional voltage (FV) [23] techniques. Others rely on measurement and comparison such as Look-up Table (LT), Linear Current Control (LCC), and Load Current (LC) techniques. Some of these approaches are based on mathematical equations such as Curve Fitting (CF), Current Sweep (CS), and Incremental Conductance (IC) techniques. Many of these methods are based on intelligent prediction such as Fuzzy Logic Control (FLC) [24], Artificial Neural Network (ANN), and Particle Swarm Optimization (PSO) [25]. The last classification is based on trial and errors such as Perturb and Observe (P&O), Array Reconfirmation (AR), and PV-Output Senseless (POS) techniques.

II.2.2 IMPLEMENTATION BASED CLASSIFICATION

Most MPPT algorithms use measurements from the output of the PV module. Using this technique, the output capacity is easily derived from the PV array. In addition, the PV generator output voltage and current are determined and the power is estimated consequently by their multiplication as shown in figure II.3.

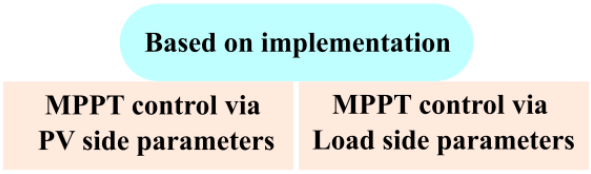

Figure II.3 Classification of MPPT based on application.

II.2.2.1 MPPT ALGORITHMS BASED ON PV SIDE PARAMETERS

Many MPPT techniques use tracking variables from the performance of the PV module. In this method, the output measurement is easily obtained from the PV array as shown in figure II.4.Second, the PV generator voltage and current at the output are determined, and the power is estimated consecutively by their multiplication.

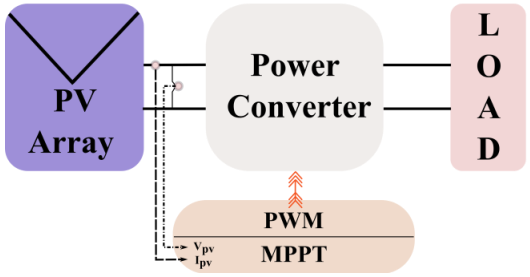

Figure II.4 Control of MPPT through PV side parameters.

II.2.2.2 MPPT ALGORITHMS BASED ON LOAD SIDE PARAMETERS

Such implementation uses measurements at the output of the DC-DC converter as tracking parameters, as shown in figure II.5. As opposed to MPPT control via input parameter control.

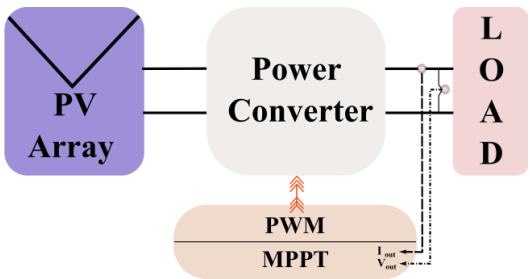

Figure II.5 Control of MPPT through load side parameters.

II.2.3 CLASSIFICATION BASED ON MODERNITY

Conventional approaches are fundamental algorithms that use have been implemented since the first used PV energy generation systems. On the other hand, advanced techniques are methods that use modern and relatively complex algorithms, as shown in figure II.6.

.

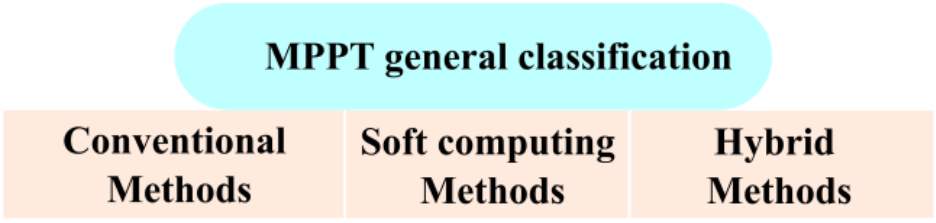

Figure II.6 General classification of MPPT methods.

II.2.3.1 CONVENTIONAL MPPT ALGORITHMS

Various conventional MPPT strategies have been used to seek the one existing MPP under uniform irradiation condition [26]. In this case, the most used techniques are shown in figure II.7.

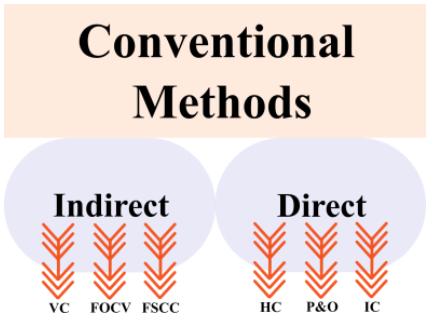

Figure II.7 Conventional Technological Grouping.

II.2.3.1.1 INDIRECT TECHNIQUES

A. MPPT BASED ON CONSTANT VOLTAGE (CV)

The MPPT based on the Constant Voltage (CV) algorithm is the easiest for implementation and has a quick response. Constant voltage methods do not require any measurements or inputs except for PV voltage calculation that allows the PI controller to change the converter duty cycle to hold the PV voltage close to the MPP. In this system, the controller controls the voltage of the PV module and operates near its MPP, matching the output

voltage of the PV module to the constant reference voltage [27]. The Constant Voltage flowchart is shown in figure II.8.

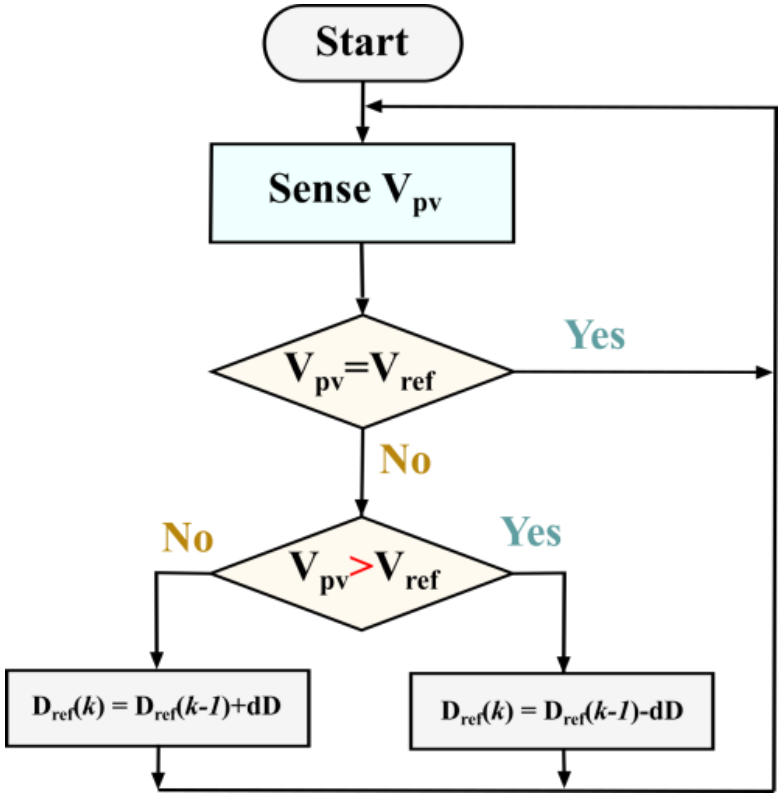

Figure II.8 Constant Voltage Flowchart.

B. FRACTIONAL VOLTAGE (FV) TECHNIQUE

The Fractional Voltage (FV) approach (Figure II.9.) is also one of the simplest MPPT techniques which is based on the principle that the MPP voltage of the PV module and its open-circuit voltage ratio is constant [28].

$$Vmpp = K_v * V_{oc} \quad \text{(II. 1)}$$

Where:

$K_v$is constant and assumes that it changes marginally in solar radiation. For K_v in the range of [0. 7–0. 8].

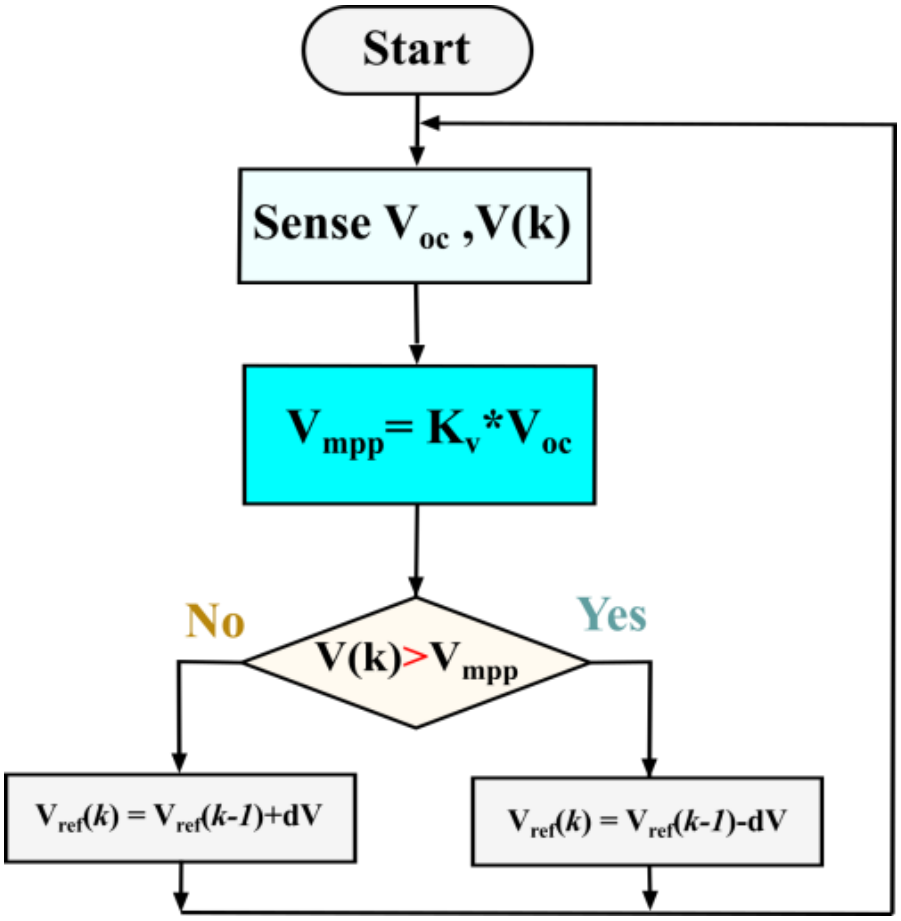

Figure II.9 Fractional Voltage Flowchart.

C. FRACTIONAL CURRENTS (FC) TECHNIQUE

The Fractional current (FC) approach is based on the calculation of the PV module's short circuit current when its voltage output is null, and the overall output current of the PV module at MPP is a direct proportion to its short circuit current [23].

$$Impp = K_i * I_{sc} \quad \text{(II. 2)}$$

Where:

K_i proportionality is constant; the constant is generally found to be between 0.78 and 0.92. The Fractional current flowchart is shown in figure II.10.

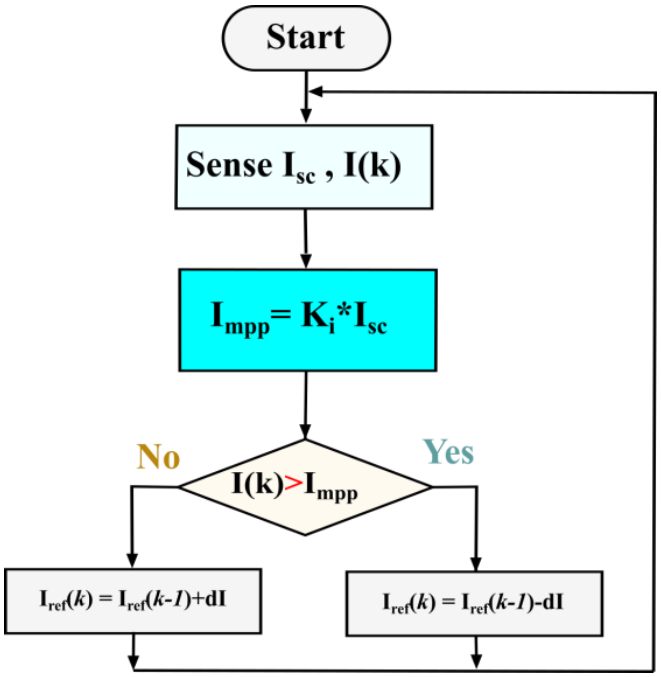

Figure II.10 Fractional current Flowchart.

II.2.3.1.2 DIRECT TECHNIQUES

Summarizing the vast majority of achievements, MPPT methods can be sorted into direct and indirect methods as summarized in. The direct MPPT method is used to describe the algorithm which theoretically doesn't require the math information of the studies system's steady-state operating points. This type of MPPT method presents more robustness, simplicity, and flexibility. These methods almost lie in the principle of the perturb and observe (P&O), or hill-climb search (HCS), which are mathematical optimization techniques used to seek for the local optimum point of a considered function.

A. HILL CLIMBING (HC) TECHNIQUE

Hill Climbing (HC) gets its name from the "hill-shaped" form of the function space [29]. If the algorithm starts at the local optimum (top of the hill), and it moves in any direction, then it will go down. Anywhere else, any axis may be chosen as long as it moves, it will be getting closer to the MPP.

Hill Climbing fails to track the MPP when the function space contains "local maxima". A local MPP is a small hill whose top is not as high as the global MPP. If a local MPP of Hill Climbing is found, the algorithm is trapped there. Any little movement in any direction

will make things temporarily worse. The condition to be verified at the maximum power is given as follows:

$$S = \frac{\Delta P/\Delta d}{P/d} \qquad (II.3)$$

Where S denotes to perturbation step size. The Hill Climbing flowchart is shown in figure II.11.

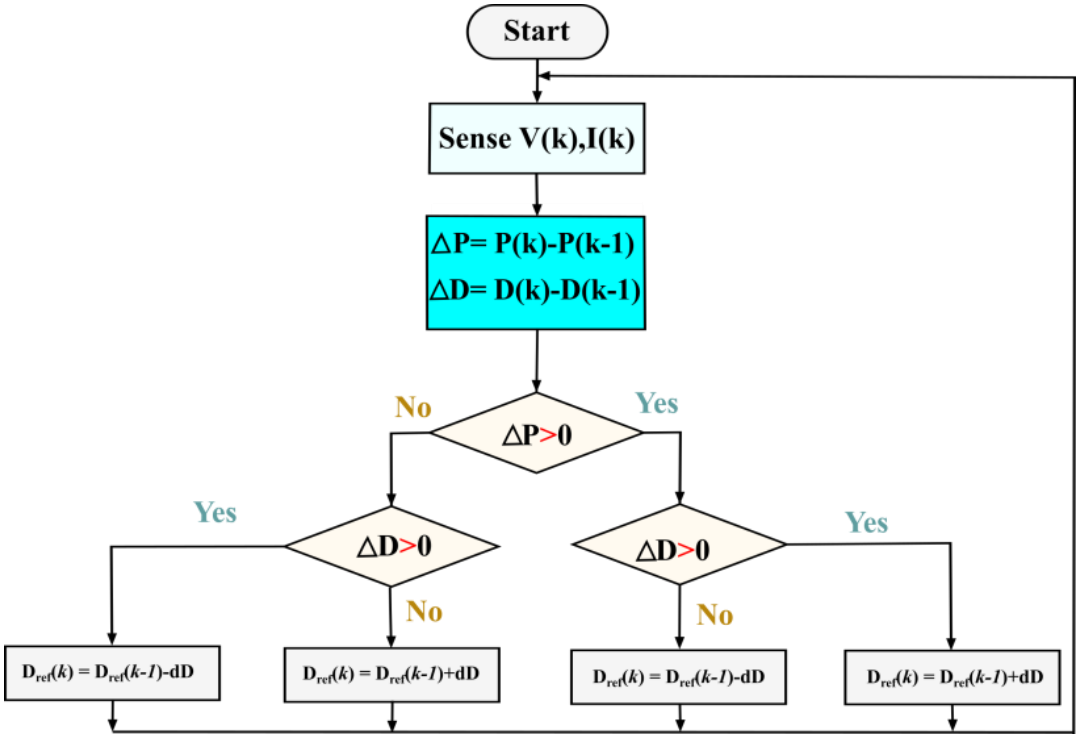

Figure II.11 Hill Climbing Flowchart.

B. PERTURB & OBSERVE (P&O) TECHNIQUE

This method is based on the perturbation of a control variable in small change and observing the target function's resulting response until the slope becomes zero.

The perturbation and observation method's operating process illustrates the movement of the steady-state operating point of the system; the perturbation step-size and the observation time step-size are the considered parameters to be adjusted [30].

The perturbation and observation method with fixed step-size (P&O-F) is one of the most used direct MPPT methods. The output power of the generator is monitored and the inverter input voltage or one of the converter variables are perturbed, such as duty cycle; input current; or input voltage. The condition to be verified at the maximum power is given as follows:

$$\frac{\Delta Ppv}{\Delta Vpv} = 0 \qquad \text{(II. 4)}$$

Where Vpv and Ppv are the PV module voltage and power respectively. The Perturb-and-Observe flowchart is shown in figure II.12.

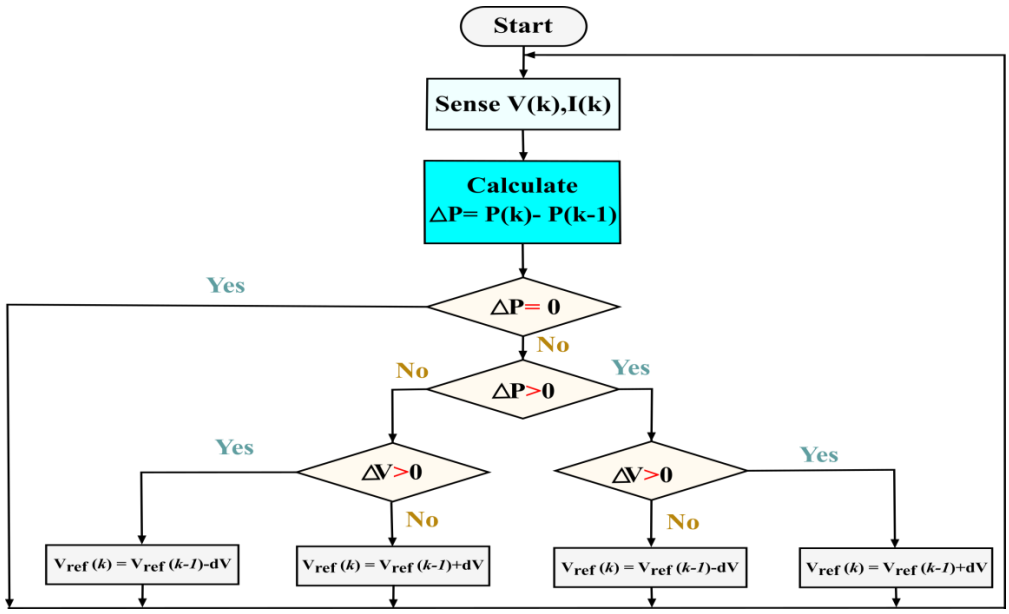

Figure II.12 Perturb-and-Observe Flowchart.

C. INCREMENTAL CONDUCTANCE (IC)

This technique has been discovered for the first time in 1983. The final version of the classical incremental conductance computational flowchart was presented in 1995. In this technique, the controller measures incremental changes in current and voltage of the PV array in order to be able to predict a voltage change effect. This technique requires additional computation time in the controller, however, it can track more rapidly changing conditions when compared with the perturb and observe (P&O) method. It is similar to the P&O algorithm for the fact that it can generate steady-state oscillations in the produced power. The condition to be verified at the maximum power is given as follows [31]:

$$\frac{dI}{dV} + \frac{I}{V} = 0 \qquad (II.5)$$

Where *I* is the PV array current. The Incremental Conductance flowchart is given in figure II.13.

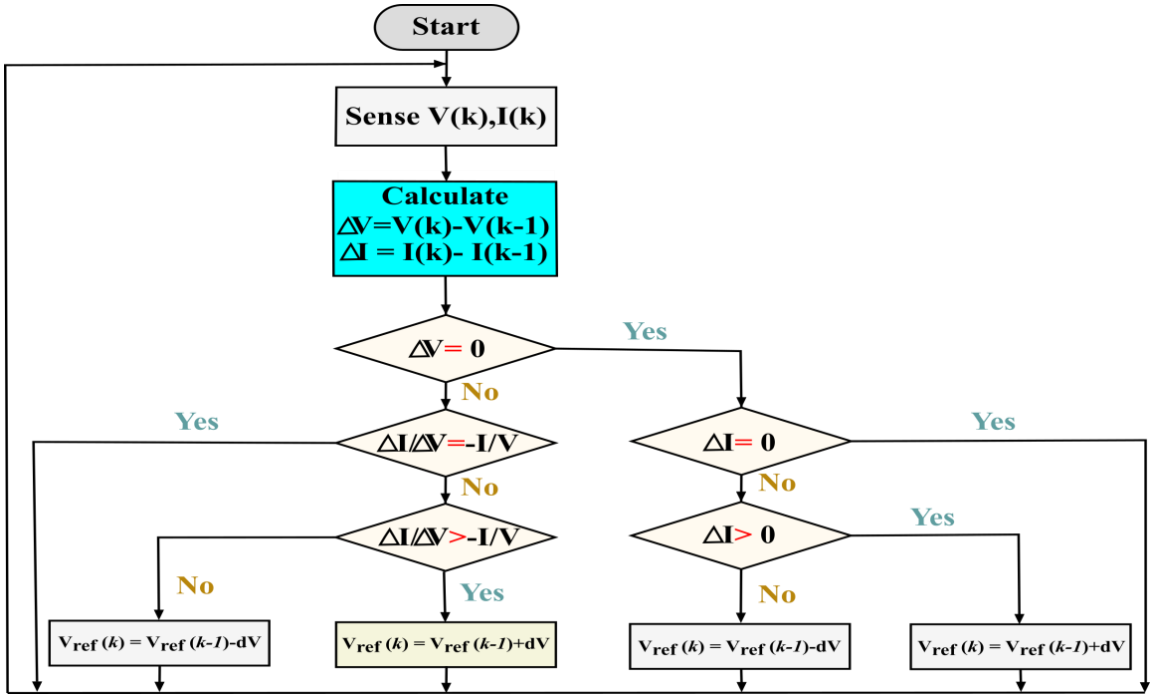

Figure II.13 Incremental Conductance Flowchart.

II.2.3.2 SOFT COMPUTING (SC) MPPT TECHNIQUES

Soft-computing is an approach used to construct computational intelligent systems [32], it encompasses a group of unique methodologies which provide flexible information processing characteristics able to solve complex optimization problems as shown in figure II.14.

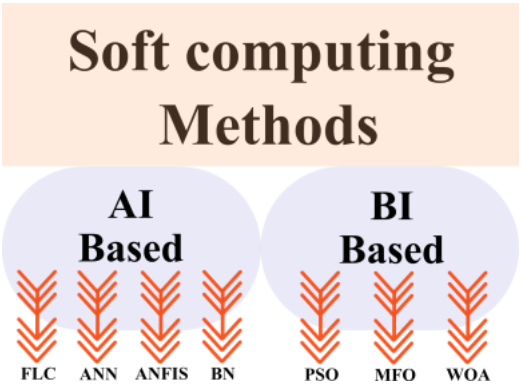

Figure II.14 Soft computing Technological Grouping.

II.2.3.2.1 MPPT TECHNIQUES BASED ON ARTIFICIAL INTELLIGENCE (AI)

A. FUZZY LOGIC CONTROL (FLC) TECHNIQUE

Initially, the theory of fuzzy logic (FL) has been known to be a well-established technique. Fuzzy logic has been used as an application for the first time in 1970 for decision support in medicine, and steam boiler fuzzy regulation in 1975 by Mamdani. A major uncertainty treatment has been initiated by fuzzy set theory, which results in advanced information systems formalization. It also has a considerable impact on modern automatic classification techniques and the renewal of some decision support approaches [33].

The words of the current language are used in fuzzy logic as values of truth, for this reason is called linguistic logic in which a combination of symbolic and digital data processing can be found.

Intelligent diagnosis may be designed using fuzzy logic-based methods based on natural language expressed knowledge. It is also human reasoning, not rigid calculations modeled approach. It is characterized by a reasoning mode that is more intuitive than conventional logic. The use of set rules and membership functions called "fuzzy sets" allows users to better understand physical phenomena, difficult and inaccurate to model otherwise. Industrial control systems use frequently fuzzy logic. The resulting control law is often effective and does not require significant theoretical-based developments. The structure of Fuzzy Logic-based Control is shown in figure II.15.

$$E(k) = \frac{P(k) - P(k-1)}{V(k) - V(k-1)} \quad \text{(II. 6)}$$

$$\Delta E(k) = E(k) - E(k-1) \quad \text{(II. 7)}$$

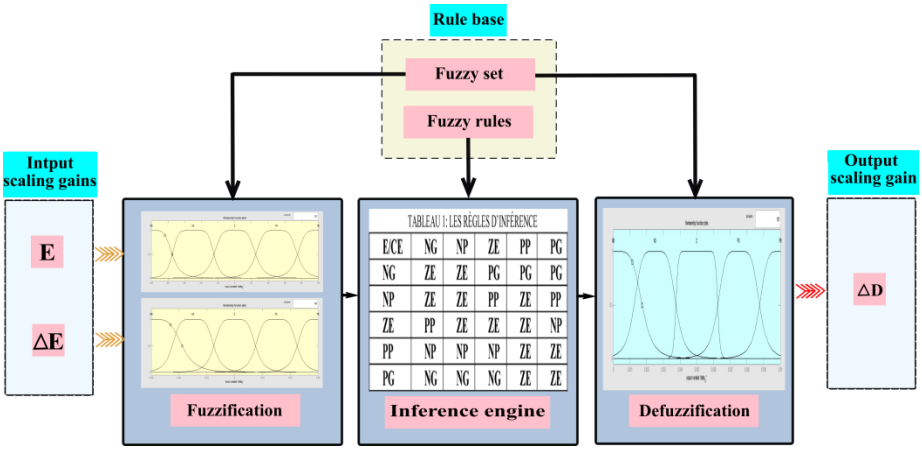

Figure II.15 Fuzzy Logic Control structure.

B. ARTIFICIAL NEURAL NETWORK (ANN)

Artificial Neural Network is composed of simple elements (usually Adaptive) massively connected in parallel with the hierarchical organization. They try to mimic biological nervous systems in their interaction with objects of the Real-world. In addition, ANN performs the algebraic function of its inputs. The ANN may be modeled by using a graph-oriented and by using connections for the interconnection of neurons and the information exchange. The calculation will be carried out in a cooperative, parallel, and distributed and approach [34].

The neural network is essentially characterized by its topology which consists of the choice of the transfer function and learning modes and type of interconnection. The neurons that construct the network characterize the structure of the model, a distributed representation in which each neuron contributes. They can be used in industrial equipment supervision problems. The fault-tolerance properties of neural networks are defined by their capacity to maintain their processing ability in the presence of network damage and execute the assigned task in the presence of information with errors. The structure of an ANN is shown in figure II.16.

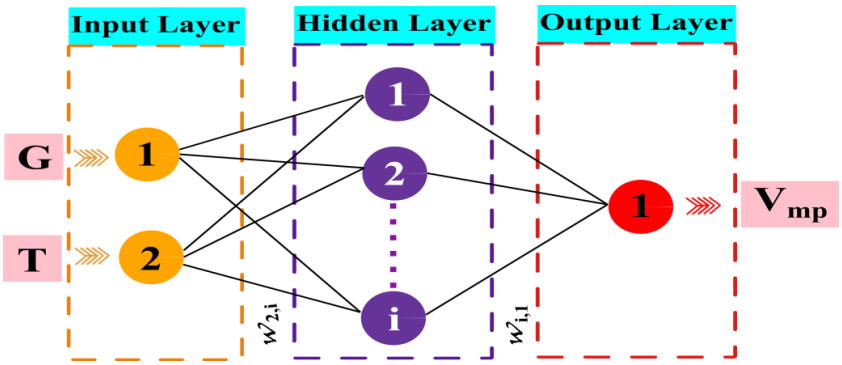

Figure II.16 Artificial Neural Network structure.

C. ADAPTIVE NEURO FUZZY INFERENCE SYSTEM (ANFIS)

Adaptive Neuro-Fuzzy Inference System (ANFIS) is implemented as part of adaptive networks fuzzy inference systems which use a hybrid learning technique. Its architecture adjusts the human expert's fuzzy rules in order to describe the input/output relationship of complex systems. ANFIS is known to give better trajectory tracking, dynamic control, signal processing, and nonlinear approximation.

In addition, when ANN and ANFIS are compared, the ANFIS algorithm gives a lower mean percentage error when compared with the one generated by ANN. ANFIS is also characterized by better performance and a learning capacity that is faster than ANN. In the case of using the largest number of inputs, ANFIS has the property of increasing the forecasting data accuracy [35]. ANFIS is a combination of data-driven and knowledge-oriented methods. In the case of prognostics based on ANFIS, a data-driven method, a stream from multidimensional data to the output is noted. The ANFIS structure is shown in figure II.17.

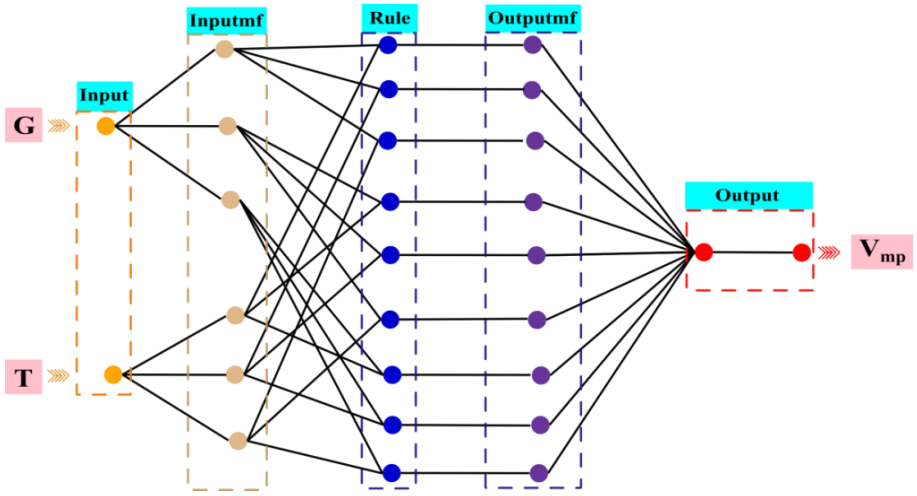

Figure II.17 Adaptive Neuro-Fuzzy Inference System structure.

D. THE BAYESIAN NETWORK (BN)

The Bayesian Network (BN) is a technique used to model multiple random variables probability distributions which is used in information fusion [36]. Bayesian Networks are used in literature to detect the correct movement direction of the actual output voltage of PV arrays. In order to verify the objective of operating at the MPP, the Bayesian Network flowchart is shown in figure II.18.

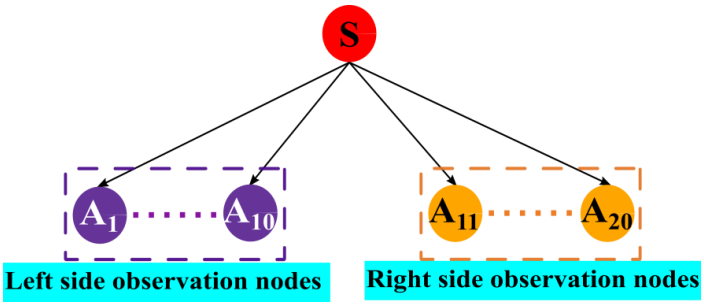

Figure II.18 Bayesian Network structure.

II.2.3.2.2 MPPT TECHNIQUES BASED ON BIO-INSPIRED (BI)

A. PARTICLE SWARM OPTIMIZATION (PSO)

PSO is a method of the large family of swarm intelligence and which mimics the social behavior and collaboration between individuals often referred to as particles [25], [37]. The analysis of the environment and the neighborhood describe the social behavior and therefore constitutes an optimum search method by analyzing the trends of neighboring particles. Each particle has the objective to optimize its chances by following the tendency of its neighborhood, which it moderates by its own experience. The algorithm is usually initialized randomly and possible solutions are randomly positioned in the objective function search space. The PSO central concept is that particles have acceleration in the direction of the best solutions [38]. They iteratively assess the suitability of candidate solutions and have a history of their best fitness value. Each particle has the property to communicate with the particles around it and has a memory of its best-visited solution. The particles move at each iteration considering their best position and the neighbor's best position. The objective is to change their trajectory so that they converge to the optimum. The processes of intelligence and movement in a dynamic system result in an optimal operating point. The PSO priorities cooperation over competition and without selection. A

particle that has poor performance at a given iteration is preserved in case it will find the best solution. According to some literature results, this technique does not have problems found in other evolutionary techniques. The flowchart of PSO is shown in figure II.19 (a).

B. WHALE OPTIMIZATION ALGORITHM (WOA)

This technique tries to mimic the bubble net hunting algorithm of humpback whales presented in [39], [40], [41]–[46]. The biggest of all whales is called Humpback which has a spiral bubble-net feeding special hunting mechanism. By generating distinctive bubbles in a circular trajectory, the whales haunt the school of krill or fishes on the surface. During the behavior of hunt and encircling, the prey is encircled by Humpback whales. The flowchart of the WOA is shown in figure II.19 (b).

C. MOTH-FLAME OPTIMISATION (MFO)

Moth-flame Optimization is based on the behavior of the moth which depends on the process of transverse orientation [47], [48], [49]–[59]. The heterocerus chase the flames which are considered the best positions of the moth, MFO begins with the random initialization of moth and flames populations. The main function of the MFO is to move the moth in search spaces to reach the flames [60]–[63]. A logarithmic spiral mechanism is used to update the position of the moth until the termination criterion is met. MFO is based on the movement of two populations which are moth and flames in search space. The flowchart of the MFO is shown in figure II.19(c).

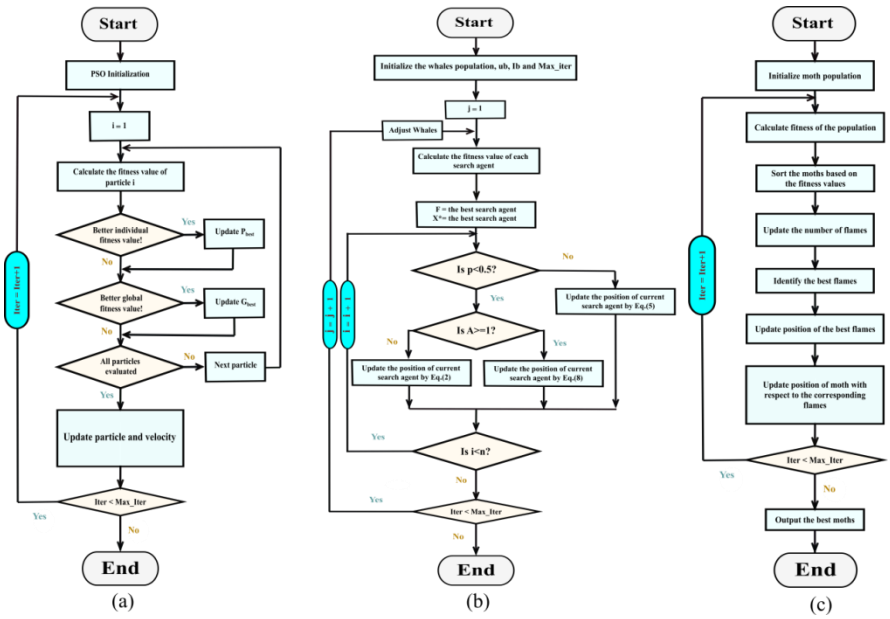

Figure II.19 Flowchart (a) PSO, (b) WOA, (c) MFO.

II.2.3.3 HYBRID MPPT TECHNIQUES

Hybrid MPPT techniques are the combination of conventional/conventional or soft computing /soft computing or conventional/soft computing as shown in figure II.20.In order to handle the partial shading conditions (PSCs) and track the Global peak (GP) accurately and efficiently. There are many variations in such combinations between different approaches[64]. In this work, an example has been selected for each hybrid category in order to illustrate the principles of hybridization.

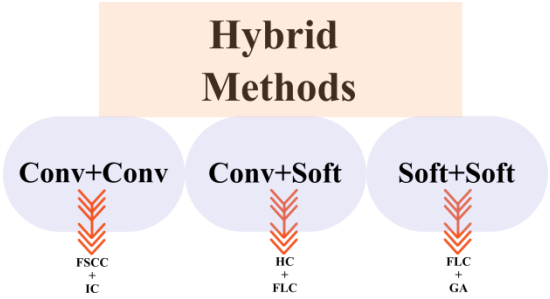

Figure II.20 Hybrid Technological Grouping.

II.2.3.3.1 CONVENTIONAL WITH CONVENTIONAL (CV/CV)

In this combination, individual conventional techniques are associated in order to achieve a common objective with enhanced performance.

A. FRACTIONAL CURRENT (FC) WITH INCREMENTAL CONDUCTANCE (IC)

The combination of the Fractional current approach and the Incremental Conductance method ensures a rapid and effective track of the MPP [65]. The FC/IC combination technique is shown in figure II.21.

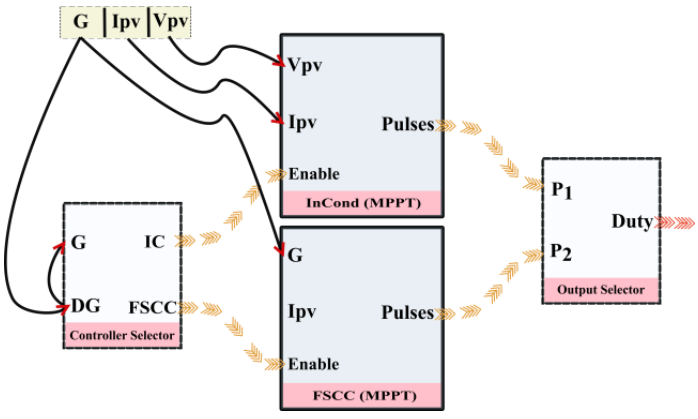

Figure II.21 Hybrid Maximum Power Point Tracking controller [65].

II.2.3.3.2 SOFT COMPUTING WITH SOFT COMPUTING (SC/SC)

Soft computing includes artificial intelligence techniques and bio-inspired algorithms which have different capabilities for searching solutions to complex problems. The combination of different approaches allows adding capacities from one domain to another to achieve a common objective.

A. FUZZY LOGIC CONTROL WITH GENETIC ALGORITHM (FLC/GA)

In [66], a Fuzzy Logic Control has been combined with some Soft computing, like the Genetic Algorithm [67]. The FLC with GA combined is shown in figure II.22.

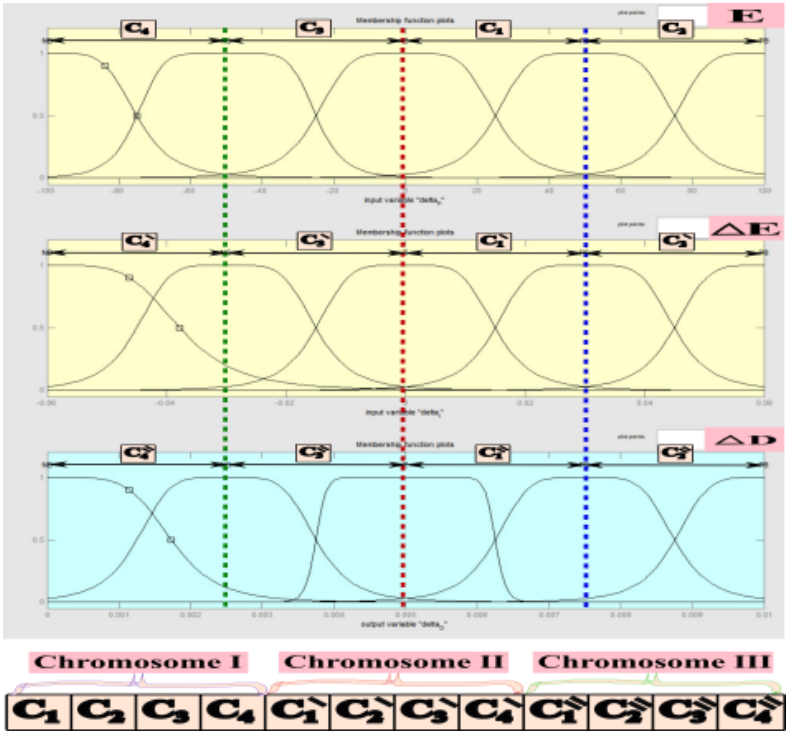

Figure II.22 Membership functions coded with Genetic Algorithm [66].

II.2.3.3.3 CONVENTIONAL WITH SOFT COMPUTING (CV/SC)

The gradual search of conventional techniques in the true seeking of MPP alleviates the drawbacks of soft computing techniques by solving issues related to the gradual variation of climatic conditions.

A. HILL CLIMBING WITH FUZZY LOGIC CONTROL (HC/ FLC)

In [68], HC has been combined with the Fuzzy Logic Control Soft computing technique. The HC/FLC combination flowchart is given in figure II.23.

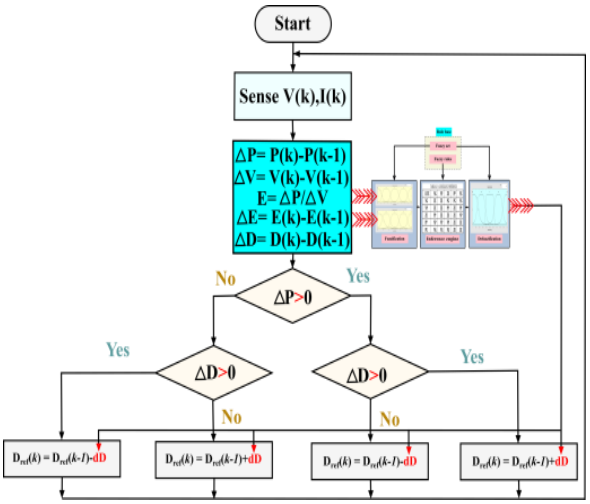

Figure II.23 Hill-Climbing with Fuzzy Logic Control [68].

A summary of the classified MPPT techniques is given in Table II.2.

Table II.2 Comparison of MPPT techniques

MPPT TECHS			COMPLEXITY	EFFICIENCY	CONVERGENCE SPEED
CONVENTIONAL	INDI	**CV**	Low	Low	Low
		FV	Low	Low	Medium
		FC	Medium	Low	Medium
	DIR	**HC**	Low	Low	Low
		P&O	Medium	Low	Medium
		INC	Medium	High	Fast
SOFT COMPUTING	(A-I)	**FLC**	High	High	Fast
		ANN	High	High	Fast
		ANFIS	High	High	Fast
		BN	High	High	Fast
	(B-I)	**PSO**	Medium	Very High	Medium
		WAO	Medium	Very High	Medium
		MFO	Medium	Very High	Medium

From the conducted research on optimization algorithms and their applications, we became aware of conventional approaches that include true seeking methods. The latter are based on gradual perturbation of the operating point and the calculation of mathematical quantities to decide the next direction of the perturbation of the P-V curve. The indirect methods are based on approximations of the maximum power point using known values such as open-circuit voltage or short circuit current. Modern MPPT techniques have been introduced to overcome drawbacks found in conventional approaches such as steady-state oscillations, rapid change in climatic conditions, or the presence of an irradiation mismatch along with PV panels. Artificial intelligence-based techniques use approximate reasoning and human brain processing architectures in order to construct trained structures able to estimate the optimal operating point at the actual climatic conditions. Bio-inspired MPPT algorithms have known increasing use to solve mismatching issues in PV arrays which

adds the functionality of using a multi-agents searching strategy that allows the convergence to the global MPP in the presence of multi-peak P-V characteristic curve. It has been shown in the literature that metaheuristic optimization-based MPPT algorithms are efficient in all operating conditions including partial shading. The MFO based MPPT is considered the best performing algorithm.

II.3 CONCLUSION

Extracting the maximum power of the PV system is recently becoming the spotlight in the solar energy sector. While PV power capacity increases continuously with newly installed PV stations, Maximum Power Point Tracking MPPT control techniques keep developing. Different MPPT techniques have been revised and discussed earlier in this Chapter, and the characteristics of these techniques have been analyzed to give a better understanding of each MPPT technique and its impact on the system performance. Based on this review, it can be concluded that the bio-inspired Maximum Power Point Tracking algorithms, especially, when these methods have been hybridized between them by taking advantage of each one, will help to construct a perfect algorithm for the Maximum Power Point Tracking search problem.

CHAPTER III

A DYNAMIC PERFORMANCE EVALUATION OF THE PV SYSTEM

CHAPTER III

III.1 INTRODUCTION

The output power of Photovoltaic (PV) energy generation systems depends mainly on operating conditions that include climatic conditions and occurrence of faults as shown in Figure Current-Voltage characteristic curves show different operating regions that are characterized by different transient responses in varying operating conditions and in the special case of the presence of the partial shading condition. Dynamic performance evaluation of the PV system is performed both in open loop and in the presence of a feedback controller.

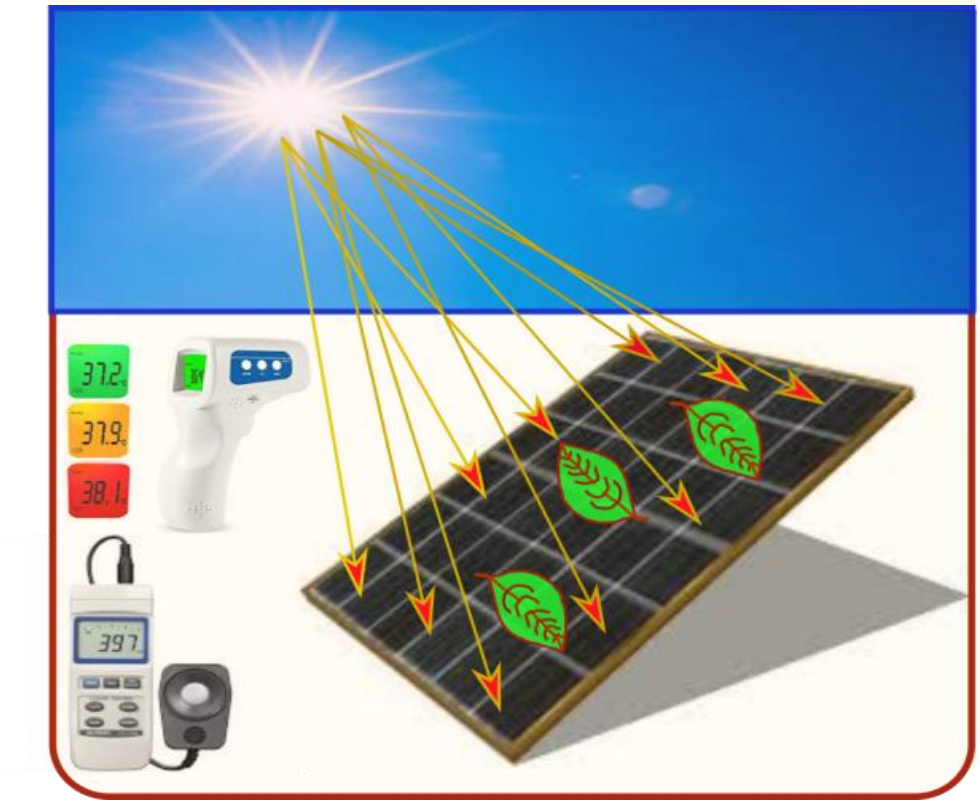

Figure III.1 Understanding the characteristics of a solar panel.

III.2 PV ARRAY CHARACTERISTIC CURVES

The PV array is usually characterized by its Current-Voltage (I-V) and Power -Voltage (P-V) relationships. Different operating regions could be shown and the effect of environmental conditions could be illustrated as well [69].

The PV array is composed of PV panels connected in series and in parallel to provide adequate voltage and current according to the load requirements. Panels connected in series (figure III.2) are used to identify the influence of the environmental conditions on the operating regions. The equivalent electric circuit model of the PV array is depicted in figure III.3.

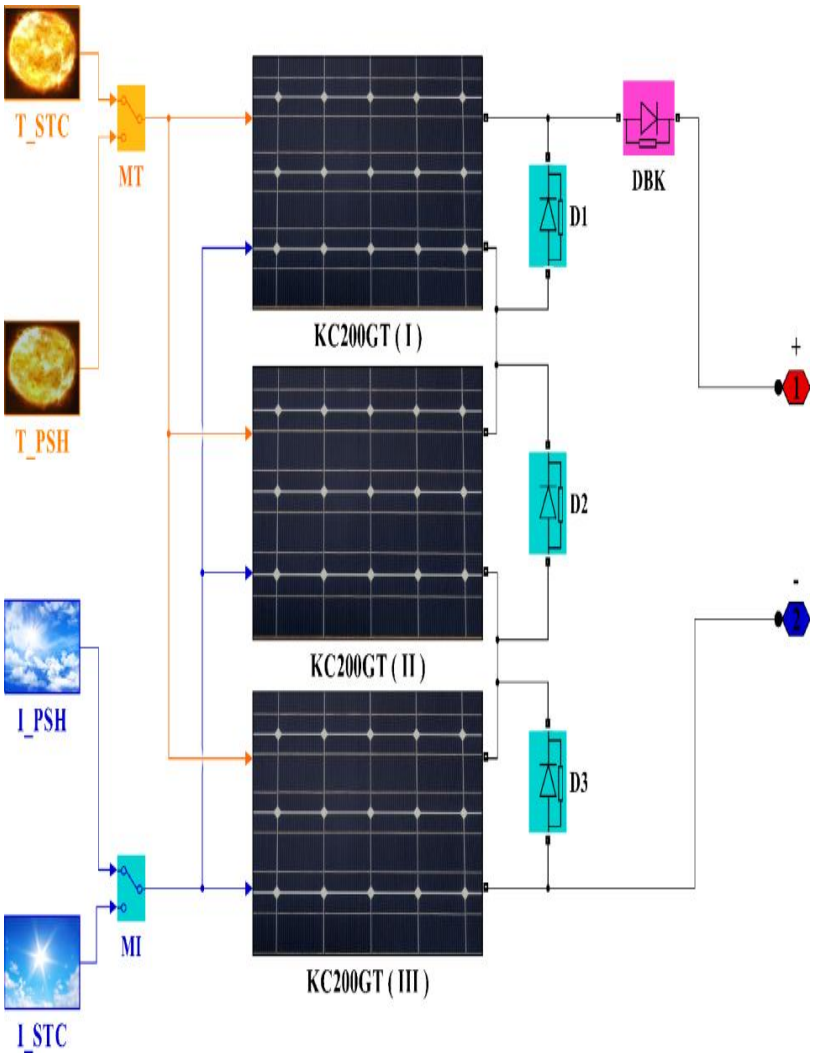

Figure III.2 PV array used to illustrate the effects of varying environmental conditions.

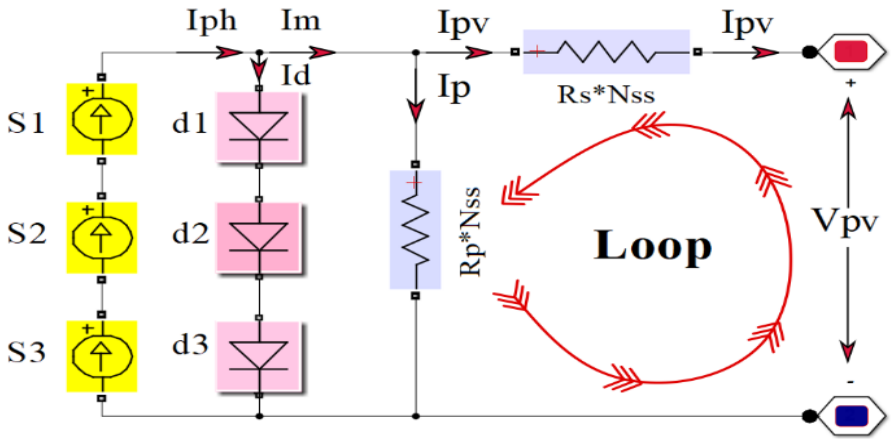

Figure III.3 Equivalent electric circuit of the used PV array.

The output current of the PV array is given by equations. (III.1-6):

$$Ipv = Im - Ip \quad \text{(III.1)}$$

$$Im = Iph - Id \quad \text{(III.2)}$$

$$Ip = \frac{Vpv + IpvRsNss}{RpNss} \quad \text{(III.3)}$$

$$Ipv = Iph - Id - \frac{Vpv + IpvRsNss}{RpNss} \quad \text{(III.4)}$$

$$Iph = (Iph,n + K_I \Delta T)\frac{G}{G_n} \quad \text{(III.5)}$$

$$Id = Io\left[\exp\left(\frac{Vpv + IpvRsNss}{aV_tNss}\right) - 1\right] \quad \text{(III.6)}$$

Where *Nss* represents the number of panels connected in series (03 in the present study), *Rs*, *Rp* the series and parallel resistances of the PV panel, respectively. The photocurrent I_{ph} depends on the irradiation *G* and Temperature *T* as shown in equation III.5. *Iph,n* is the nominal generated current (given at nominal conditions: $T = 25\ °C$ and $G = 1000\ W/m^2$), K_I is the short-circuit current/temperature coefficient, $\Delta T = T - T_n$ (*T* and T_n are the current and nominal temperatures), *G* and G_n are the current and nominal irradiations. I_d the current in the diode as shown in equation III.6. *Io* the reverse saturation current, *a* is the diode ideality constant, *Vt* is the thermal voltage of the PV array.

The characteristic curve of the PV has been identified for the first time to include two distinctive operating regions namely current and voltage source regions as in [70] and four (04) operating regions with additional Power region I and II as in [71]. The suitable classification to Maximum Power Point Tracking algorithms is the three (03) regions

proposed in [72], where the characteristic curve is sub-devised into the current source, power and voltage source regions.

figure III.4 shows the operating regions of the PV array at Standard Test Conditions (STC) using the PV panel with the characteristics given in Table III.1(appendix B). The I-V characteristic curve presents three (03) operating regions that include the current source region characterized by almost constant current, power region characterized by constant power and voltage source region characterized by almost constant voltage.

Temperature Variations induce a change in the open circuit voltage of the PV array as shown in figure III.5 (a) which in turn have a major impact on the constant voltage and power regions. Irradiation changes affect mainly the short circuit current and a slight change is noticed in the open circuit voltage. The irradiation change also modifies largely the constant current and power regions as shown in figure III.5 (b).

The major impact on all operating regions is noticed when the partial shading condition is introduced. The partial shading condition creates several patterns of superposed I-V curves with a repetitive current source and power regions terminating by a voltage region in the vicinity of the open circuit voltage operating point as shown in figure III.5 (c).

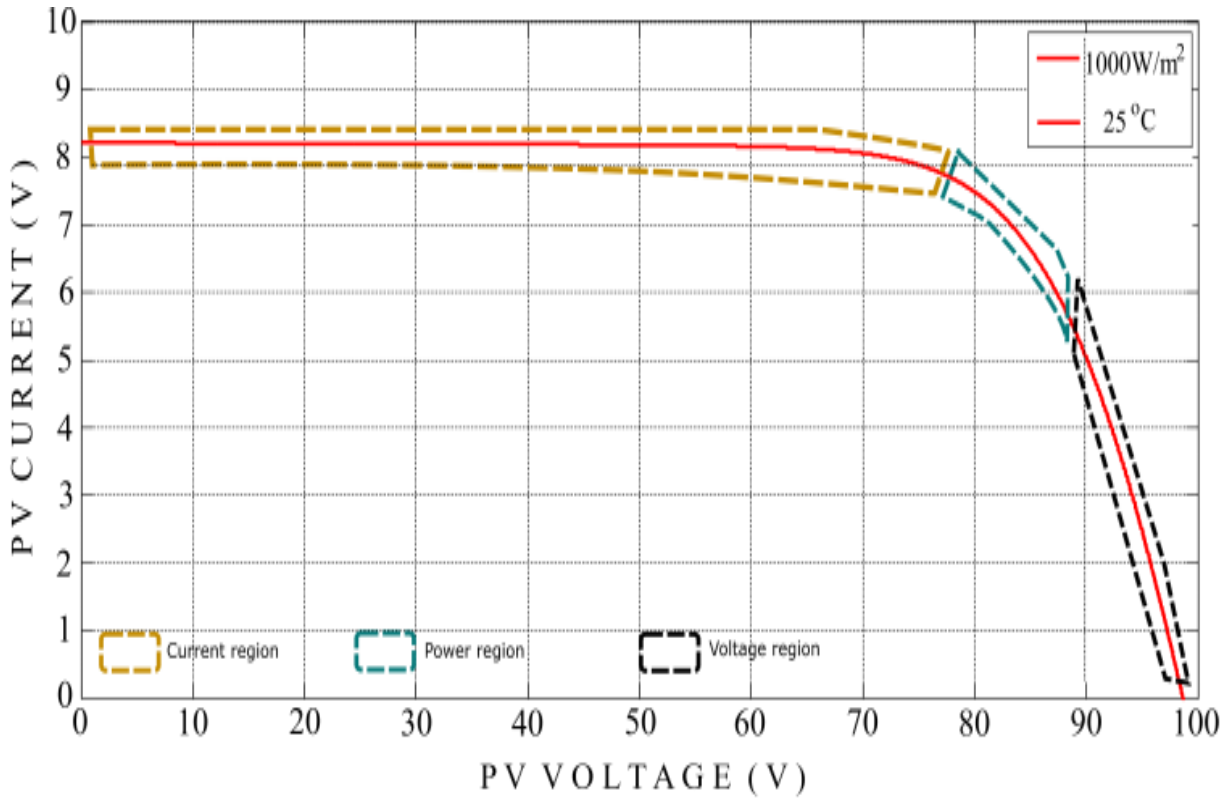

Figure III.4 Operating regions of PV array at STC.

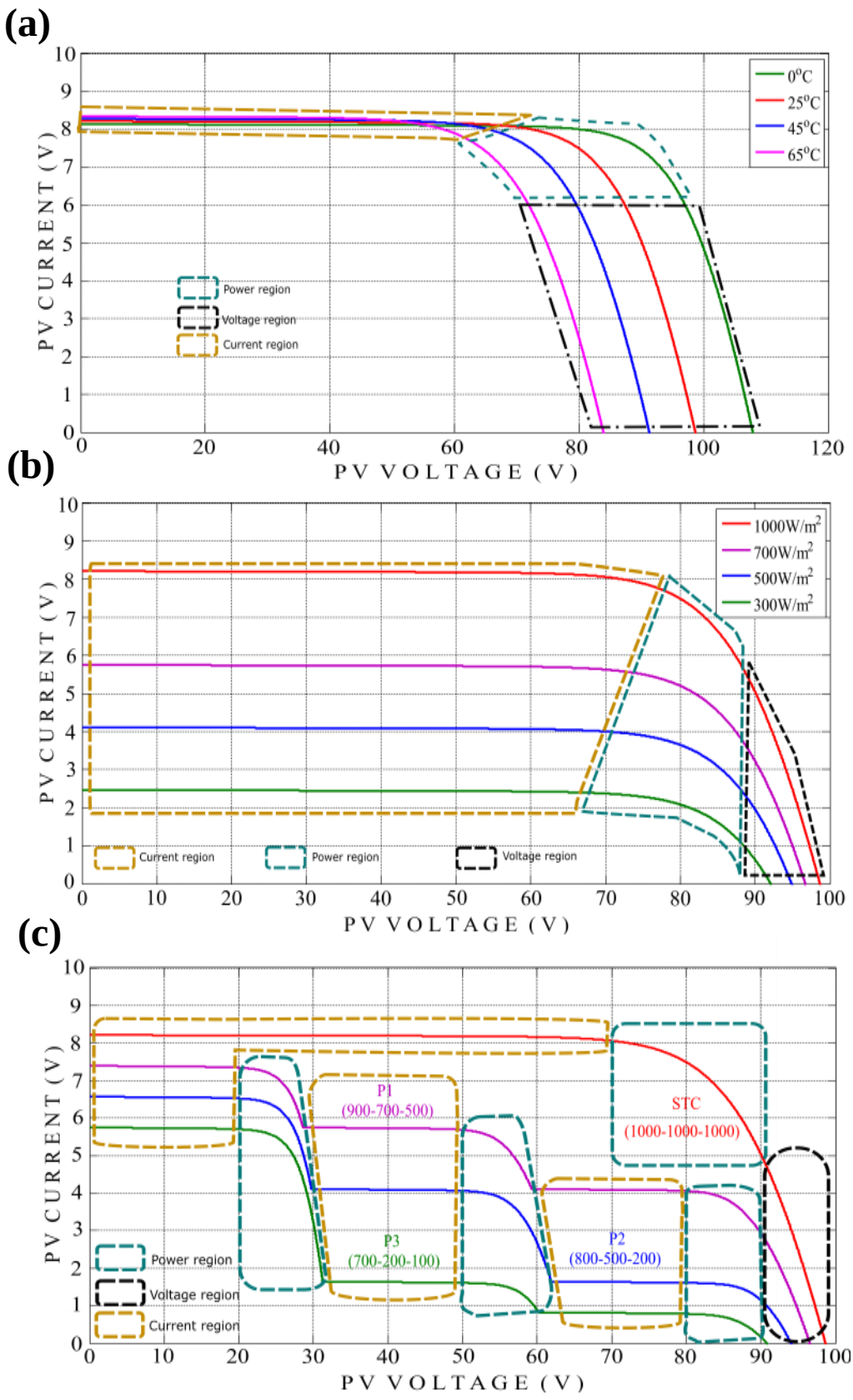

Figure III.5 Operating regions of PV array at different operating conditions:

(a) variation of temperature, (b) variation of irradiation, (c) partial shading.

Table III.1 Kyocera KC200GT PV panel characteristics at STC(appendix B).

Maximum power, P_{max}	200 W (+10%/-5%)
Open circuit voltage,V_{DC}	32.9 V
Short circuit current, I_{SC}	8.21 A
Temperature coefficient of current, K_i	3.18e-3 A/°C
Temperature coefficient of voltage, K_v	-1.23e-1 V/°C
Maximum power voltage	26.3 V
Maximum power current	7.61 A

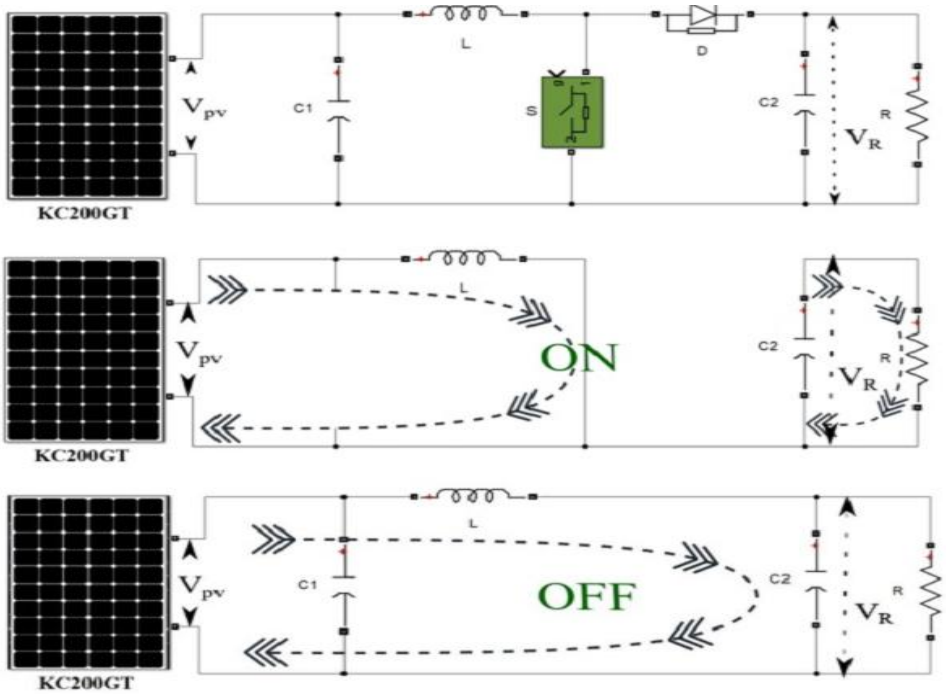

Figure III.6 Association PV array/boost DC-DC converter and its operation.

III.3 PV ARRAY DYNAMIC PERFORMANCE EVALUATION

III.3.1 OPEN LOOP RESPONSE OF PV ARRAY/BOOST DC-DC CONVERTER

In order to show the effect of the operating condition on the photovoltaic energy generation system, the PV array is associated with a boost DC-DC converter as shown in figure III.6 in which its operation is also illustrated(appendix C). The association PV array/boost DC-DC converter is then evaluated in an open loop scheme as illustrated in figure III.7 using the duty cycle presented in figure III.8 under variations of temperature and irradiation in addition to the case of the presence of partial shading.

It can be noted that the open loop response in the case of a change in temperature or irradiation has minor changes on the responses in each operating region (figure III.9 and figure III.10). However, the change in the shape of the response in terms of overshoot and response time is noticeable in the case of the partial shading condition as shown in figure III.11.

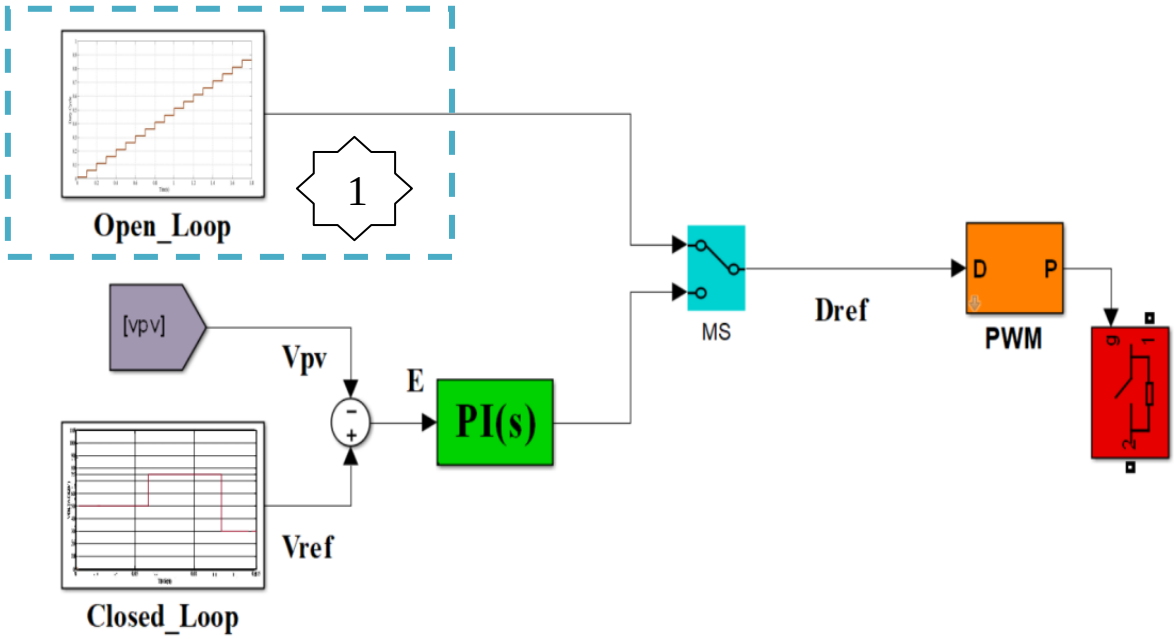

Figure III.7 Association PV array/boost DC-DC converter (Open Loop).

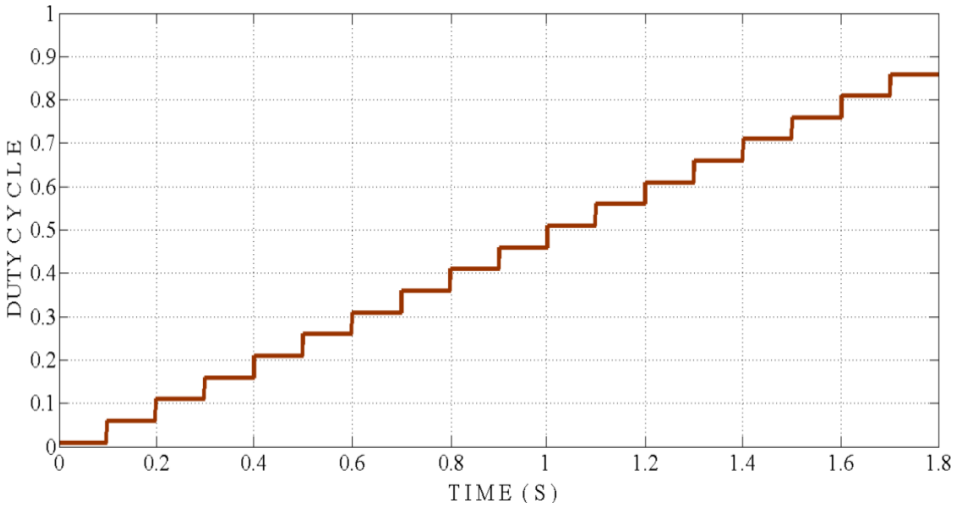

Figure III.8 Duty cycle evolution used to drive the open loop response of the association PV array/boost DC-DC converter.

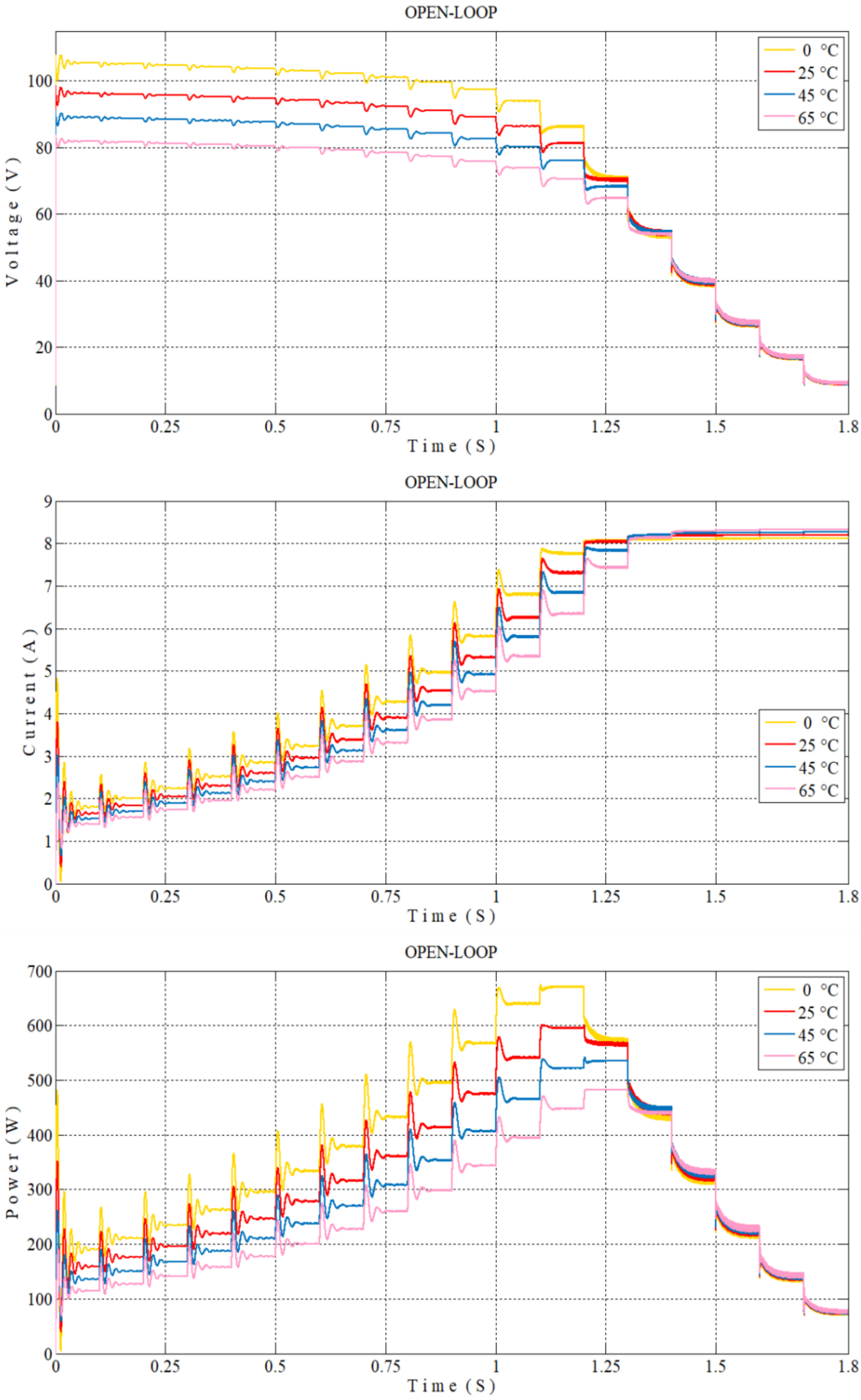

Figure III.9 Open loop response to variation of temperature.

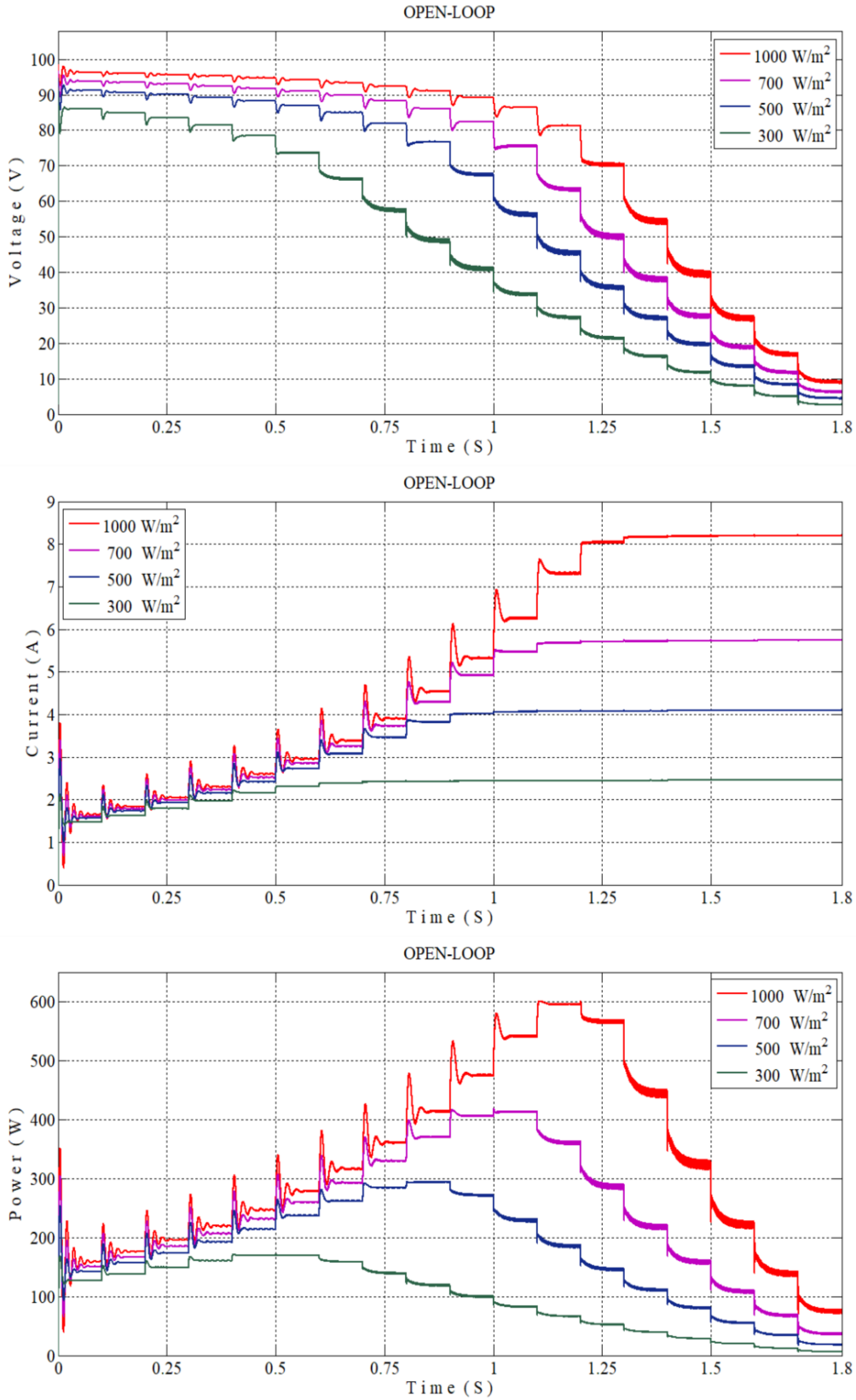

Figure III.10 Open loop response to variation of irradiation.

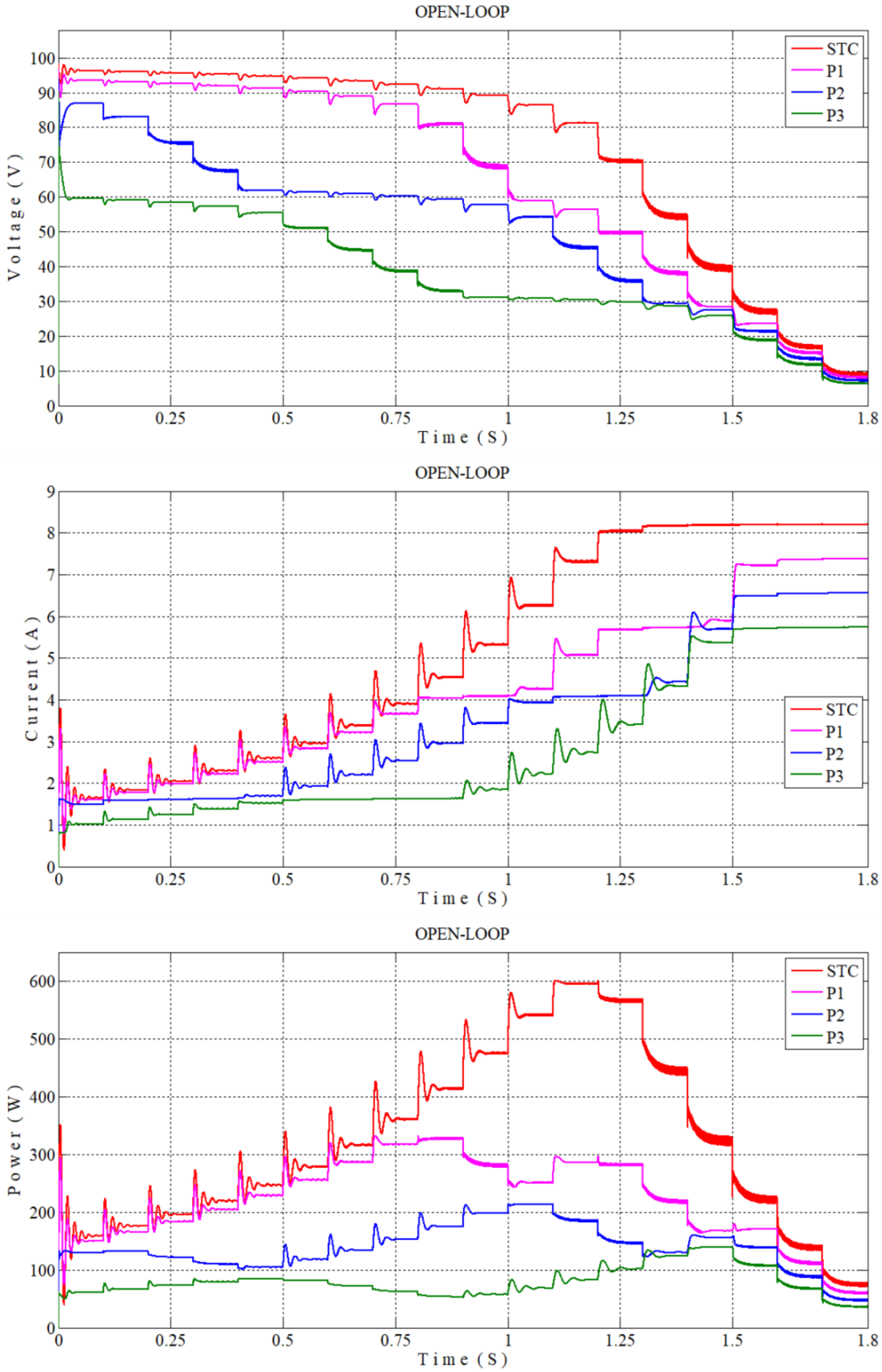

Figure III.11 Open loop response at partial shading.

III.3.2 CLOSED LOOP RESPONSE OF PV ARRAY/BOOST DC-DC CONVERTER

The PV energy generation system shown in figure III.12 is controlled using PV voltage and a Proportional Integral (PI) controller as shown in figure III.12. The reference voltage used to evaluate the PV system at various operating regions is shown in figure III.13. In addition temperature variation has been introduced which results in a change of overshoot as shown in figure III.14 (a). The change in irradiation increases the time response as shown in figure III.14 (b). The partial shading affects the response of the PV system in an unpredicted effect as in figure III.14 (c).

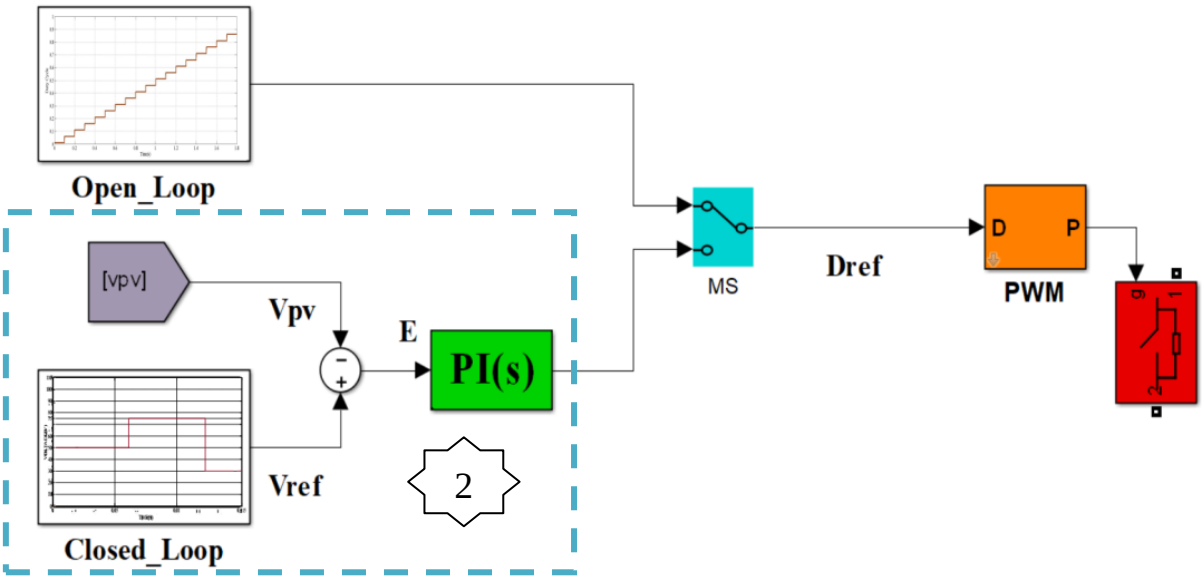

Figure III.12 Association PV array/boost DC-DC converter and its operation (Closed Loop).

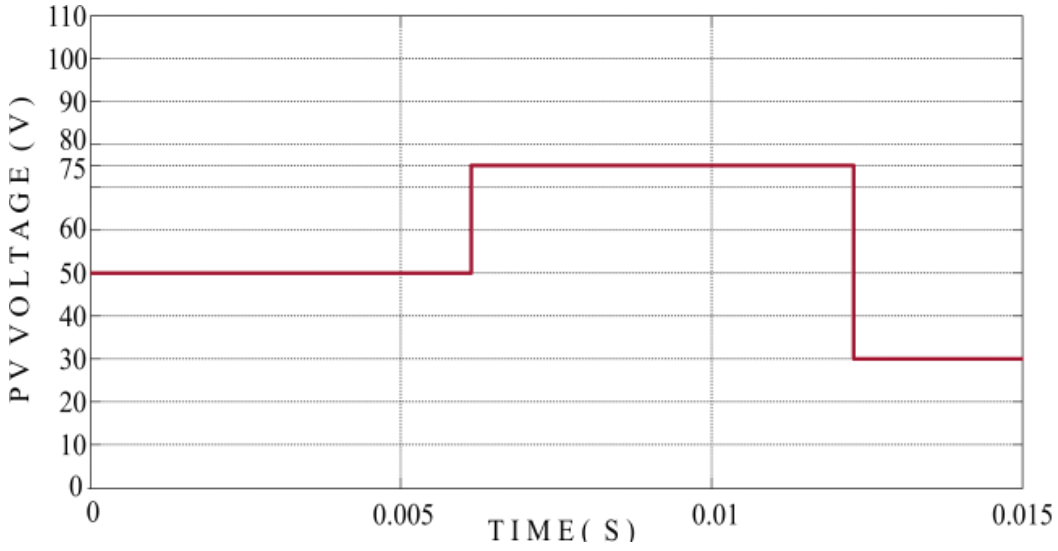

Figure III.13 Closed loop response of association PV array/DC-DC converter along the characteristic curve: Voltage reference

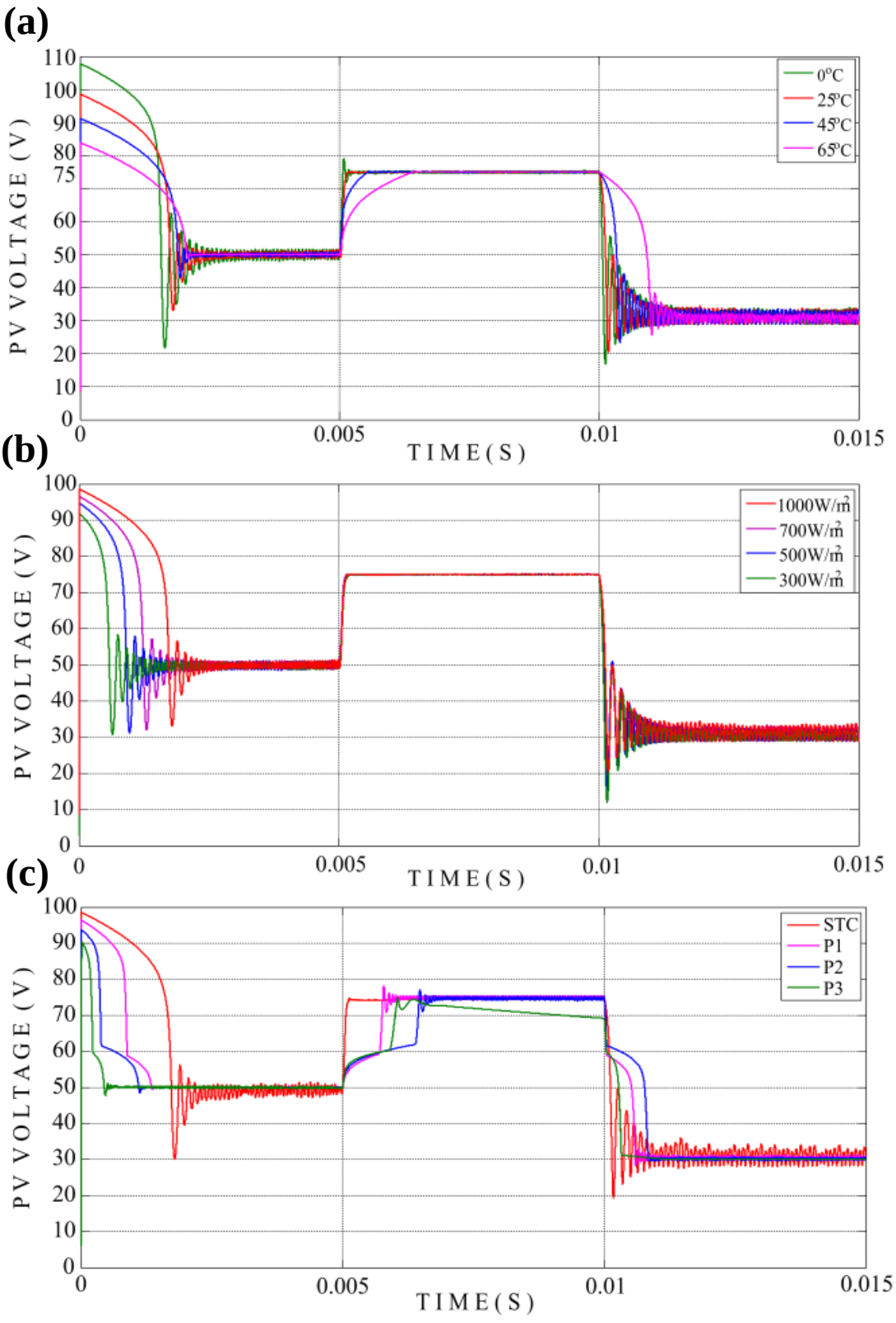

Figure III.14 Closed loop response of association PV array/DC-DC converter along the characteristic curve: (b) variation of temperature, (c) variation of irradiation, (d) partial shading.

In figure III.14, The initial voltage is that of the open circuit (Voc) because the boost converter is used as the main power converter. We can also notice that the starting point is influenced by the variation of climatic conditions. Depending on the operating conditions, the convergence of the voltage towards that of the reference takes a considerable time. Oscillations are even present in some cases. The PSH condition clarifies the previous observations in the transient response.

It has been shown in previous research works that PV arrays Power-Voltage characteristic curves are characterized by three operating regions which are multiplied in the case of partial shading occurrence. The mathematical model of PV systems could be affected by the region at which it was introduced. The conventional fixed parameters controller is efficient only in the power region. Analysis of the effect of the climatic conditions on the PV system shows that the transient response gives different behavior at the fixed input and the same environmental conditions. This is mainly due to the existence of multiple models depending on the operating region. In addition, the present research work has shown that controller tuning has a direct effect on the Maximum Power Tracking algorithm performance.

III.4 CONCLUSION

The dynamic performance of PV energy generation systems is affected by the operating region, climatic conditions and the occurrence of unexpected operating conditions such as faults and partial shading. The PV system operation in different regions and with the presence of environmental conditions is characterized by a complex dynamic behavior.

The dynamic response of the PV system, both in open and closed-loop has been identified. Variations in overshoot and response time could be so easily depicted. Such dynamic effects are further noticeable along the characteristic curve when the partial shading condition occurs.

CHAPTER IV

THE PROPOSED STRATEGY, RESULTS AND DISCUSSIONS

CHAPTER IV

IV.1 INTRODUCTION

The MPPT algorithms use controllers to modify the operating point of the PV energy generation system in order to correspond to the generated reference. Different versions of MPPT are found in the literature with various choices of the tracking variable [73]. Figure IV.1 shows some of the variants for the choice of controlled variable that include open loop duty cycle (figure IV.1 (a)), voltage (figure IV.1 (b)) and current (figure IV.1 (c)) regulation.

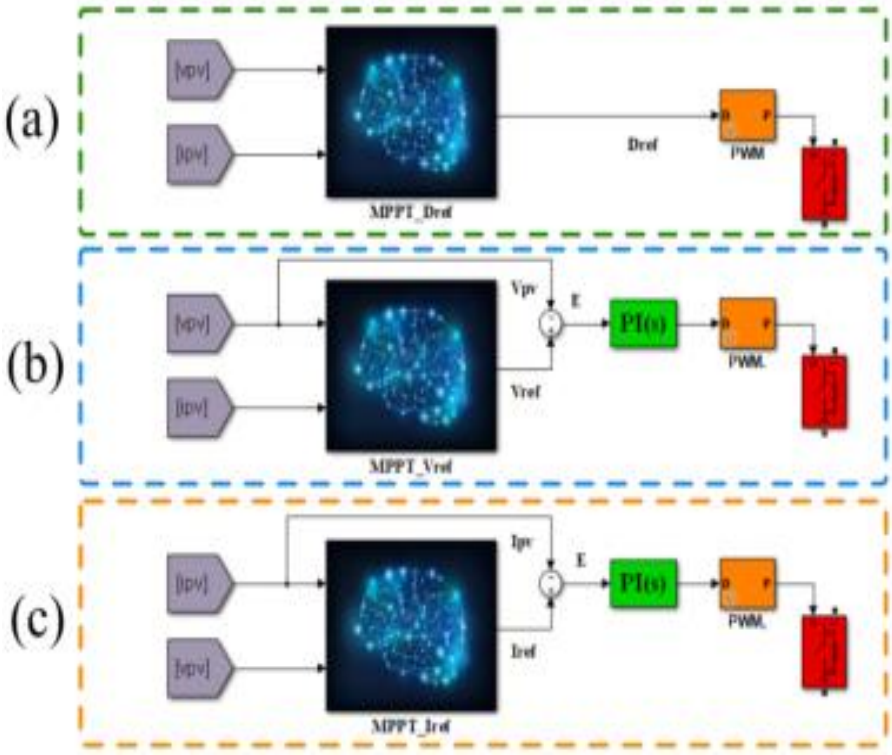

Figure IV.1 Different versions of the MPPT algorithms: (a) Duty cycle based MPPT, (b) Voltage regulation based MPPT, (c) Current regulation based MPPT.

As it has been presented in the previous section, where the dynamics of the PV system exhibit complex behavior which may controller design challenging.

An adapted control strategy is proposed in order to improve The PV system dynamics. The PV voltage is regulated using a Fractional Order PID controller tuned in various regions and partial shading patterns using Particle Swarm Optimization. The PV current is regulated using a sliding mode controller that does not require using Pulse Width Modulation (PWM). It is also shown that MPPT algorithms are affected by the conventional tuning approach of the feedback controller. To remedy this issue, the Moth Flame Optimization based MPPT technique is implemented and associated with the proposed control strategy to improve the performance PV system in different operating conditions.

The cascade control loop is suggested for electrical systems and especially for boost converter [74]. The current control was considered as an inner loop due to the fastness of current compared to the voltage. The cascade control loop is considered for the PV system voltage control. The dynamic behaviour of the closed loop system is so improved and, consequently, the MPPT algorithm reached a high performance.

In the proposed control strategy, a combination between sliding mode control technique and fractional order control approach has been used. The transient performance enhancement of the PV system subject to different operating conditions has been obtained. The bio-inspired MPPT strategy based on Moth flame optimization has been used to track global maximum power point.

IV.2 PROPOSED CONTROL STRATEGY

The PV system voltage and current regulation loops are cascaded [74] as illustrated in figure IV.2. The linear PV voltage is regulated using a Fractional Order Controller tuned offline by the particle swarm optimization algorithm for various operating regions and different partial shading patterns.

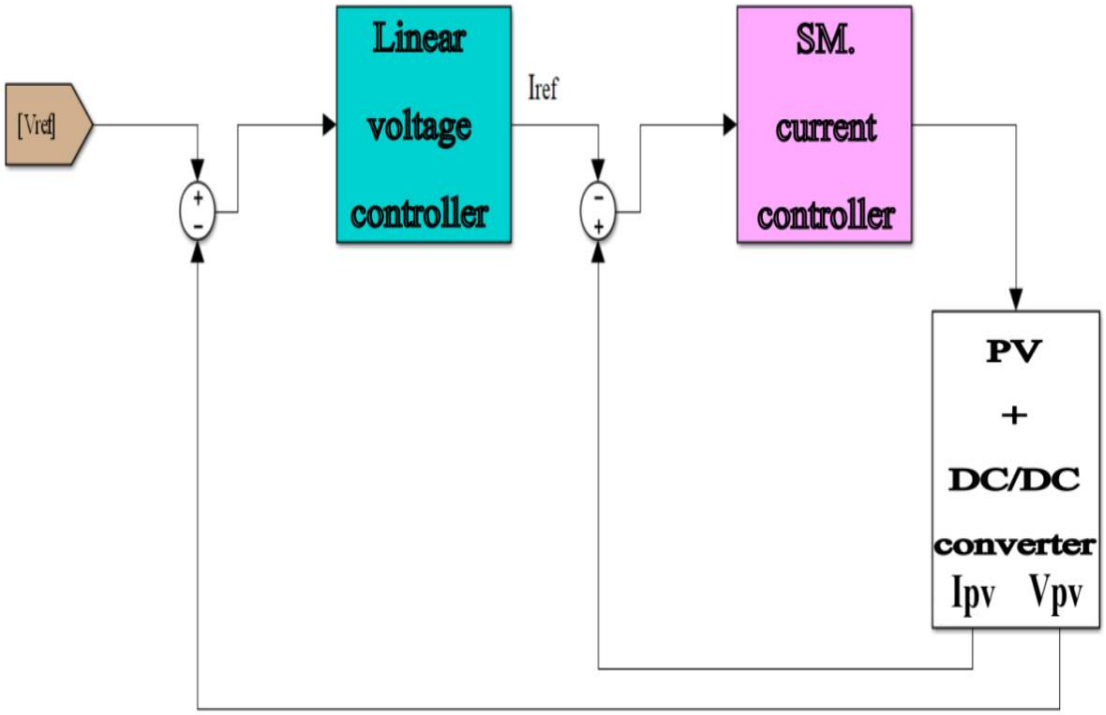

Figure IV.2 Cascade control strategy of the PV system.

IV.2.1 SLIDING MODE CONTROLLER

Sliding mode control (SMC) is considered a powerful tool for robust control of nonlinear systems [74]. The basis of this control is the construction of a sliding surface *S* defined by trend error to zero then application a control effort which guarantees that the dynamics of the controlled system will approach this surface.

In the low frequency range for a boost converter, the work presented in [75] demonstrated the equivalence between the Pulse Width Modulation (PWM) and the Sliding Mode Controller (SMC) [74]. The SMC is used to control the PV current where the switching signal u of the sliding mode controller takes discrete values set as {0,1}, whereas the sliding surface for PV current regulation is given as follows:

$$s = e(t) = i_{pv} - i_{ref} \quad \text{(IV.1)}$$

The control signal of the sliding mode controller is given as follows:

$$u = \frac{1}{2}(1 - sign(s)) \quad \text{(IV.2)}$$

The controller given by equation IV.2 is easily implemented without a need of tuning parameters which simplifies its applicability.

IV.2.2 FRACTIONAL ORDER CONTROLLER

The fractional order PID controller noted $PI^{\lambda}D^{\mu}$ which is a generalization of the conventional integer order PID controller was proposed in [76]. Its form is given in time domain as follows (equation IV.3):

$$u(t) = K_P e(t) + K_I D^{-\lambda} e(t) + K_D D^{\mu} e(t) \quad \text{(IV.3)}$$

The corresponding transfer function is given as follows (equation IV.4):

$$G_c(s) = \frac{U(s)}{E(s)} = K_P + K_I s^{-\lambda} + K_D s^{\mu} (\lambda, \mu > 0) \quad \text{(IV.4)}$$

As shown in equations IV. 3 – 4, the fractional order controller has additional parameters when compared with the classical PID which gives additional flexibility. The two additional parameters which are the fractional order integral λ and the fractional order derivative μ are used to improve the dynamic behavior of the closed loop system.

From figure IV.3, it is illustrated that the classical P, PI, PD and PID controllers are particular cases of the fractional PID controller when additional parameters λ and μ takes integer values 0 or 1. Indeed, the use of the $PI^{\lambda}D^{\mu}$ controller offers more flexibility and a more possibility for the generation of control signal u(t) of equation IV.3 which extends the control space.

From equation IV.4, the transfer function of the $PI^{\lambda}D^{\mu}$ controller seems to be irrational. Therefore, the implementation of this controller needs an approximation by a rational transfer function. Several methods exist in the literature which allows the approximation of fractional order operators by a rational transfer function in a limited frequency band. The most widely used techniques are presented in [77] and [78].

IV.2.3 FRACTIONAL ORDER CONTROLLER PARAMETERS TUNING

The tuning of the parameters of the fractional order controller may be classified as in [79]. Two main approaches are adopted. Model-based-tuning as in [80], [81], [82] and model-free tuning as in [83], [84].

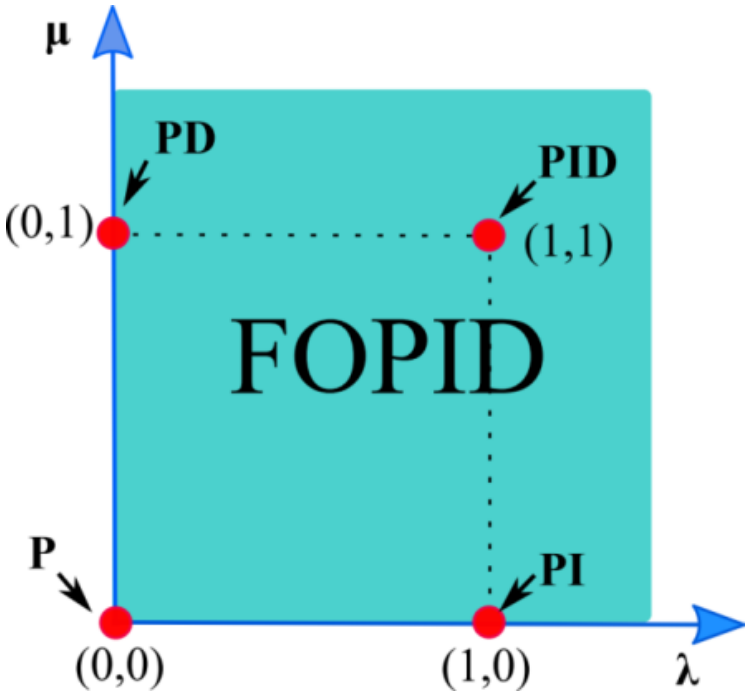

Figure IV.3 Fractional $PI^{\lambda}D^{\mu}$ Controller.

A model-based approach for parameters tuning is carried out using the Particle Swarm Optimization technique by minimizing the Integral Square Error performance index as shown in figure IV.4 (b). The position of the swarm particles is updated using equations.(IV.5-6) where c_1 and c_2 are constants and give the movement weight towards personal best or global best respectively. r_1, r_2 are randomly generated numbers in the range [0, 1]. w is the adaptive inertia factor. The movement of the swarm is illustrated in figure IV.4 (a). The resulting tuned fractional order controller is then used for PV voltage regulation to track reference given by the MPPT block as shown in figure IV.4.

$$V_i(t+1) = wV_i(t) + c_1 r_1\big(P_i(t) - X_i(t)\big) + c_2 r_2\big(G_b(t) - X_i(t)\big) \quad \text{(IV.5)}$$

$$X_i(t+1) = X_i(t) + V_i(t+1) \quad \text{(IV.6)}$$

Figure IV.3 (b) shows the flowchart of the used algorithm for tuning five parameters of the fractional order PID controller. The main idea of this tuning is to optimize the performance criteria under different operation regions presented in figure III.5 (c). The proposed controller overcomes the imperfections of the conventional controller designed for the power region. The latter has the disadvantage of reducing the performance of other regions and slows down the convergence of the MPPT algorithm as well.

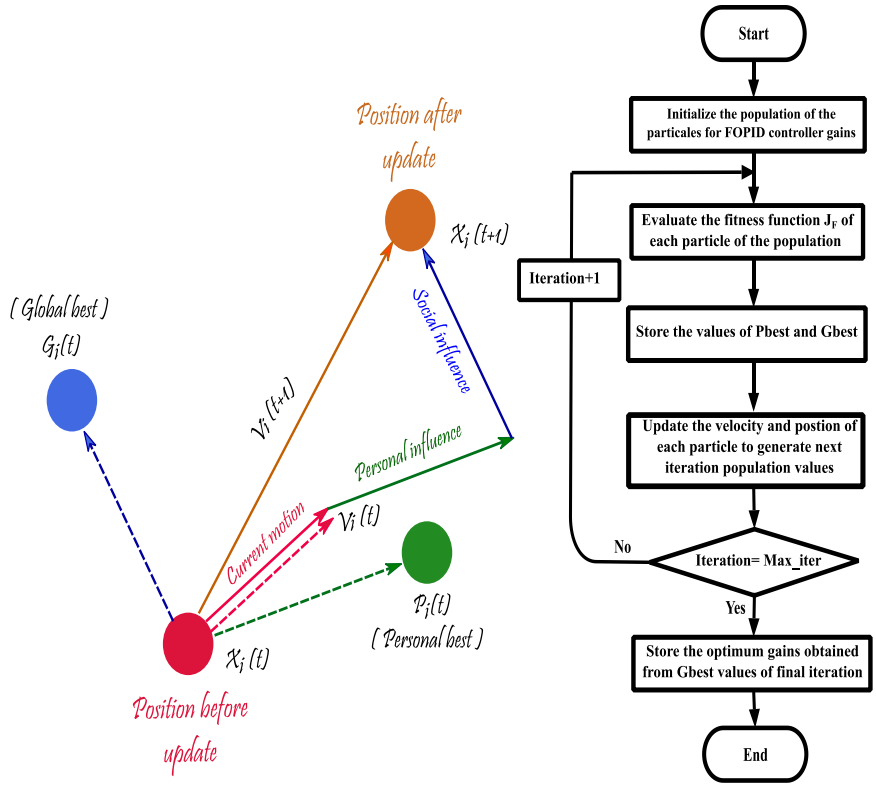

Figure IV.4 Tuning of the parameters of the Fractional Order PID using the PSO algorithm: (a) Operation of PSO swarm, (b) Flowchart of PSO tuning algorithm.

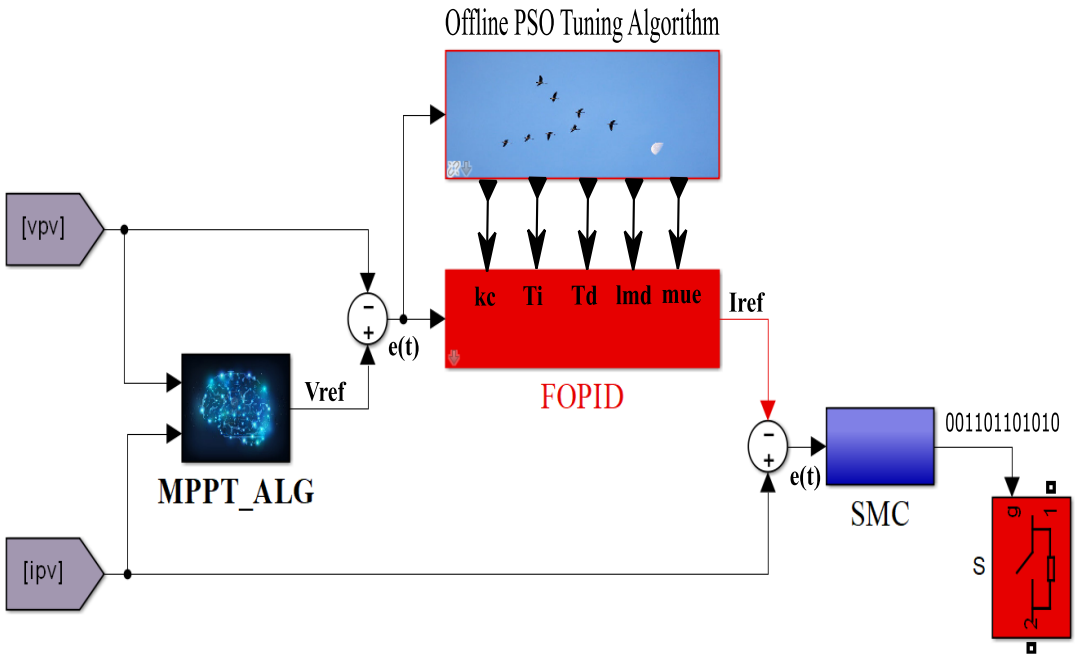

Figure IV.5 Proposed control strategy for voltage and current regulation of the PV system.

The controller's parameters are fixed for each agent by means of offline tuning. The corresponding PSO algorithm searches the optimal controller and the tuning procedure is carried out for different scenarios. The latter are selected by the designer and include the partial shading condition before the system start-up.

The proposed tuning strategy allows us to obtain a robust controller that can work in different operating conditions. The complex dynamic performance presented in the previous chapter could be defined and well analyzed.

IV.3 GLOBAL MPPT ALGORITHM

The Moth Flame Optimization algorithm is based on the navigation method of moths at night using a light source [47]. The original navigation mechanism is based on using the moonlight to maintain a fixed angle when traveling for long distances. However, when moths are exposed to artificial light sources, their behavior changes to a deadly spiral motion around the flame.

The MFO technique [24] mimics the movement of moths as they navigate at night towards a light source. The original navigation mechanism is based on using the moonlight to maintain a fixed angle when traveling for long distances. However, when moths have exposed to artificial light sources their behavior changes to a deadly spiral motion around the flame.

The position (M_i) and Flames (F_j) and the corresponding fitness (Fit_M) and (Fit_F) respectively of the moths in 1-D search space are defined as follows (equation IV.7) [47]:

$$M_i = \begin{bmatrix} m_1 \\ m_2 \\ \vdots \\ m_n \end{bmatrix}, Fit_M = \begin{bmatrix} Fit_{M_1} \\ Fit_{M_2} \\ \vdots \\ Fit_{M_n} \end{bmatrix}, F_j = \begin{bmatrix} F_1 \\ F_2 \\ \vdots \\ F_m \end{bmatrix}, Fit_F = \begin{bmatrix} Fit_{F_1} \\ Fit_{F_2} \\ \vdots \\ Fit_{F_m} \end{bmatrix} \quad \text{(IV.7)}$$

Where n represents the number of moths. As iterations increase, the flames number decreases as follows: $m = round\left(N - l * \frac{N-1}{T}\right)$. N represents the maximum number of flames, the current number of iteration is represented by l, and T indicates the maximum number of iterations.

The position of moths *M* represents the position of the searching agents and *F* the best positions of moths which represents the flames. The positions of moths are evaluated as follows (equation IV.8):

$$M_i = D_i e^{bt} cos(2\pi t) + F_j \quad \text{(IV.8)}$$

where D_i represents the distance between the i^{th} moth and j^{th} flame which is calculated as follows (equation IV.9):

$$D_i = \left|F_j - M_i\right| \quad \text{(IV.9)}$$

in which b represents a constant that defines the shape of the spiral, *t* is a random number in [-1,1].

(a)

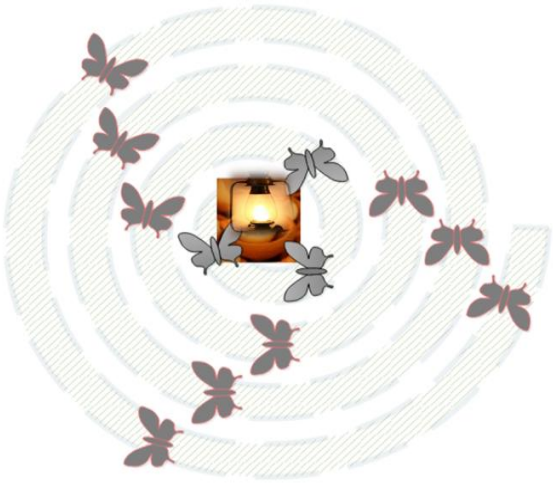

(b)

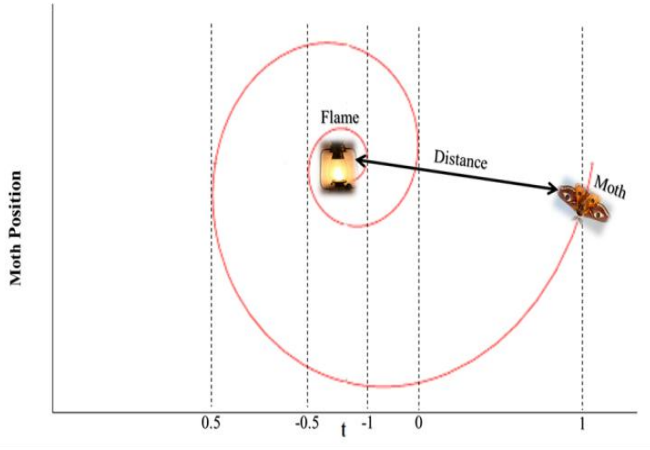

Figure IV.6 Movement of the moth: (a) illustration of the navigation mechanism of moths, (b) Mathematical description of the movement.

The displacement of the moths in a spiral trajectory around the flame is illustrated in figure IV.6 (a). The mathematical model in equation (IV.8) is simulated in figure IV.6 (b) where the parameter *t* is +1 when the moth is the farthest from the flame and -1 when it is the closest to the flame. Figure IV.7 shows the displacement in the P-V curve with its corresponding interpretation using the spiral motion. The MPPT is started by positioning the Moths along with the range [0 v_{oc}], then each one makes a transition to the next iteration by displacing by an amount of D_i *(i=1..n)* towards the flame F_j *(j=1..N)* until the convergence of the algorithm to the GMPP. The flowchart of the MFO algorithm including the steps for its implementation is given in figure IV.8 [85].

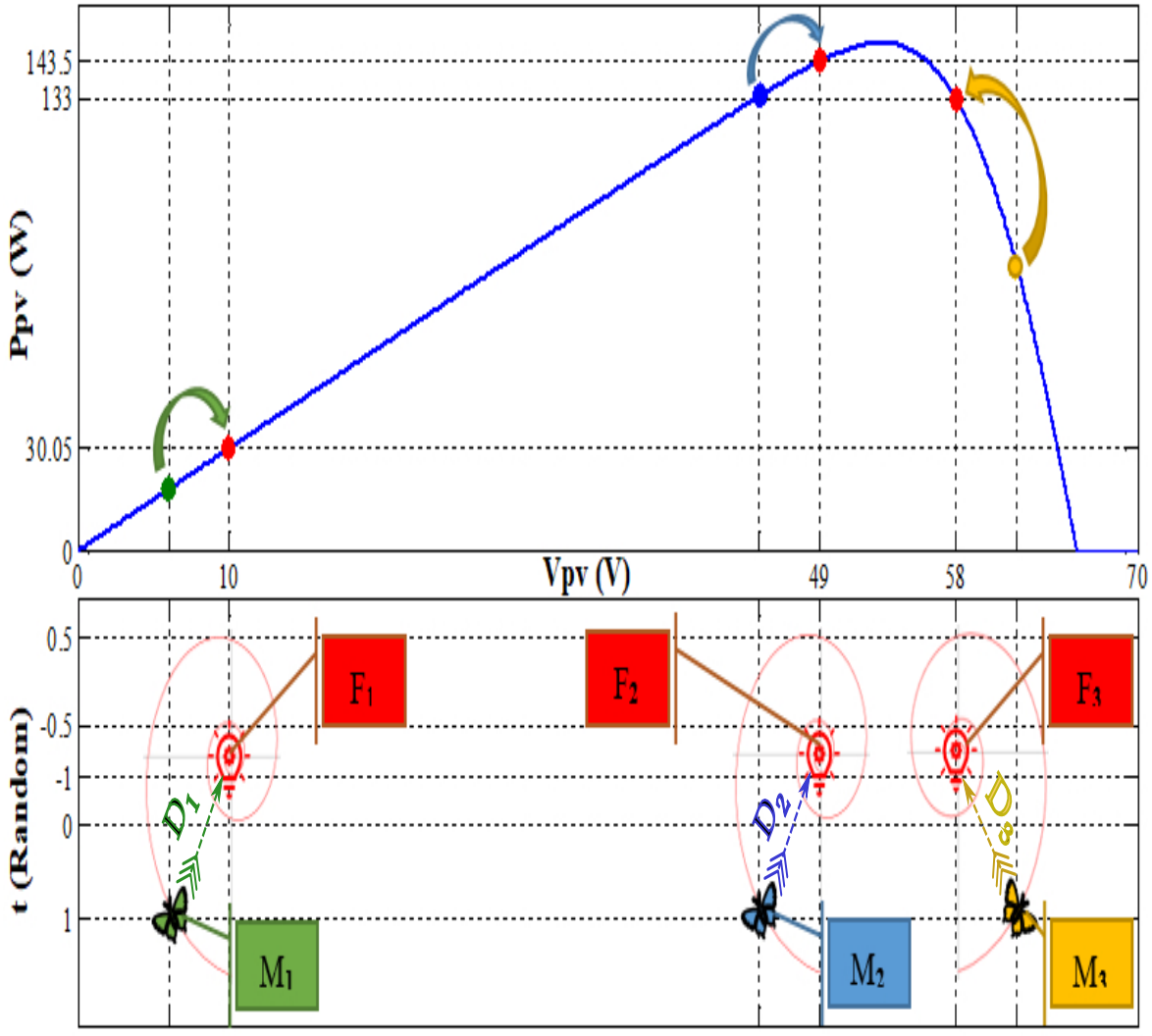

Figure IV.7 Displacement in the P-V curve with its corresponding interpretation using the spiral motion.

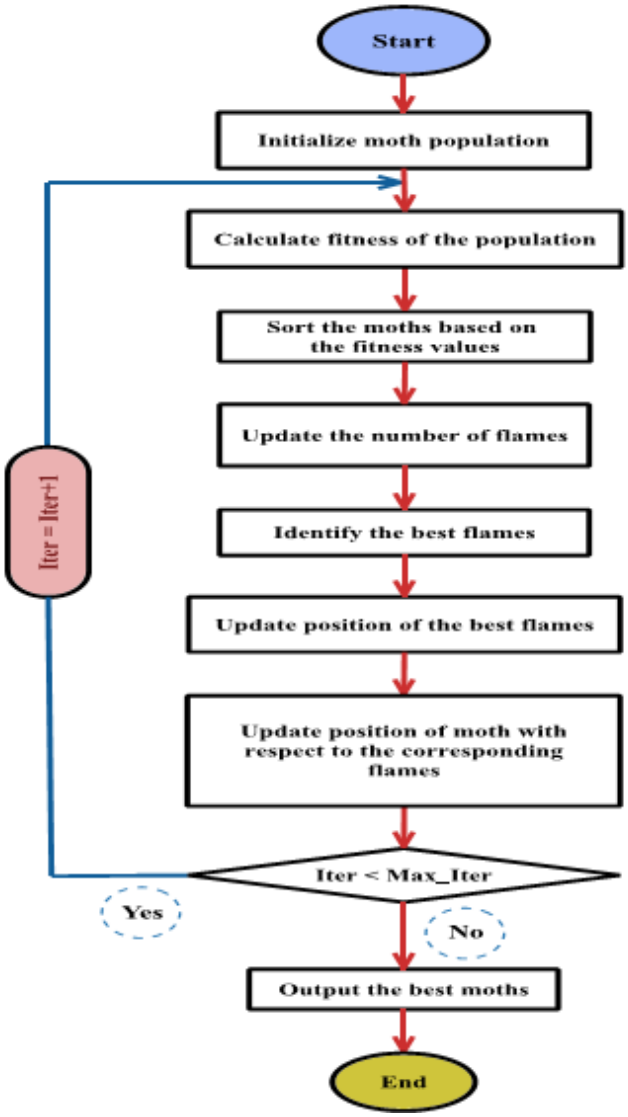

Figure IV.8 Flowchart of the MFO algorithm.

IV.4 RESULTS AND DISCUSSION

The PV generation system shown in figure IV.9 composed of three PV panels in series with selectable temperature and irradiation patterns is associated with a boost DC-DC converter and evaluated using the proposed control strategy under different operating conditions.

The characteristic curves for the considered simulation scenarios are presented in figure IV.10 (a) where different operating points are chosen at different operating regions for each operating condition. The patterns have the characteristics given in Table IV.1, where different positions of the GMPP are selected to cover all possible cases (left, center, right).

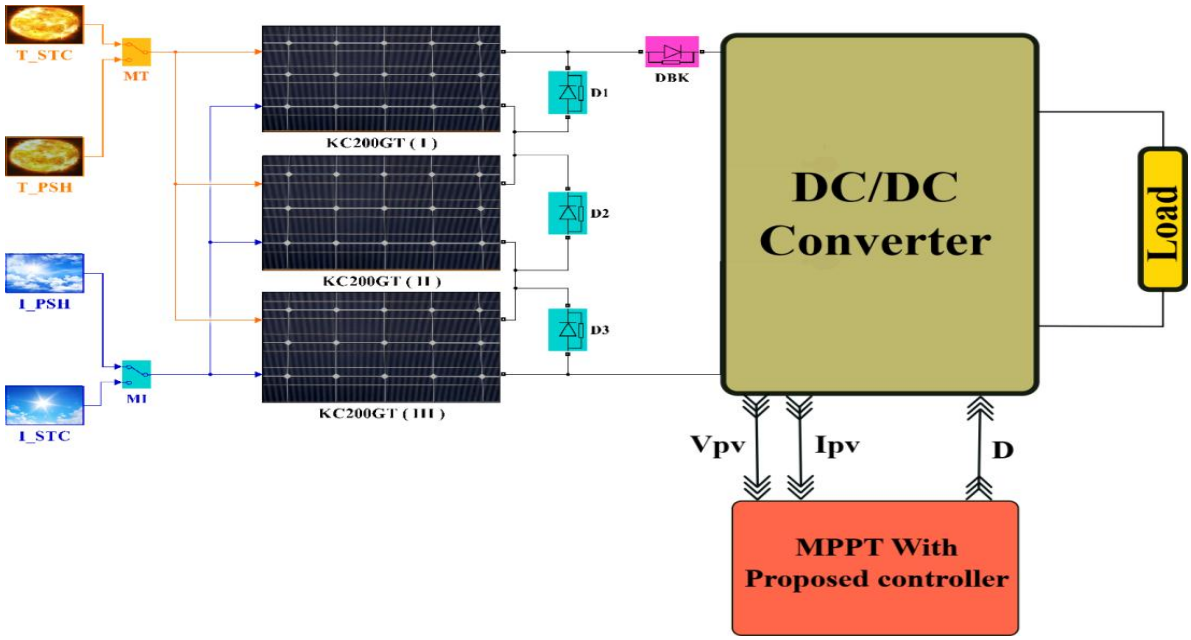

Figure IV.9 PV array associated with boost DC-DC converter and load.

The partial shading pattern P1 exposes the first PV panel to 900 W/m², the second PV panel to 700 W/m² and the third PV panel to 500 W/m². The partial shading pattern P2 exposes the three PV panels to the values (800,500,200) W/m² respectively. Whereas P3 considers the pattern (700,200,100) W/m² as irradiation values for the PV panels.

The response of the PV energy generation system equipped with the combined fractional order controller and sliding mode controller for successive setpoint change is given in figure IV.10 (b). It can be noted that the controlled system has good performance in CPR and VSR regions, and have an oscillating response in CSR. Such an effect has been previously highlighted in [71].

From figure IV.10 (b) it can be seen that the dynamic behavior of the PV system in the current source region presents an oscillatory mode bounded from 0 to 70 volts for STC region (as C point at 35 volts). However, in the same region [0 70], and with different condition (P1, P2 and P3) the six points (F L R) and (H L T) present an intermediate power region with an over damped dynamics modes. In addition there is a special behavior that occurred with a different degree as it is shown in point T compared to the H.

From the obtained results, it can be concluded that at the same operation point from the known viewpoint of the three regions [13] the PV system can have different dynamic behavior depending on the climatic condition. As an example, the operation point (V=25

volts) of the system has four different dynamics as shown in figure IV.10 (b) horizontally (H, N, T and C). These phenomena may affect the convergence of the MPPT algorithms to track the true MPP.

Table IV.1 Maximum power points of the PV array for simulation scenarios.

Patterns	Solar irradiance Level (W/m^2)	Voltage at MPP, V	Current at MPP, A	Power at MPP, W	Position of GMPP
STC	1000,1000,1000	78.90	7.61	600.43	Center
P1	900,700,500	83.527	3.97	331.6	Right
P2	800,500,200	54.554	3.926	214.193	Center
P3	700,200,100	26.17	5.317	139.15	Left

Figure IV.11 shows the displacement in the P-V curve with its corresponding interpretation using the spiral motion.

The proposed strategy is first tested in STC where both algorithms (MFO-FOPID and MFO-PI) converge to the MPP as shown in figure IV.12 (a)-(c). Furthermore, the proposed MFO-FOPID technique has provided the best capability with respect to three different performance evaluation criteria over the test period that are the steady state oscillations (ΔV_{PV}), tracking accuracy (ξ) and tracking time (Tr) as shown in Table IV.2.

For the partial shading patterns P1, P2 and P3, the proposed tracking strategy (MFO-FOPID) is characterized by the convergence to the GMPP whereas the MFO-PI converges to a local MPP (figure IV.12 (a)-(c)). The gain in power is evaluated at 35.33W for the case of the pattern P1 which is the highest in the considered scenarios (Table IV.1).

As mentioned above, the tuning of the classical controller PI is designed by only considering the STC in which this controller can provide almost similar results as the proposed FOPID controller that is designed by considering all kinds of voltage, power, and current regions according to different test conditions. But, when the region in which the PV system works is changed, the classical controller PI based MFO fails to converge to the GMPP whereas the MFO- FOPID always converges to global MPP.

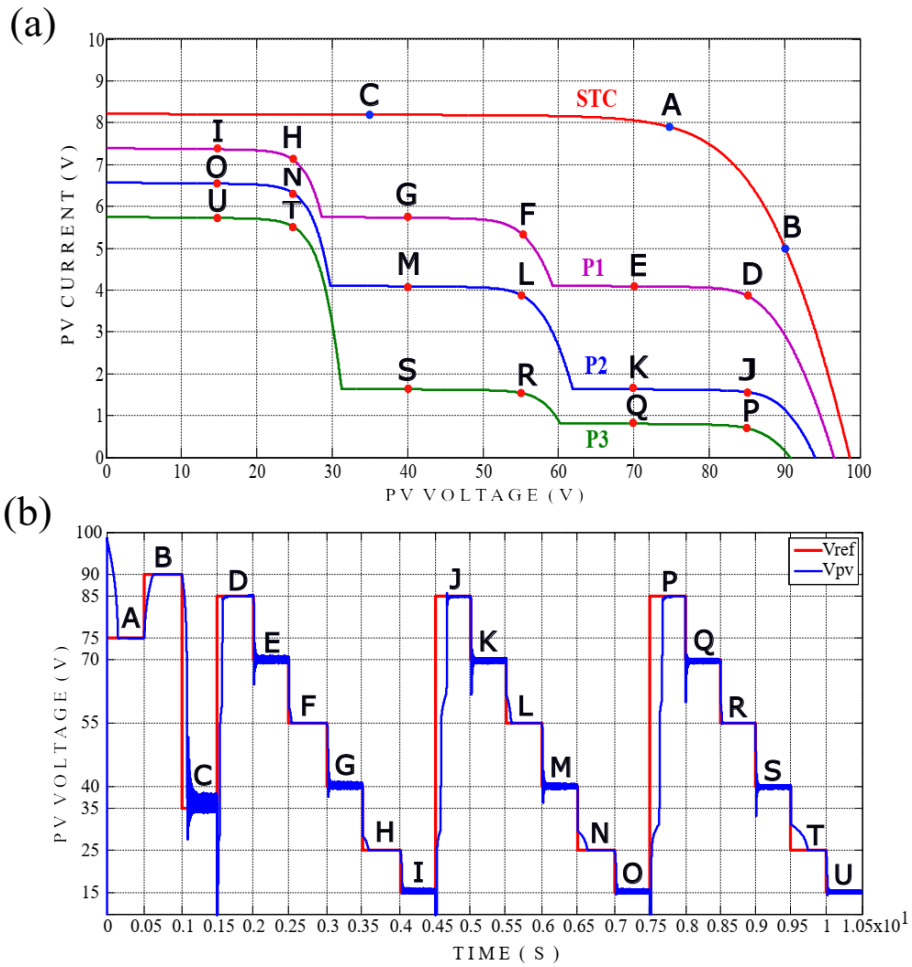

Figure IV.10 Evaluation of the PV energy generation system using the proposed strategy:
(a) The characteristic curves for the considered simulation scenarios,
(b) Response in various operating regions and climatic conditions.

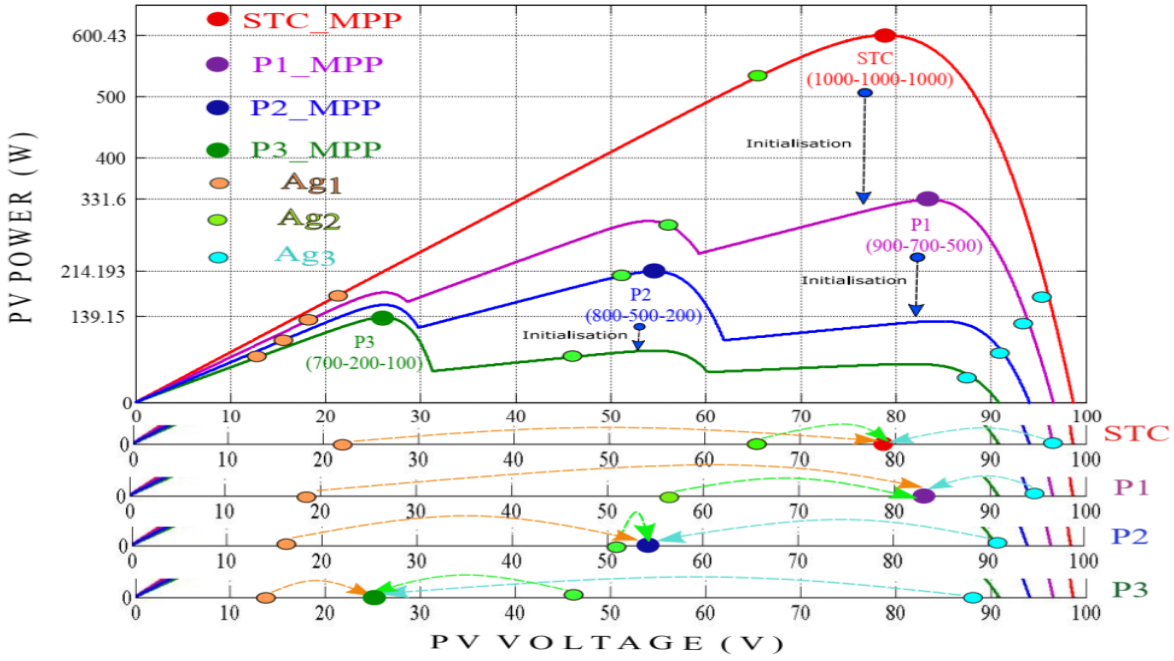

Figure IV.11 Movement of agents of the MFO MPPT algorithms during transitions.

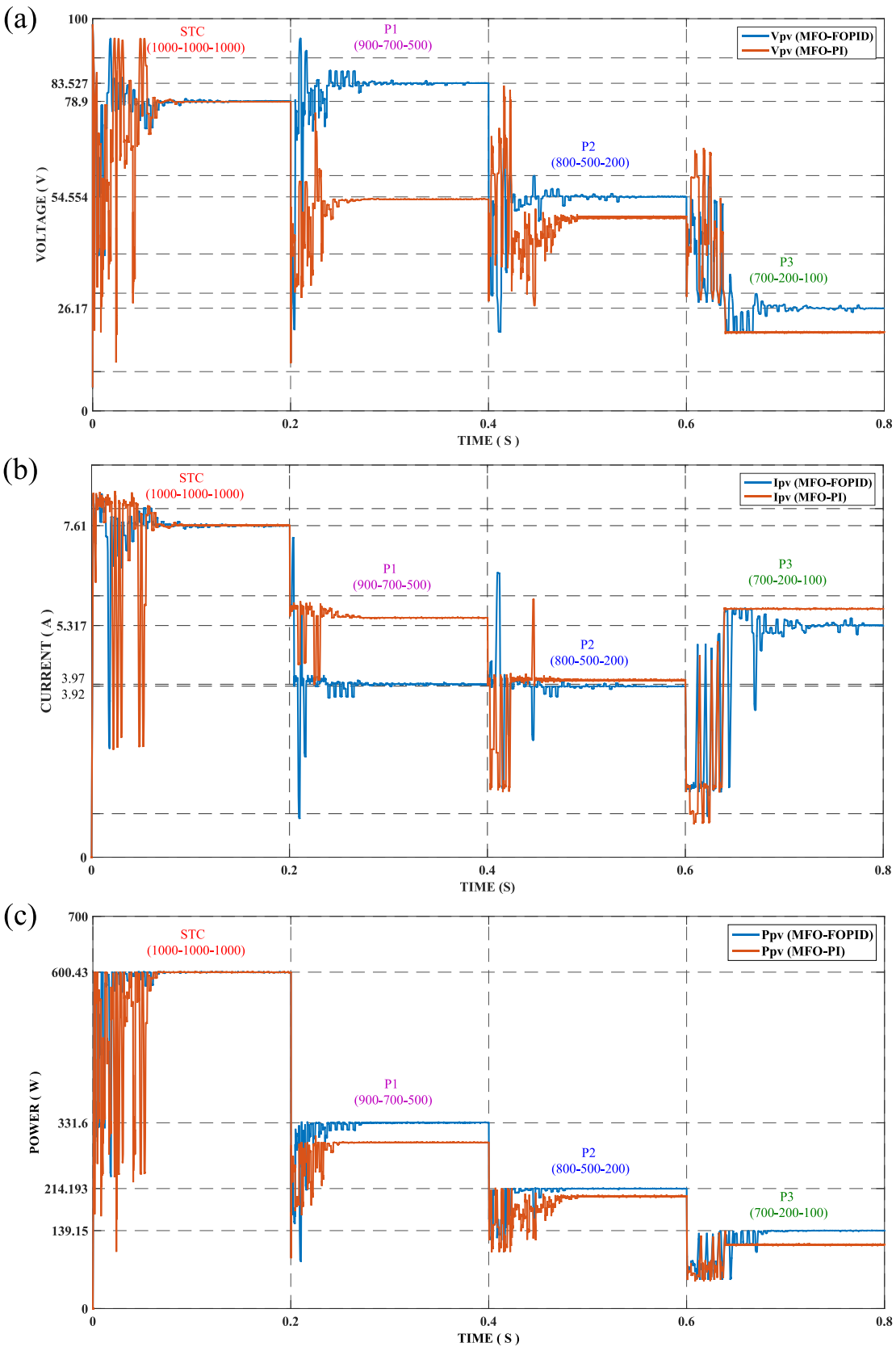

Figure IV.12 Response of the proposed MPPT strategy to various operating conditions: (a) PV voltage, (b) PV current, (c) PV power.

Table IV.2 Comparative results between the proposed approach and the conventional technique.

		V_{PV} (V)	I_{PV} (A)	P_{PV} (W)	ΔV_{PV} (V)	ξ (V)	Tr (S)
STC	**MFO-PI**	78,8178	7,6162	600,3	0,129	0,0822	0,0685
	MFO-FOPID	78,9546	7,6024	600,39	0,055	0,0546	0,0657
P1	**MFO-PI**	53,9795	5,4880	296,24	0,09	29,5475	0,06615
	MFO-FOPID	83,579	3,9671	331,57	0,111	0,052	0,0728
P2	**MFO-PI**	49,3019	4,0637	200,35	0,61	5,2521	0,09065
	MFO-FOPID	54,6139	3,9217	214,1825	0,0537	0,0599	0,08385
P3	**MFO-PI**	20,0293	5,6967	114,1025	0,42	6,1407	0,04
	MFO-FOPID	26,14625	5,3194	139,064	0,0185	0,02375	0,0865

IV.5 CONCLUSION

The MPPT algorithm has been found to be sensitive to the feedback controller tuning region particularly in the power region which leads to a decreased performance. A fractional order controller tuned with the Particle Swarm Optimization technique around various operating regions and with the presence of partial shading patterns has been used for PV voltage regulation to overcome this disadvantage. In addition, the PV current is regulated using a Sliding Mode Controller which eliminates the need for a pulse width modulation. The combination of both regulation loops are used to enhance the dynamic performance of the PV array.

The Moth Flame Optimization algorithm has been used and combined with the proposed control strategy to search the GMPP for various patterns of partial shading and operating regions. Simulation results show a better performance of the MFO-based MPPT associated with the proposed control strategy when compared with the conventional approach.

CHAPTER V

CONCLUSIONS, RECOMMENDATIONS AND FUTURE WORKS

CHAPTER V

In this chapter the main conclusions obtained within the present thesis are given, followed by personal recommendations and suggestions for future works related to photovoltaic panels based solar energy generation systems integrated in electric power systems.

V.1. CONCLUSIONS

The main focus of this thesis has been the design of a novel maximum power point tracking algorithm with enhanced control strategy under partial shading conditions.

Significant technical challenge has been addressed to define the best possible uses of solar energy. The impact of humanity's increasing energy demand on the environment and climatic conditions makes the subject very timely and deserves it to be highlighted.

The search of different possible combinations between conventional and modern MPPT techniques for PV energy generation systems has been carried out. It has been pointed out that the best combination is settled between the Bio-inspired/Bio-inspired methods by selecting the advantages of each one. Although this approach seems to be complex and induces certain additional costs, its implementation is promising for the search of a best performance of PV energy generation systems operating with the presence of STC and partial shading conditions. The latter impose a constraining dynamic behavior for the PV systems operation.

The effect of different climatic conditions on the I-V characteristic has been analyzed. The resulting rate of change of current concerning PV voltage gives a hint in developing a new idea for optimal extraction of power from PV array under STC and partial shading conditions.

The PV system operation in different regions and with the presence of environmental conditions is characterized by a complex dynamic behaviour.

The dynamic response of the PV system, both in open and closed loop has been identified. Variations in overshoot and response time could be so easily depicted. Such dynamic effects are further noticeable along the characteristic curve when the partial shading condition occurs.

The conventional techniques related to MPPT algorithms fail to determine the MPP under varying atmospheric conditions which degrades the PV array's performance and reduces the system's overall efficiency. Thus to improve the PV system's performance, the MFO has been developed and implemented for various operating conditions to improve the power extraction efficiency, reduce tracking time, and decrease power fluctuations. The objectives of the work have been successfully achieved.

V.2 RECOMMENDATIONS AND FUTURE WORKS

There is a broad scope for extending this research work by integrating the system with standalone load, grid, hybrid system, Etc. Some of the extensions of the research work that can be made in the future are listed as follows:

- The MPPT analysis for the PV inverter systems tied with AC commercial and household loads could be performed based on findings of the present thesis.
- Sun tracker based MPPT algorithms can be implemented to improve the efficiency of the PV systems.
- Future research could investigate other converters' topologies such as buck, buck-boost, cuk, sepic along with the proposed MPPT techniques.
- PV system's performance can be determined for the different types of loads such as batteries or motors instead of resistive load.
- The proposed algorithm may be implemented with advanced microcontrollers such as Texas Instruments C2000 DSP and FPGA boards. By doing so, the efficiency of the PV system control can be validated.
- The PV system cannot continuously deliver energy to the load throughout the day, and so battery backup is necessary for a PV-based standalone system. A power management concept can be implemented in such systems to be extracted from PV and the remaining from batteries.

APPENDICES

APPENDIX

« A »

LIST OF PUBLICATIONS

2020 International Conference on Mathematics and Information Technology, Adrar, Algeria, February 18-19, 2020 159

ANN based MPPT Algorithm Design using Real Operating Climatic Condition

Mohammed Salah Bouakkaz
Department of Electrical Engineering, Laboratoire d'électrotechnique de Skikda «LES», Université du 20 Août 1955, Skikda 21000, Algeria
ms.bouakkaz@univ-skikda.dz

Ahcene Boukadoum
Department of Electrical Engineering, Laboratoire d'électrotechnique de Skikda «LES», Université du 20 Août 1955, Skikda 21000, Algeria

Omar Boudebbouz
Department of Electrical Engineering, Laboratoire d'électrotechnique de Skikda «LES», Université du 20 Août 1955, Skikda 21000, Algeria

Ahmed Bouraiou
Unité de Recherche en Energie Renouvelables en Milieu Saharien, URERMS, Centre de Développement des Energies Renouvelables, CDER, 01000, Adrar, Algeria
bouraiouahmed@gmail.com

Nadir boutasseta
Research Center in Industrial Technologies CRTI, P.O. Box 64, Cheraga, Algeria
boutasseta@gmail.com

Issam Attoui
Research Center in Industrial Technologies CRTI, P.O. Box 64, Cheraga, Algeria
atoui_article@yahoo.fr

***Abstract*— Maximum Power Point Tracking (MPPT) controller is an indispensable component to ensure the transfer of maximum energy from the photovoltaic generator to the load. In this paper, an intelligent MPPT based on Artificial Neural Network (ANN) is designed using Real Operating Conditions and implemented in Matlab/Simulink. The algorithm gives a reference operating point to a Step-up DC-DC converter with the objective of reaching the Maximum Power Point (MPP) in photovoltaic energy generation system. Simulation results prove the capability of the ANN-MPPT algorithm in tracking the MPP rapidly and accurately with low ripple.**

Keywords—Photovoltaic (PV) module, Maximum Power Point Tracking (MPPT), Artificial Neural Network (ANN), Real Operating Conditions (ROC).

I. INTRODUCTION

The integration of renewable energy in the different sectors of energy has become an important key for mitigating the Greenhouse Gas (GHG) emission and reducing the dependence to fossil sources [1]. Solar energy generation is widely used in the world due to its abundance especially in the desert regions [2]. Maximum energy extraction from the PV generator is an indispensable task the optimum operation of photovoltaic solar energy generation systems. For this purpose, Maximum Power Point Tracking (MPPT) algorithms are implemented to control a DC/DC converter in order to optimize the power transfer to the load [3], [4].

Several MPPT techniques have been proposed using different approaches [5]. The perturb and observe (P&O) algorithm is the conventional technique used to track the MPP in uniform irradiation operating conditions [6]. The steady state oscillations of the perturbation step is the main drawback of this method compared with the advantage of its simple hardware implementation. The availability of meteorological data allows the determination of the maximum power operating point in real operating conditions using artificial intelligence based identification techniques.

978-1-7281-2580-0/20/$31.00 ©2020 IEEE

Artificial Neural Network (ANN) has been used in several applications like identification, prediction, control, classification and digital image processing [7]–[9]. The structure of ANN is composed of an input layer that varies in size depending on the training data, a hidden layer which its configuration depends on the complexity of the considered problem, the output layer which gives the value of the ANN evaluation of the presented inputs [10]. The ANN has been used for forecasting grid parameters such as voltage and frequency in [11]. The MPPT in wind energy generation systems has been evaluated using ANN and Sliding Mode Control in [12].

In this paper, an ANN-based MPPT algorithm implemented using Real Operating Climatic Condition (ROC) is proposed to ensure maximum power transfer from a PV module generator to the load.

II. PV SYSTEM DESIGN AND ANN APPLICATION

A. PV system design

The PV system modeling was implemented using the Simulink tool of the Matlab software, it consists of following blocks:

- PV module
- Step-up converter
- Resistive load
- ANN-MPPT block

Fig. 1 presents the Matlab/Simulink platform used for simulation.

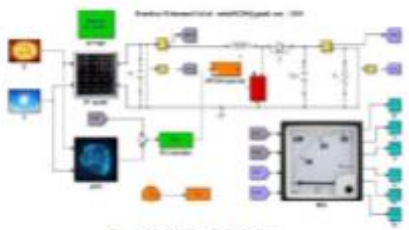

Fig. 1. Matlab/Simulink platform.

Solar Energy 199 (2020) 411–424

Contents lists available at ScienceDirect

Solar Energy

journal homepage: www.elsevier.com/locate/solener

Dynamic performance evaluation and improvement of PV energy generation systems using Moth Flame Optimization with combined fractional order PID and sliding mode controller

Mohammed Salah Bouakkaz[a], Ahcene Boukadoum[a], Omar Boudebbouz[a], Nadir Fergani[b], Nadir Boutasseta[b,*], Issam Attoui[b], Ahmed Bouraiou[c], Ammar Necaibia[c]

[a] Department of Electrical Engineering, Laboratoire d'électrotechnique de Skikda «LES», Université du 20 Août 1955, Skikda 21000, Algeria
[b] Research Center in Industrial Technologies, CRTI, P.O. Box 64, Cheraga, Algiers, Algeria
[c] Unité de recherche en Energie Renouvelables en milieu saharien, URERMS, Centre de Développement des Energies Renouvelables, CDER, 01000 Adrar, Algeria

ARTICLE INFO

Keywords:
Photovoltaic (PV) energy generation systems
Dynamic performance
Global Maximum Power Point Tracking (GMPPT)
Moth Flame optimization (MFO)
Fractional Order Controller
Sliding Mode Controller (SMC)

ABSTRACT

The output power of Photovoltaic (PV) energy generation systems depends mainly on operating conditions that include climatic conditions and occurrence of faults. Current-Voltage characteristic curves show different operating regions that are characterized by different transient responses in varying operating conditions and in the special case of the presence of the partial shading condition. In this paper, a dynamic performance evaluation of the PV system is performed both in open loop and in the presence of a feedback controller. Analysis shows that the PV system is affected when operating in different regions and environmental conditions and is characterized by a complex dynamic behavior. To improve the PV system dynamics, an adapted control strategy is proposed where the PV voltage is regulated using a Fractional Order PID controller tuned in various regions and partial shading patterns using Particle Swarm Optimization, whereas the PV current is regulated using a sliding mode controller that does not require using Pulse Width Modulation (PWM). In the present study, it is also shown that MPPT algorithms are affected by the conventional tuning approach of the feedback controller. To remedy to this issue, the Moth Flame Optimization based MPPT technique is implemented associated with the proposed control strategy to improve the performance PV system in different operating conditions. The proposed dynamic performance improvement strategy shows excellent transient responses in various operating scenarios.

1. Introduction

Photovoltaic energy generation systems are subject to outdoor operating conditions that affect their operation and may lead to a considerable energy loss (Necaibia, 2018; Boutasseta et al., 2018). Hot dry climatic conditions especially have direct effect on the degradation of PV arrays as studied in Bouraiou (2018, 2017), where the operation of PV arrays in the south of Algeria has been assessed (Bouraiou, 2019). Climatic conditions have direct effect on the energy generation efficiency of PV arrays as it is well known that temperature increase induces a decrease in the generated power and irradiation decrease leads to reduced output power (Bouraiou, 2015; Villalva et al., 2009). The effect of partial shading on the conversion efficiency of PV arrays has been well studied in the literature (Boutasseta et al., 2018; Alonso-García et al., 2006; Karatepe et al., 2007; Sánchez Reinoso et al., 2013). Under uniform irradiation environmental conditions, the Power-Voltage (P-V) characteristic curve of the PV array is characterized by a single Maximum Power Point (MPP) which constitutes a simple objective for Maximum Power Point Tracking (MPPT) algorithm. Whereas in the case where PV cells or panels receive different irradiation levels as in the case of the partial shading condition, multiple peaks or MPPs are introduced in the PV curve which makes the tracking of the global MPP challenging. The effect of these operating conditions in addition to occurrence of faults on the power conversion efficiency in the steady state region has been the subject of most of the research works that study their effect on the PV array or propose Maximum Power Point Techniques (MPPT) that optimize the power conversion efficiency in such conditions (Belhachat and Larbes, 2019; Boutasseta et al., 2013).

On the other hand, the transient response of the association PV array/DC-DC converter in different regions of the current-voltage (I-V)

* Corresponding author.
E-mail address: n.boutasseta@crti.dz (N. Boutasseta).

https://doi.org/10.1016/j.solener.2020.02.055
Received 7 November 2019; Received in revised form 26 January 2020; Accepted 12 February 2020

2020 International Conference on Computing and Information Technology, University of Tabuk, Kingdom of Saudi Arabia.
Volume: 01, Issue: ICCIT- 1441, Page No.: 248 – 252, 9th & 10th Sep. 2020.

Fuzzy Logic based Adaptive Step Hill Climbing MPPT Algorithm for PV Energy Generation Systems

Mohammed Salah Bouakkaz
Department of Electrical Engineering, Laboratoire d'électronique de Skikda (LES), Université du 20 Aout 1955 Skikda 21000
Skikda, Algeria
ms.bouakkaz@univ-skikda.dz

Ahcen Boukadoum
Department of Electrical Engineering, Laboratoire d'électronique de Skikda (LES), Université du 20 Aout 1955 Skikda 21000
Skikda, Algeria.
a.boukadoum@univ-skikda.dz

Omar Boudebbouz
Department of Electrical Engineering, Laboratoire d'électronique de Skikda (LES), Université du 20 Aout 1955 Skikda 21000
Skikda, Algeria.
o.boudebbouz@univ-skikda.dz

Issam Attoui
Research Center in Industrial Technologies CRTI, P.O. Box 64, 16014
Algiers, Algeria
i.atoui@crti.dz

Nadir Boutasseta
Research Center in Industrial Technologies CRTI, P.O. Box 64, 16014
Algiers, Algeria
n.boutasseta@crti.dz

Ahmed Bouraiou
Unité de Recherche en Energie Renouvelables en Milieu Saharien, URERMS, Centre de Développement des Energies Renouvelables, CDER, 01000,
Adrar, Algeria
bouraiouahmed@gmail.com

***Abstract*— This paper presents a modified Hill Climbing (HC) based Maximum Power Point Tracking MPPT algorithm with adaptive duty cycle step using Fuzzy Logic Controller (FLC). The conventional HC MPPT algorithm is usually used in numerous applications because of its simplicity; however, it is highly affected by sudden changes in climatic conditions, and it is characterized by ripple around the Maximum Power Point MPP and slow rate of convergence. In order to overcome these issues, a modified Hill Climbing MPPT method using FLC is presented. The robustness of this method has been demonstrated using a boost DC-DC converter connected to a Kyocera kc 200st model.**

Keywords—Hill Climbing HC, Fuzzy Logic Control FLC, Pulse Width Modulation PWM, Maximum Power Point Tracking MPPT, Photovoltaic PV systems

I. INTRODUCTION

In the current years, the world demand for energy and the phenomenon of global warming have increased due to population growth and expanding manufacturing industry [1]. To minimize the effects of such problem, many studies have been conducted to use renewable energies in order to face it [2]. A solar photovoltaic (PV) system is one of the most attractive renewable energy resources. However, the productivity of a PV system is low for the reason that the output power of a PV system relies on irradiance and temperature. The MPPT technique is an effective way to improve the efficiency of a PV system [3],[4]. They are designed to improve its production, including cost, efficiency, lost energy, and type of implementation.

The Hill Climbing-MPPT is a common method for PV-MPPT due to its low cost and simple implementation [5]. But it poses several challenges, such as lower converging speed when a small duty cycle step is used and high oscillation around a maximum power point MPP when a large duty cycle step is used [6]. In the proposed algorithm, in order to solve this problem, the duty cycle step is adjusted for each time instant using the FLC depending on the variation of the power and current of PV system.

II. PV SYSTEM DESIGN AND HC MPPT APPLICATION

a. PV system Design

The PV system modeling was implemented using the Matlab software based on the Simulink tool, it consists of following blocks:

- PV module
- Boost converter
- Resistive load
- Adaptive HC-MPPT block

Fig. 1 presents the Matlab/Simulink platform used for simulation.

The modeling of PV module is based on a single diode model [7] presented in Fig.2. Its power and current characteristic curves are given in Fig.3 and Fig.4 respectively.

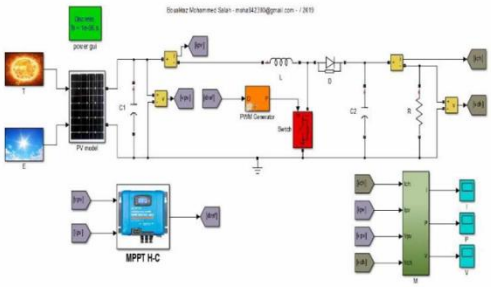

Fig. 1. Matlab/Simulink platform

The PV current is calculated using the following formula:

$$Id = Io\left[\exp\left(\frac{Vpv + IpvRsNss}{aV_tNss}\right) - 1\right] \quad (1)$$

978-1-7281-2680-7/20/$31.00 ©2020 IEEE

International Journal of Energy for a Clean Environment 22(4):63–82 (2021)

ANFIS-BASED MAXIMUM POWER POINT TRACKING USING GENETIC ALGORITHM TUNED FRACTIONAL-ORDER PROPORTIONAL-INTEGRAL-DERIVATIVE CONTROLLER AND ON-SITE MEASURED CLIMATIC DATA

Mohammed Salah Bouakkaz,[1] Ahcene Boukadoum,[1] Omar Boudebbouz,[1] Nadir Boutasseta,[2,] Issam Attoui,[2] Nadir Fergani,[2] Ahmed Bouraiou,[3] & Ammar Neçaibia[3]*

[1]*Department of Electrical Engineering, Laboratoire d'électrotechnique de Skikda "LES," Universite du 20 Août 1955, Skikda 21000, Algeria*

[2]*Research Center in Industrial Technologies, CRTI P.O. Box 64, Cheraga, Algiers, Algeria*

[3]*Unité de Recherche en Energies Renouvelables en Milieu Saharien, URERMS, Centre de Développement des Energies Renouvelables, CDER, 01000 Adrar, Algeria*

*Address all correspondence to: Nadir Boutasseta, Research Center in Industrial Technologies, CRTI P.O. Box 64, Cheraga, Algiers, Algeria, E-mail: n.boutasseta@crti.dz

Original Manuscript Submitted: 7/15/2020; Final Draft Received: 10/20/2020

Solar energy in the region of Adrar which is located in the south of Algeria is considered one of the favorable renewable sources for the deployment of solar-based energy generation systems. This source of energy changes during the day according to several environmental conditions such as solar radiation, temperature, sand storms, and dust accumulation. In order to transfer the maximum amount of energy from the photovoltaic (PV) system to the load, maximum power point tracking (MPPT) techniques are implemented to control the power converter using different approaches. In this work, an adaptive neuro-fuzzy inference system (ANFIS)-based MPPT algorithm which uses a fractional-order proportional integral derivative (FOPID) controller tuned by genetic algorithm (GA) is proposed to track the optimal operating point using real on-site measured climatic data. For this purpose, the duty cycle of the DC–DC converter which has been connected between the solar panel and the load is controlled using the proposed method. The FOPID controller is optimized by a genetic algorithm in order to both improve the transient response performance and overcome the PV systems nonlinearity. The robustness and effectiveness of the proposed methodology have been validated based on simulation results under real climatic conditions using on-site measurements from the region of Adrar.

Algerian Journal of Renewable Energy and Sustainable Development Volume: 3 | Number: 1 | 2021| June

Survey of Six Maximum Power Point Tracking Algorithms under Standard Test conditions

Mohammed Salah Bouakkaz[1*], Ahcene Boukadoum[1], Omar Boudebbouz[1], Issam Attoui[2], Nadir Boutasseta[2], Ahmed Bouraiou[3]

[1]Department of Electrical Engineering, LES laboratory, University of Skikda, Algeria.

[2]Research Center in Industrial Technologies CRTI P.O. Box 64, Cheraga, Algiers, Algeria.

[3]Research unit in Renewable energies in Saharan Medium, URERMS, Renewable Energy Development Center, CDER, 01000 Adrar, Algeria.

[*]Corresponding author; Email: ms.bouakkaz@univ-skikda.dz.

Article Info

Article history:

Received 01 May 2021
Revised 07 May 2021
Accepted 15 May 2021

Keywords:

Perturb and Observe (P&O)
Hill Climbing (HC)
Fuzzy Logic (FL)
Proportional Integral (PI)
Voltage Open Circuit (VOC)

ABSTRACT

In this work, a survey is carried out on six MPPT algorithms which include conventional and artificial intelligence based approaches. Maximum Power Point Tracking (MPPT) algorithms are used in PV systems to extract the maximum power in varying climatic conditions. The following most popular MPPT techniques are being reviewed and studied: Hill Climbing (HC), Perturb and Observe (P&O), Incremental Conductance (INC), Open-Circuit Voltage (OCV), Short Circuit Current (SCC), and Fuzzy Logic Control (FLC). The algorithms are evaluated, analyzed, and interpreted using a Matlab-Simulink environment to show the performance and limitations of each algorithm.

I. Introduction

Photovoltaic solar energy is one of the renewable energy sources which consists of transforming solar radiation into electricity using the photoelectric effect [1]–[3]. In photovoltaic systems, the transfer of the energy from the PV generator via converters needs an MPPT controller for ensuring the optimal power transfer. In current literature, several MPPT algorithms are being classified into two main categories that are conventional and intelligent [4]–[10]. In order to differentiate the characteristics of available algorithms and properly use the appropriate algorithm for a given situation, MPPT techniques have to be evaluated in the same system configuration and environmental conditions. In this context, this work aims to evaluate the considered algorithms on a PV system subject to fixed STC climatic conditions. Hill Climbing (HC), Perturb and Observe (P&O), Incremental Conductance (INC), Open-Circuit Voltage (OCV), Short Circuit Current (SCC), and Fuzzy Logic Control (FLC) MPPT algorithms are implemented in Matlab-Simulink environment in order to give an insight on the performance and limitations of each algorithm.

Global Maximum Power Point Tracking Using Genetic Algorithm Combined with PSO Tuned PID Controller

Mohammed Salah Bouakkaz, Ahcene Boukadoum, Omar Boudebbouz, Abdel Djabar Bouchaala, Nadir Boutasseta, Issam Attoui, Ahmed Bouraiou, and Saad Motahhir

Abstract Several techniques have been proposed to track the global maximum power point (GMPP) in the presence of multiple local peaks introduced when the PV generator is affected by partial shading. Such methods include scanning methods and advanced optimization-based strategies. In this paper, a Genetic Algorithm based MPPT, combined with PID controller tuned using PSO, is proposed to track the MPP. The GA algorithm is applied to give the reference voltage and measured PV voltage to the PID controller that its parameters were tuned using PSO. The obtained results give a good tracking performance of the GMPP under STC conditions and partial shading scenarios.

Keywords Maximum power point tracking (MPPT) · Genetic algorithm (GA) · PID controller · Particle Swarm Optimization (PSO)

1 Introduction

Photovoltaic (PV) solar energy is one of the most important renewable energies for the following reasons: clean and non-polluting energy, economical and maintainable, the availability of solar radiation in most countries of the world [1, 2]. The photovoltaic solar system consists of a group of elements which include: photovoltaic solar panels, charge controller (including MPPT), storage batteries, and the power inverter (for AC loads). In general; solar photovoltaic energy in terms of load connection into two

M. S. Bouakkaz (✉) · A. Boukadoum · O. Boudebbouz · A. D. Bouchaala
Department of Electrical Engineering, Laboratoire d'électrotechnique de Skikda «LES», Université du 20 Août 1955, 21000 Skikda, Algeria

N. Boutasseta · I. Attoui
Research Center in Industrial Technologies CRTI, P.O. Box 64, Cheraga, Algiers, Algeria

A. Bouraiou
Unité de Recherche en Energies Renouvelables en Milieu Saharien (URERMS), Centre de Développement des Energies Renouvelables (CDER), 01000 Adrar, Algeria

S. Motahhir
ENSA, SMBA University, Fez, Morocco

S. Motahhir and B. Bossoufi (eds.), *Digital Technologies and Applications*,
Lecture Notes in Networks and Systems 211,
https://doi.org/10.1007/978-3-030-73882-2_107

APPENDIX

« B »

DATASHEET OF PANEL

THE NEW VALUE FRONTIER

KYOCERA

KC200GT

HIGH EFFICIENCY MULTICRYSTAL
PHOTOVOLTAIC MODULE

UL LISTED

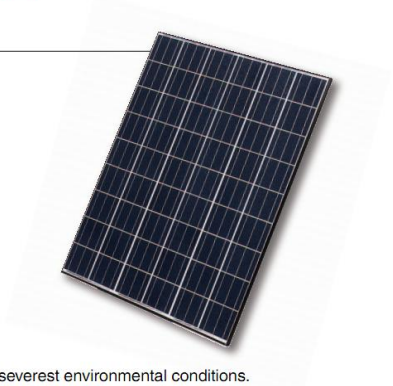

HIGHLIGHTS OF KYOCERA PHOTOVOLTAIC MODULES

Kyocera's advanced cell processing technology
and automated production facilities produce a highly efficient
multicrystal photovoltaic module.
The conversion efficiency of the Kyocera solar cell is over 16%.
These cells are encapsulated between a tempered glass cover
and a pottant with back sheet to provide efficient protection from the severest environmental conditions.
The entire laminate is installed in an anodized aluminum frame to provide structural strength and ease of installation.
Equipped with plug-in connectors.

APPLICATIONS

KC200GT is ideal for grid tie system applications.

- Residential roof top systems
- Large commercial grid tie systems
- Water Pumping systems
- High Voltage stand alone systems
- etc.

QUALIFICATIONS

- **MODULE** : UL1703 certified
- **FACTORY** : ISO9001 and ISO 14001

QUALITY ASSURANCE

Kyocera multicrystal photovoltaic modules have passed the following tests.

- Thermal cycling test
- Thermal shock test
- Thermal / Freezing and high humidity cycling test
- Electrical isolation test
- Hail impact test
- Mechanical, wind and twist loading test
- Salt mist test
- Light and water-exposure test
- Field exposure test

LIMITED WARRANTY

※1 year limited warranty on material and workmanship
※20 years limited warranty on power output: For detail, please refer to "category IV" in Warranty issued by Kyocera

(Long term output warranty shall warrant if PV Module(s) exhibits power output of less than 90% of the original minimum rated power specified at the time of sale within 10 years and less than 80% within 20 years after the date of sale to the Customer. The power output values shall be those measured under Kyocera's standard measurement conditions. Regarding the warranty conditions in detail, please refer to Warranty issued by Kyocera)

ELECTRICAL CHARACTERISTICS

Current-Voltage characteristics of Photovoltaic Module KC200GT at various cell temperatures

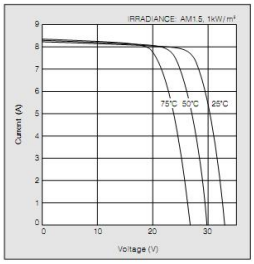

Current-Voltage characteristics of Photovoltaic Module KC200GT at various irradiance levels

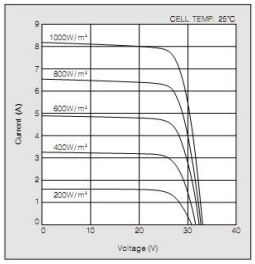

SPECIFICATIONS

KC200GT

■ Physical Specifications

Unit : mm (in.)

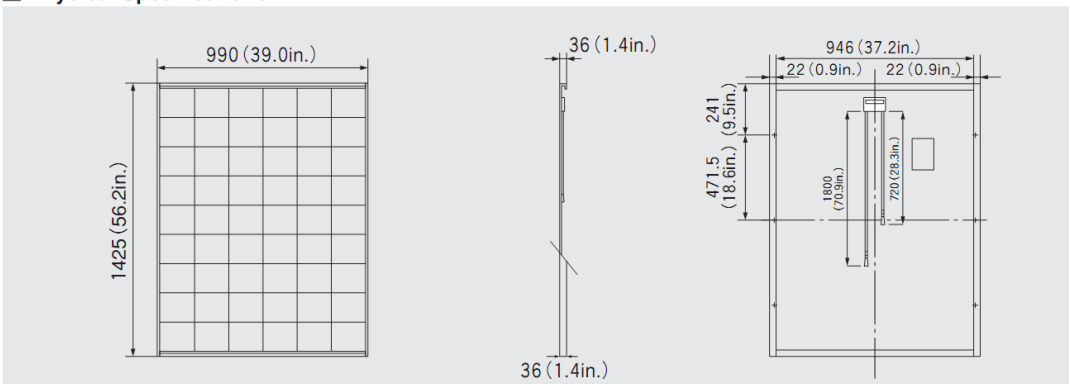

■ Specifications

■ Electrical Performance under Standard Test Conditions (*STC)	
Maximum Power (Pmax)	200W (+10%/−5%)
Maximum Power Voltage (Vmpp)	26.3V
Maximum Power Current (Impp)	7.61A
Open Circuit Voltage (Voc)	32.9V
Short Circuit Current (Isc)	8.21A
Max System Voltage	600V
Temperature Coefficient of Voc	-1.23×10^{-1} V/℃
Temperature Coefficient of Isc	3.18×10^{-3} A/℃

*STC : Irradiance 1000W/m², AM1.5 spectrum, module temperture 25℃

■ Electrical Performance at 800W/m², NOCT, AM1.5	
Maximum Power (Pmax)	142W
Maximum Power Voltage (Vmpp)	23.2V
Maximum Power Current (Impp)	6.13A
Open Circuit Voltage (Voc)	29.9V
Short Circuit Current (Isc)	6.62A

NOCT (Nominal Operating Cell Temperature) : 47℃

■ Cells	
Number per Module	54

■ Module Characteristics	
Length × Width × Depth	1425mm(56.2in)×990mm(39.0in)×36mm(1.4in)
Weight	18.5kg(40.7lbs.)
Cable	(+)720mm(28.3in),(-)1800mm(70.9in)

■ Junction Box Characteristics	
Length × Width × Depth	113.6mm(4.5in)×76mm(3.0in)×9mm(0.4in)
IP Code	IP65

■ Reduction of Efficiency under Low Irradiance	
Reduction	7.8%

Reduction of efficiency from an irrandiance of 1000W/m² to 200W/m² (module temperature 25℃)

Please contact our office for further information

KYOCERA

KYOCERA Corporation

■ KYOCERA Corporation Headquarters
CORPORATE SOLAR ENERGY DIVISION
6 Takeda Tobadono-cho
Fushimi-ku, Kyoto
612-8501, Japan
TEL:(81)75-604-3476 FAX:(81)75-604-3475
http://www.kyocera.com

● KYOCERA Solar, Inc.
7812 East Acoma Drive
Scottsdale, AZ 85260, USA
TEL:(1)480-948-8003 or (800)223-9580 FAX:(1)480-483-6431
http://www.kyocerasolar.com

● KYOCERA Solar do Brasil Ltda.
Av. Guignard 661, Loja A
22790-200, Recreio dos Bandeirantes, Rio de Janeiro, Brazil
TEL:(55)21-2437-8525 FAX:(55)21-2437-2338
http://www.kyocerasolar.com.br

● KYOCERA Solar Pty Ltd.
Level 3, 6-10 Talavera Road, North Ryde
N.S.W. 2113, Australia
TEL:(61)2-9870-3948 FAX:(61)2-9888-9588
http://www.kyocerasolar.com.au/

● KYOCERA Fineceramics GmbH
Fritz Muller strasse 107, D-73730 Esslingen, Germany
TEL:(49)711-93934-917 FAX:(49)711-93934-950
http://www.kyocerasolar.de/

● KYOCERA Asia Pacific Pte. Ltd.
298 Tiong Bahru Road, #13-03/05
Central Plaza, Singapore 168730
TEL:(65)6271-0500 FAX:(65)6271-0600

● KYOCERA Asia Pacific Ltd.
Room 801-802, Tower 1 South Seas Centre, 75 Mody Road,
Tsimshatsui East, Kowloon, Hong Kong
TEL:(852)2-7237183 FAX:(852)2-7244501

● KYOCERA Asia Pacific Ltd. Taipei Office
10 Fl., No.66, Nanking West Road, Taipei, Taiwan
TEL:(886)2-2555-3609 FAX:(886)2-2559-4131

● KYOCERA(Tianjin) Sales & Trading Corporation
19F, Tower C HeQiao Building 8A GuangHua Rd.,
Chao Yang District, Beijing 100026, China
TEL:(86)10-6583-2270 FAX:(86)10-6583-2250

LIE/I09M0703-SAGKM

APPENDIX

« C »

DESIGN OF BOOST CONVERTER

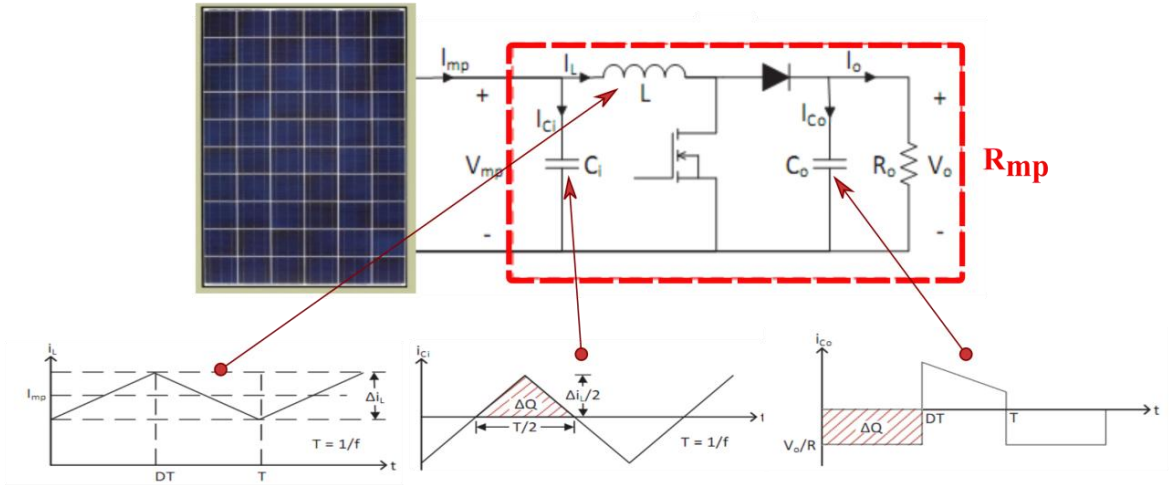

The schematic of the boost converter.

Component	Calculation
Minimum inductance, L_{min} (H)	$L_{(min,com)} = \frac{R_{mp(max)}}{\gamma_{I_L} f}\left(1-\sqrt{\frac{R_{mp(max)}}{R_{o(max)}}}\right)$ *Where* $R_{o(ming)} \leqslant R_{o(max)} \leqslant R_{o(maxg)}$ For the fixed R_o, $L_{(min,fixed)} = \frac{4}{27}\frac{R_o}{\gamma_{I_L} f}$
Minimum input capacitance, $C_{i(min)}$ (F)	$C_{i(min,com)} = \frac{D_{max}}{8L\gamma_{Vmp} f^2}$ *if* $R_{o(max)} \geqslant R_{o(max,G)}$ $C_{i(min,lim)} = \frac{1-\sqrt{\frac{R_{mp(min)}}{R_{o(max)}}}}{8L\gamma_{Vmp} f^2}$ *if* $R_{o(max)} < R_{o(max,G)}$ For the fixed R_o, $R_{o(max)} = R_{o(op)}$
Minimum output capacitance, $C_{o(min)}$ (F)	• For the fixed R_o $C_{o(min,op)} = \frac{1}{\gamma_{V_O} f}\left(\frac{1}{R_{o(op)}} - \sqrt{\frac{R_{mp(min)}}{R^3_{o(op)}}}\right)$ • For the limited R_o with $R_{o(max)} < \frac{9}{4}R_{mp(min)}$ *and* $D_{max} > 1-\sqrt{R_{mp(min)}/R_{o(max)}}$ $C_{o(min,lim)} = \frac{1}{\gamma_{V_O} f}\left(\frac{1}{R_{o(max)}} - \sqrt{\frac{R_{mp(min)}}{R^3_{o(max)}}}\right)$ • For other condition $C_{o(min,com)} = \frac{4}{27R_{mp(min)}\gamma_{V_O} f}$ *if* $D_{min} \leqslant \frac{1}{3}$ *and* $D_{max} \geqslant \frac{1}{3}$ $C_{o(min,Dmin)} = \frac{D_{min}(1-D_{min})^2}{R_{mp(min)}\gamma_{V_O} f}$ *if* $D_{min} > \frac{1}{3}$ $C_{o(min,Dmax)} = \frac{D_{max}(1-D_{max})^2}{R_{mp(min)}\gamma_{V_O} f}$ *if* $D_{max} < \frac{1}{3}$

Calculation of the minimum inductance, input capacitance, and output capacitance

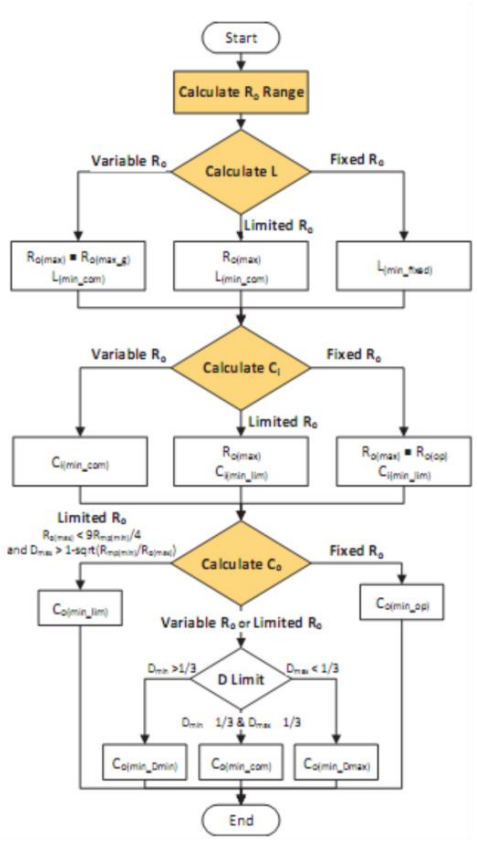

The flowchart of the boost converter design.

BIBLIOGRAPHY

[1] Z. Liu *et al.*, “Near-real-time monitoring of global CO2 emissions reveals the effects of the COVID-19 pandemic,” *Nat. Commun.*, vol. 11, no. 1, p. 5172, 2020, doi: 10.1038/s41467-020-18922-7.

[2] Bloomberg NEF, “BNEF Executive Factbook,” *Bloomberg*, p. All, 2020, [Online]. Available: https://data.bloomberglp.com/promo/sites/12/678001-BNEF_2020-04-22-ExecutiveFactbook.pdf?link=cta-text.

[3] SOLSRGIS, “© 2019 The World Bank, Source: Global Solar Atlas 2.0, Solar resource data: Solargis.,” *Solargis*, p. All, 2019, [Online]. Available: https://solargis.com/maps-and-gis-data/download/world.

[4] SOLSRGIS, “© 2019 The World Bank, Source: Global Solar Atlas 2.0, Solar resource data: Solargis.,” *Solargis*, p. All, 2019, [Online]. Available: https://solahttps//solargis.com/maps-and-gis-data/download/algeria.

[5] pvXchange, “Price Index,” *pvXchange*, 2021.

[6] NREL, “National Renewable Energy Laboratory, Andasol-1,” *Data Conc. Sol. power Proj.*, pp. 9–10, 2008, [Online]. Available: http://www.nrel.gov/csp/solarpaces/project_detail.cfm/projectID=3.

[7] V. Muteri *et al.*, “Review on life cycle assessment of solar photovoltaic panels,” *Energies*, vol. 13, no. 1, 2020, doi: 10.3390/en13010252.

[8] J. Assadeg, K. Sopian, and A. Fudholi, “Performance of grid-connected solar photovoltaic power plants in the Middle East and North Africa,” *Int. J. Electr. Comput. Eng.*, vol. 9, no. 5, pp. 3375–3383, 2019, doi: 10.11591/ijece.v9i5.pp3375-3383.

[9] V. G. R. Kummara *et al.*, “A comprehensive review of DC–DC converter topologies and modulation strategies with recent advances in solar photovoltaic systems,” *Electron.*, vol. 9, no. 1, 2020, doi: 10.3390/electronics9010031.

[10] A. O. Baba, G. Liu, and X. Chen, “Classification and Evaluation Review of Maximum Power Point Tracking Methods,” *Sustain. Futur.*, vol. 2, p. 100020, 2020, doi: 10.1016/j.sftr.2020.100020.

[11] A. Badis and M. H. Boujmil, “Cascade control based on TLBO-FOPID for grid-connected PV systems,” *Smart Innov. Syst. Technol.*, vol. 147, pp. 156–166, 2020, doi: 10.1007/978-3-030-21009-0_14.

[12] K. M. Passino, “Biomimicry of Bacterial Foraging for Distributed Optimization and Control,” *IEEE Control Syst.*, vol. 22, no. 3, pp. 52–

67, 2002, doi: 10.1109/MCS.2002.1004010.

[13] S. Mirjalili, S. M. Mirjalili, and A. Lewis, “Grey Wolf Optimizer,” *Adv. Eng. Softw.*, vol. 69, pp. 46–61, 2014, doi: 10.1016/j.advengsoft.2013.12.007.

[14] X. S. Yang, “Firefly algorithms for multimodal optimization,” *Lect. Notes Comput. Sci. (including Subser. Lect. Notes Artif. Intell. Lect. Notes Bioinformatics)*, vol. 5792 LNCS, pp. 169–178, 2009, doi: 10.1007/978-3-642-04944-6_14.

[15] B. Yang *et al.*, “Novel bio-inspired memetic salp swarm algorithm and application to MPPT for PV systems considering partial shading condition,” *J. Clean. Prod.*, vol. 215, pp. 1203–1222, 2019, doi: 10.1016/j.jclepro.2019.01.150.

[16] S. Mirjalili, “Dragonfly algorithm: a new meta-heuristic optimization technique for solving single-objective, discrete, and multi-objective problems,” *Neural Comput. Appl.*, vol. 27, no. 4, pp. 1053–1073, 2016, doi: 10.1007/s00521-015-1920-1.

[17] S. A. Chu, P. W. Tsai, and J. S. Pan, “Cat swarm optimization,” *Lect. Notes Comput. Sci. (including Subser. Lect. Notes Artif. Intell. Lect. Notes Bioinformatics)*, vol. 4099 LNAI, pp. 854–858, 2006, doi: 10.1007/11801603_94.

[18] X. S. Yang, “A new metaheuristic Bat-inspired Algorithm,” *Stud. Comput. Intell.*, vol. 284, pp. 65–74, 2010, doi: 10.1007/978-3-642-12538-6_6.

[19] R. Rao, “Jaya: A simple and new optimization algorithm for solving constrained and unconstrained optimization problems,” *Int. J. Ind. Eng. Comput.*, vol. 7, no. 1, pp. 19–34, 2016, [Online]. Available: http://growingscience.com/beta/ijiec/2072-jaya-a-simple-and-new-optimization-algorithm-for-solving-constrained-and-unconstrained-optimization-problems.html.

[20] Q. J. Li LX, Shao ZJ, “An optimizing method based on autonomous animals: fish-swarm algorithm. Syst Eng Theory Practice,” *Syst Eng Theory Pract.*, vol. 22, pp. 32–38, 2002.

[21] D. Karaboga, “An idea based on Honey Bee Swarm for Numerical Optimization,” *Tech. Rep. TR06, Erciyes Univ.*, no. TR06, p. 10, 2005, [Online]. Available: http://mf.erciyes.edu.tr/abc/pub/tr06_2005.pdf.

[22] M. A. M. Ramli, S. Twaha, K. Ishaque, and Y. A. Al-Turki, “A review on maximum power point tracking for photovoltaic systems with and

without shading conditions," *Renew. Sustain. Energy Rev.*, vol. 67, pp. 144–159, 2017, doi: 10.1016/j.rser.2016.09.013.

[23] D. Baimel, S. Tapuchi, Y. Levron, and J. Belikov, "Improved fractional open circuit voltage MPPT methods for PV systems," *Electron.*, vol. 8, no. 3, 2019, doi: 10.3390/electronics8030321.

[24] H. M. H. Farh, A. M. Eltamaly, and M. F. Othman, "Hybrid PSO-FLC for dynamic global peak extraction of the partially shaded photovoltaic system," *PLoS One*, vol. 13, no. 11, 2018, doi: 10.1371/journal.pone.0206171.

[25] A. M. Eltamaly, M. S. Al-Saud, and A. G. Abo-Khalil, "Performance improvement of PV systems' maximum power point tracker based on a scanning PSO particle strategy," *Sustain.*, vol. 12, no. 3, 2020, doi: 10.3390/su12031185.

[26] B. Subudhi and R. Pradhan, "A comparative study on maximum power point tracking techniques for photovoltaic power systems," *IEEE Trans. Sustain. Energy*, vol. 4, no. 1, pp. 89–98, 2013, doi: 10.1109/TSTE.2012.2202294.

[27] E. Prasetyono, L. Mohammad, and F. D. Murdianto, "Performance of ACO-MPPT and constant voltage method for street lighting charging system," *Int. Rev. Electr. Eng.*, vol. 15, no. 3, pp. 235–244, 2020, doi: 10.15866/iree.v15i3.17309.

[28] A. Vijayakumari, "A non-iterative MPPT of PV array with online measured short circuit and open circuit quantities," *J. King Saud Univ. - Eng. Sci.*, 2020, doi: 10.1016/j.jksues.2020.04.007.

[29] S. Motahhir, A. El Hammoumi, and A. El Ghzizal, "The most used MPPT algorithms: Review and the suitable low-cost embedded board for each algorithm," *J. Clean. Prod.*, vol. 246, 2020, doi: 10.1016/j.jclepro.2019.118983.

[30] E. Mamarelis, G. Petrone, and G. Spagnuolo, "A two-steps algorithm improving the P&O steady state MPPT efficiency," *Appl. Energy*, vol. 113, pp. 414–421, 2014, doi: 10.1016/j.apenergy.2013.07.022.

[31] M. A. Elgendy, B. Zahawi, and D. J. Atkinson, "Assessment of the incremental conductance maximum power point tracking algorithm," *IEEE Trans. Sustain. Energy*, vol. 4, no. 1, pp. 108–117, 2013, doi: 10.1109/TSTE.2012.2202698.

[32] C. H. Basha and C. Rani, "Different conventional and soft computing MPPT techniques for solar PV systems with high step-up boost

converters: A comprehensive analysis," *Energies*, vol. 13, no. 2, 2020, doi: 10.3390/en13020371.

[33] C. L. Liu, J. H. Chen, Y. H. Liu, and Z. Z. Yang, "An asymmetrical fuzzy-logic-control-based MPPT algorithm for photovoltaic systems," *Energies*, vol. 7, no. 4, pp. 2177–2193, 2014, doi: 10.3390/en7042177.

[34] Ruchira, R. N. Patel, and S. K. Sinha, "Comparison of ANN-based MPPT controller and incremental conductance for photovoltaic system," *Lect. Notes Electr. Eng.*, vol. 476, pp. 295–305, 2019, doi: 10.1007/978-981-10-8234-4_26.

[35] H. M. El-Zoghby and A. F. Bendary, "A Novel Technique for Maximum Power Point Tracking of a Photovoltaic Based on Sensing of Array Current Using Adaptive Neuro-Fuzzy Inference System (ANFIS)," *Int. J. Emerg. Electr. Power Syst.*, vol. 17, no. 5, pp. 547–554, 2016, doi: 10.1515/ijeeps-2016-0049.

[36] F. Keyrouz, "Enhanced Bayesian Based MPPT Controller for PV Systems," *IEEE Power Energy Technol. Syst. J.*, vol. 5, no. 1, pp. 11–17, 2018, doi: 10.1109/jpets.2018.2811708.

[37] A. M. Eltamaly, H. M. H. Farh, and M. S. Al Saud, "Impact of PSO reinitialization on the accuracy of dynamic global maximum power detection of variant partially shaded PV systems," *Sustain.*, vol. 11, no. 7, 2019, doi: 10.3390/su1102091.

[38] Y. H. Liu, S. C. Huang, J. W. Huang, and W. C. Liang, "A particle swarm optimization-based maximum power point tracking algorithm for PV systems operating under partially shaded conditions," *IEEE Trans. Energy Convers.*, vol. 27, no. 4, pp. 1027–1035, 2012, doi: 10.1109/TEC.2012.2219533.

[39] S. Mirjalili and A. Lewis, "The Whale Optimization Algorithm," *Adv. Eng. Softw.*, vol. 95, pp. 51–67, 2016, doi: 10.1016/j.advengsoft.2016.01.008.

[40] A. A. Z. Diab, "MPPT of PV system under partial shading conditions based on hybrid whale optimization-simulated annealing algorithm (WOSA)," *Green Energy Technol.*, pp. 355–378, 2020, doi: 10.1007/978-3-030-05578-3_13.

[41] M. Abdel-Basset, G. Manogaran, D. El-Shahat, and S. Mirjalili, "A hybrid whale optimization algorithm based on local search strategy for the permutation flow shop scheduling problem," *Futur. Gener. Comput. Syst.*, vol. 85, pp. 129–145, 2018, doi: 10.1016/j.future.2018.03.020.

[42] K. ben oualid Medani, S. Sayah, and A. Bekrar, “Whale optimization algorithm based optimal reactive power dispatch: A case study of the Algerian power system,” *Electr. Power Syst. Res.*, vol. 163, pp. 696–705, 2018, doi: 10.1016/j.epsr.2017.09.001.

[43] B. Bentouati, L. Chaib, and S. Chettih, “A hybrid whale algorithm and pattern search technique for optimal power flow problem,” *Proc. 2016 8th Int. Conf. Model. Identif. Control. ICMIC 2016*, pp. 1048–1053, 2017, doi: 10.1109/ICMIC.2016.7804267.

[44] R. H. Bhesdadiya, S. A. Parmar, I. N. Trivedi, P. Jangir, M. Bhoye, and N. Jangir, “Optimal Active and Reactive Power Dispatch Problem Solution using Whale Optimization Algorithm,” *Indian J. Sci. Technol.*, vol. 9, no. S1, 2016, doi: 10.17485/ijst/2016/v9is1/101941.

[45] Q. T. Bui, M. Van Pham, Q. H. Nguyen, L. X. Nguyen, and H. M. Pham, “Whale Optimization Algorithm and Adaptive Neuro-Fuzzy Inference System: a hybrid method for feature selection and land pattern classification,” *Int. J. Remote Sens.*, vol. 40, no. 13, pp. 5078–5093, 2019, doi: 10.1080/01431161.2019.1578000.

[46] C. H. Santhan Kumar and R. Srinivasa Rao, “A novel global MPP tracking of photovoltaic system based on whale optimization algorithm,” *Int. J. Renew. Energy Dev.*, vol. 5, no. 3, pp. 225–232, 2016, doi: 10.14710/ijred.5.3.225-232.

[47] S. Mirjalili, “Moth-flame optimization algorithm: A novel nature-inspired heuristic paradigm,” *Knowledge-Based Syst.*, vol. 89, pp. 228–249, 2015, doi: 10.1016/j.knosys.2015.07.006.

[48] M. S. Bouakkaz *et al.*, “Dynamic performance evaluation and improvement of PV energy generation systems using Moth Flame Optimization with combined fractional order PID and sliding mode controller,” *Sol. Energy*, vol. 199, pp. 411–424, 2020, doi: 10.1016/j.solener.2020.02.055.

[49] K. D. Frank, “Effects of artificial night lighting on moths,” *Ecol. Consequences Artif. Night Light.*, pp. 305–344, 2006, [Online]. Available: http://books.google.com/books?hl=en&lr=&id=dEEGtAtR1NcC&pgis=1%5Cnhttp://books.google.com/books?hl=en&lr=&id=dEEGtAtR1NcC&oi=fnd&pg=PA305&dq=Effects+of+Artificial+Night+Lighting+on+Moths&ots=82_8j687jI&sig=OcVL2Sp2PBaJoMTWDq8CYiFuKQ0.

[50] D. Allam, D. A. Yousri, and M. B. Eteiba, “Parameters extraction of the three diode model for the multi-crystalline solar cell/module using

Moth-Flame Optimization Algorithm," *Energy Convers. Manag.*, vol. 123, pp. 535–548, 2016, doi: 10.1016/j.enconman.2016.06.052.

[51] I. N. Trivedi, A. Kumar, A. H. Ranpariya, and P. Jangir, "Economic Load Dispatch problem with ramp rate limits and prohibited operating zones solve using Levy flight Moth-Flame optimizer," *2016 Int. Conf. Energy Effic. Technol. Sustain. ICEETS 2016*, pp. 442–447, 2016, doi: 10.1109/ICEETS.2016.7583795.

[52] B. Bentouati, L. Chaib, and S. Chettih, "Optimal power flow using the moth flam optimizer: A case study of the algerian power system," *Indones. J. Electr. Eng. Comput. Sci.*, vol. 1, no. 3, pp. 431–445, 2016, doi: 10.11591/ijeecs.v1.i3.pp431-445.

[53] O. Ceylan, "Harmonic elimination of multilevel inverters by moth-flame optimization algorithm," *2016 Int. Symp. Ind. Electron. INDEL 2016 - Proc.*, 2016, doi: 10.1109/INDEL.2016.7797803.

[54] P. Garg and A. Gupta, "Optimized open shortest path first algorithm based on moth flame optimization," *Indian J. Sci. Technol.*, vol. 9, no. 48, 2016, doi: 10.17485/ijst/2016/v9i48/104255.

[55] N. Jangir, M. H. Pandya, I. N. Trivedi, R. H. Bhesdadiya, P. Jangir, and A. Kumar, "Moth-Flame optimization Algorithm for solving real challenging constrained engineering optimization problems," *2016 IEEE Students' Conf. Electr. Electron. Comput. Sci. SCEECS 2016*, 2016, doi: 10.1109/SCEECS.2016.7509293.

[56] Z. Li, Y. Zhou, S. Zhang, and J. Song, "Lévy-Flight Moth-Flame Algorithm for Function Optimization and Engineering Design Problems," *Math. Probl. Eng.*, vol. 2016, 2016, doi: 10.1155/2016/1423930.

[57] N. Muangkote, K. Sunat, and S. Chiewchanwattana, "Multilevel thresholding for satellite image segmentation with moth-flame based optimization," *2016 13th Int. Jt. Conf. Comput. Sci. Softw. Eng. JCSSE 2016*, 2016, doi: 10.1109/JCSSE.2016.7748919.

[58] Vikas and S. J. Nanda, "Multi-objective Moth Flame Optimization," *2016 Int. Conf. Adv. Comput. Commun. Informatics, ICACCI 2016*, pp. 2470–2476, 2016, doi: 10.1109/ICACCI.2016.7732428.

[59] T. H. M. A.-E.-E. Ghada M. A. Soliman, Motaz M. H. Khorshid, "MODiFIED MOTH-FLAME OPTIMIZATION ALGORITHMS FOR TERRORISM PREDICTION," *Int. J. Appl. or Innov. Eng. Manag.*, vol. 5, no. 7, 2016.

[60] H. M. Zawbaa, E. Emary, B. Parv, and M. Sharawi, “Feature selection approach based on moth-flame optimization algorithm,” *2016 IEEE Congr. Evol. Comput. CEC 2016*, pp. 4612–4617, 2016, doi: 10.1109/CEC.2016.7744378.

[61] W. Yamany, M. Fawzy, A. Tharwat, and A. E. Hassanien, “Moth-flame optimization for training Multi-Layer Perceptrons,” *2015 11th Int. Comput. Eng. Conf. Today Inf. Soc. What’s Next?, ICENCO 2015*, pp. 267–272, 2016, doi: 10.1109/ICENCO.2015.7416360.

[62] H. Buch, I. N. Trivedi, and P. Jangir, “Moth flame optimization to solve optimal power flow with non-parametric statistical evaluation validation,” *Cogent Eng.*, vol. 4, no. 1, 2017, doi: 10.1080/23311916.2017.1286731.

[63] M. Raju, L. C. Saikia, and D. Saha, “Automatic generation control in competitive market conditions with moth-flame optimization based cascade controller,” *IEEE Reg. 10 Annu. Int. Conf. Proceedings/TENCON*, pp. 734–738, 2017, doi: 10.1109/TENCON.2016.7848100.

[64] A. Mohapatra, B. Nayak, P. Das, and K. B. Mohanty, “A review on MPPT techniques of PV system under partial shading condition,” *Renew. Sustain. Energy Rev.*, vol. 80, pp. 854–867, 2017, doi: 10.1016/j.rser.2017.05.083.

[65] K. Labeeb, S. Shankar, and J. Ramprabhakar, “Hybrid MPPT controller for accurate and quick tracking,” *2016 IEEE Int. Conf. Recent Trends Electron. Inf. Commun. Technol. RTEICT 2016 - Proc.*, pp. 1533–1537, 2017, doi: 10.1109/RTEICT.2016.7808089.

[66] C. Larbes, S. M. Aït Cheikh, T. Obeidi, and A. Zerguerras, “Genetic algorithms optimized fuzzy logic control for the maximum power point tracking in photovoltaic system,” *Renew. Energy*, vol. 34, no. 10, pp. 2093–2100, 2009, doi: 10.1016/j.renene.2009.01.006.

[67] M. S. Bouakkaz *et al.*, “Global Maximum Power Point Tracking Using Genetic Algorithm Combined with PSO Tuned PID Controller,” in *Digital Technologies and Applications*, 2021, pp. 1171–1180.

[68] M. S. Bouakkaz, A. Boukadoum, O. Boudebbouz, I. Attoui, N. Boutasseta, and A. Bouraiou, “Fuzzy Logic based Adaptive Step Hill Climbing MPPT Algorithm for PV Energy Generation Systems,” *2020 Int. Conf. Comput. Inf. Technol. ICCIT 2020*, 2020, doi: 10.1109/ICCIT-144147971.2020.9213737.

[69] Y. Zhu and W. Xiao, “A comprehensive review of topologies for photovoltaic I–V curve tracer,” *Sol. Energy*, vol. 196, pp. 346–357, Jan. 2020, doi: 10.1016/j.solener.2019.12.020.

[70] M. G. Villalva, J. R. Gazoli, and E. R. Filho, “Comprehensive Approach to Modeling and Simulation of Photovoltaic Arrays,” *IEEE Trans. Power Electron.*, vol. 24, no. 5, pp. 1198–1208, May 2009, doi: 10.1109/TPEL.2009.2013862.

[71] W. Xiao, W. G. Dunford, P. R. Palmer, and A. Capel, “Regulation of photovoltaic voltage,” *IEEE Trans. Ind. Electron.*, vol. 54, no. 3, pp. 1365–1374, 2007, doi: 10.1109/TIE.2007.893059.

[72] J. Kivimaki, S. Kolesnik, M. Sitbon, T. Suntio, and A. Kuperman, “Revisited Perturbation Frequency Design Guideline for Direct Fixed-Step Maximum Power Point Tracking Algorithms,” *IEEE Trans. Ind. Electron.*, vol. 64, no. 6, pp. 4601–4609, 2017, doi: 10.1109/TIE.2017.2674589.

[73] H. Rezk *et al.*, “A novel statistical performance evaluation of most modern optimization-based global MPPT techniques for partially shaded PV system,” *Renew. Sustain. Energy Rev.*, vol. 115, p. 109372, Nov. 2019, doi: 10.1016/j.rser.2019.109372.

[74] V. Utkin, J. Guldner, and J. Shi, *Sliding Mode Control in Electro-Mechanical Systems, Second Edition*, vol. 31. CRC Press, 2009.

[75] H. SIRA-RAMIREZ, “Sliding-mode control on slow manifolds of DC-to-DC power converters,” *Int. J. Control*, vol. 47, no. 5, pp. 1323–1340, May 1988, doi: 10.1080/00207178808906099.

[76] I. Podlubny, “Fractional-order systems and PI/sup/spl lambda//D/sup/spl mu//-controllers,” *IEEE Trans. Automat. Contr.*, vol. 44, no. 1, pp. 208–214, 1999.

[77] A. Charef, “Analogue realisation of fractional-order integrator, differentiator and fractional PIλDμ controller,” *IEE Proc. - Control Theory Appl.*, vol. 153, no. 6, pp. 714–720, Nov. 2006, doi: 10.1049/ip-cta:20050019.

[78] A. Oustaloup, F. Levron, B. Mathieu, and F. M. Nanot, “Frequency-band complex noninteger differentiator: characterization and synthesis,” *IEEE Trans. Circuits Syst. I Fundam. Theory Appl.*, vol. 47, no. 1, pp. 25–39, 2000, doi: 10.1109/81.817385.

[79] P. Shah and S. Agashe, “Review of fractional PID controller,” *Mechatronics*, vol. 38, pp. 29–41, Sep. 2016, doi:

10.1016/j.mechatronics.2016.06.005.

[80] C. A. Monje, B. M. Vinagre, V. Feliu, and Y. Chen, “Tuning and auto-tuning of fractional order controllers for industry applications,” *Control Eng. Pract.*, vol. 16, no. 7, pp. 798–812, Jul. 2008, doi: 10.1016/j.conengprac.2007.08.006.

[81] Y. Luo, Y. Q. Chen, C. Y. Wang, and Y. G. Pi, “Tuning fractional order proportional integral controllers for fractional order systems,” *J. Process Control*, vol. 20, no. 7, pp. 823–831, Aug. 2010, doi: 10.1016/j.jprocont.2010.04.011.

[82] M. Bettayeb and R. Mansouri, “Fractional IMC-PID-filter controllers design for non integer order systems,” *J. Process Control*, vol. 24, no. 4, pp. 261–271, Apr. 2014, doi: 10.1016/j.jprocont.2014.01.014.

[83] J. Cao and B. Cao, “Design of Fractional Order Controllers Based on Particle Swarm Optimization,” in *2006 1ST IEEE Conference on Industrial Electronics and Applications*, May 2006, pp. 1–6, doi: 10.1109/ICIEA.2006.257091.

[84] R. S. Barbosa, M. F. Silva, and J. A. T. Machado, “Tuning and Application of Integer and Fractional Order PID Controllers,” in *Intelligent Engineering Systems and Computational Cybernetics*, Dordrecht: Springer Netherlands, pp. 245–255.

[85] S. Sapre and S. Mini, “Optimized Relay Nodes Positioning to Achieve Full Connectivity in Wireless Sensor Networks,” *Wirel. Pers. Commun.*, vol. 99, no. 4, pp. 1521–1540, Apr. 2018, doi: 10.1007/s11277-018-5290-8.